Chemical Weathering of Basalts and Andesites: Evidence from Weathering Rinds

GEOLOGICAL SURVEY PROFESSIONAL PAPER 1246

Chemical Weathering of Basalts and Andesites: Evidence from Weathering Rinds

By STEVEN M. COLMAN

GEOLOGICAL SURVEY PROFESSIONAL PAPER 1246

Weathering rinds preserve a wide spectrum of uncontaminated alteration products, and allow documentation of the mineralogic and chemical changes accompanying the weathering of basalts and andesites

UNITED STATES GOVERNMENT PRINTING OFFICE, WASHINGTON: 1982

UNITED STATES DEPARTMENT OF THE INTERIOR

JAMES G. WATT, *Secretary*

GEOLOGICAL SURVEY

Dallas L. Peck, *Director*

Library of Congress Cataloging in Publication Data
Colman, Steven M.
Chemical weathering of basalts and andesites.
(Geogical Survey Professional Paper 1246)
Includes bibliographical references.
1. Basalt. 2. Andesite. 3. Weathering.
I. Title. II. Series.
QE462.B3C64 552'26 81–6803 AACR2

For sale by the Branch of Distribution, U.S. Geological Survey,
604 South Pickett Street, Alexandria, VA 22304

CONTENTS

ILLUSTRATIONS

TABLES

CHEMICAL WEATHERING OF BASALTS AND ANDESITES: EVIDENCE FROM WEATHERING RINDS

By STEVEN M. COLMAN

ABSTRACT

Weathering rinds on basaltic and andesitic stones preserve the alteration products of these lithologies under conditions that preclude detrital contamination, physical removal, and uncertainty of original composition. The mineralogy and chemistry of samples of weathering rinds on andesitic and basaltic stones from several areas with temperate climates in the Western United States were studied using a variety of analytical methods, including thin- and polished sections, X-ray diffraction, differential thermal analysis, scanning electron microscopy, X-ray energy spectrometry, and bulk chemical analysis.

Volcanic glass and olivine are the least stable phases in the rocks examined, and early stages of rind development are largely defined by oxidation colors produced by the alteration of these materials. At the other extreme are the remarkably stable opaque minerals, primarily titanomagnetites, which are commonly the only recognizable primary mineral in severely altered weathering rinds. Pyroxene and plagioclase have intermediate stabilities, which vary with the chemical composition of these minerals. Grain size, degree of fracturing, and chemical zonation of mineral grains are important controls in determining the location and severity of alteration.

The alteration processes that produce weathering rinds on basalts and andesites appear to be mostly degradational; only minor secondary mineral formation was observed. Alteration products appear to result mostly from hydrolysis, leaching, oxidation, and destruction of primary mineral structures, and the sequence from primary minerals to the most weathered products appears to be nearly continuous. The end product of the intensities and durations of weathering observed in this study is a mixture of allophane, amorphous iron oxide-hydroxide, and poorly developed clay minerals. Because many of the samples are from well-developed argillic B horizons formed in deposits more than 10^5 yr old, the poor development of clay minerals in the weathering rinds suggests that the clay minerals form more slowly than is commonly assumed and that the well-developed clay minerals in the argillic B horizons are from sources other than the weathering of primary minerals.

Chemical trends during weathering-rind formation, as indicated by several weathering indices based on molecular percentages, include large losses of bases (Ca, Mg, Na, and K), lesser depletion of SiO_2, relative concentration of sesquioxides, oxidation of iron, and incorporation of water. Absolute chemical changes are best estimated by assuming the immobility of a reference consitituent, because volume reduction apparently occurs during weathering-rind formation. Titanium appears to be the least mobile major element in the rinds, and both aluminum and iron are depleted relative to titanium. Relative elemental mobilities in the rinds are:

$$Ca \geqslant Na > Mg > Si > Al \geqslant K > Fe > Ti.$$

The rate of loss of most elements appears to decrease with time.

INTRODUCTION

Weathering rinds on andesitic and basaltic rocks are an important source of mineralogic and chemical data for the weathering of these lithologies. Most previous studies of basalt and andesite weathering have dealt with well-developed residual soils on highly altered bedrock in tropical to semitropical climates (Carroll, 1970, references, p. 179). Of the few studies in temperate climates, that by Hendricks and Whittig (1968) on andesites in northern California and that by Roberson (1963) on volcanic ash in Oregon, examined rock compositions and environments most similar to those examined in this study.

Weathering rinds offer a number of unique advantages for weathering studies. First, the parent material involved in the weathering is known with certainty. Thin-section examination confirms that weathering rinds are the altered part of the original stones and that the rinds contain no detrital contamination. This relation usually cannot be demonstrated for residual soil profiles. The fresh rock, the altered rock forming the rind, and the soil matrix are easily differentiated.

Second, because weathering rinds on basalts and andesites are cohesive, and because they were sampled from below the ground surface, material can be removed from the weathered stone only in solution; physical erosion of the weathered material does not affect comparisons among samples.

Finally, weathering rinds contain the products of all stages of weathering, both in the transition from the altered rind to the fresh core of a single stone and in stones that have been subjected to weathering for different lengths of time. In contrast, well-preserved residual soils of a wide spectrum of ages on a single lithology are uncommon.

This report is divided into two sections, based on the mineralogic and the chemical changes that occur during weathering-rind formation. The mineralogic section examines various stages of mineral alteration, identifies secondary weathering products, and documents primary mineral stabilities. The chemical sec-

tion assesses bulk chemical changes accompanying weathering and relative elemental mobilities.

A companion report (Colman and Pierce, 1981) describes in detail the sample sites and their geology and contains detailed descriptions of the sampling methods and other background information.

METHODS

SAMPLING PROCEDURES

Weathering rinds were sampled on stones from within soil profiles at depths of about 20–50 cm. This interval represents the upper part of the B horizon for the soils sampled, or the upper part of the C horizon where a B horizon was not developed; it was selected because that part of the profile is the most weathered. Between 30 and 60 stones were sampled at each site for measuring weathering-rind thicknesses (Colman and Pierce, 1981); of these, several stones having approximately the average rind thickness for the site were selected for the mineralogical and chemical analyses reported here.

Deposits sampled were primarily till, outwash, or fluvial gravels. Sampling sites on these deposits were located where the land surface has been most stable. Most sampling sites were located on broad moraine crests or on terrace surfaces where disturbance of the weathering profile by erosion or by colluvial or eolian deposition has been negligible.

General sample localities and descriptions are given in figure 1 and table 1; detailed sampling methods and site descriptions and localities are discussed in Colman and Pierce (1981).

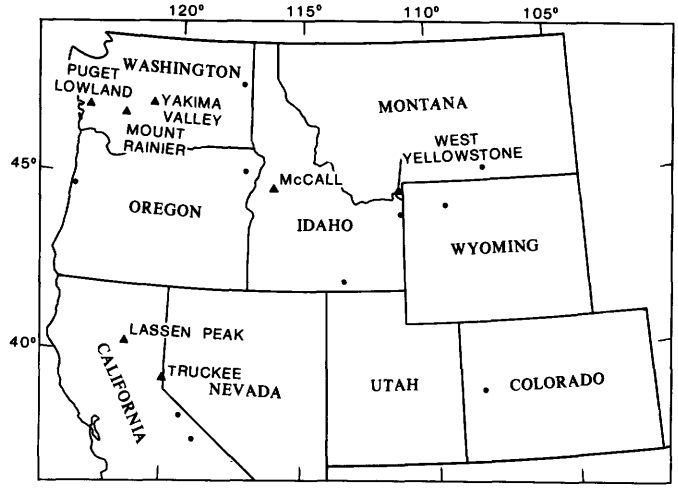

FIGURE 1.—Index map of sample localities. Labeled triangles are areas for which analytical data for weathering-rind samples are presented here. Circles are other localities where weathering-rind thicknesses were measured (Colman and Pierce, 1981).

TABLE 1.—*General description of samples*

[For detailed descriptions of sample localities, see Colman and Pierce (1981, appendixes 1 and 2). All deposits are till, except for Thorp (outwash(?) gravels) and Logan Hill (genesis uncertain)]

Sample No.	Area	Rock type	Deposit
98	West Yellowstone	Basalt	Pinedale.
95	—do—	—do—	Bull Lake.
102	—do—	—do—	Do.
105	McCall	—do—	Pinedale.
104	—do—	—do—	Bull Lake.
109	—do—	—do—	Do.
119	Mt. Rainier	Andesite	Evans Creek.
120	—do—	—do—	Hayden Creek.
121	—do—	—do—	Wingate Hill.
118	—do—	—do—	Logan Hill.
84	Lassen Peak	—do—	Tioga.
89	—do—	—do—	Early Tioga.
85	—do—	—do—	Tahoe.
86	—do—	—do—	Pre-Tahoe.
75	Truckee	—do—	Tioga.
83	—do—	—do—	Tahoe.
79	—do—	—do—	Donner Lake.
134	Yakima Valley	Basalt	Indian John.
135	—do—	—do—	Swauk Prairie.
140	—do—	—do—	Thorp.

ANALYTICAL PROCEDURES

Mineral alteration was studied using a variety of analytical tools, including: (1) microscopic examination of thin and polished sections, (2) X-ray diffraction (XRD), (3) differential thermal analysis (DTA), (4) scanning electron microscopy (SEM), and (5) X-ray energy spectrometry (XES).

About 55 thin sections were examined with transmitted light, and many of these also were polished and examined with reflected light in oil immersion. Weathered portions of the rocks were impregnated with polymerized methyl methacrylate (Plexiglas), and so the thin sections contained both the unaltered rock and the undisturbed weathering rind.

About 30 samples of the clay-size fraction of weathering rinds, along with 30 samples of the associated soil matrices, were examined by XRD using Ni-filtered CuKα radiation. Several replicate sets of samples were prepared: One set was mixed with a dispersing agent (sodium pyrophosphate); another set was mixed with the dispersing agent and placed in an ultrasonic bath for 30 minutes. Selected samples of the second set also were treated with a dithionite-citrate-bicarbonate solution to remove free iron (Mehra and Jackson, 1960). The clay-size fractions (< 2 μm) of all samples were separated by sedimentation and were oriented by evaporation onto warm ceramic tiles.

Nineteen of the clay-size samples prepared for XRD and 14 of the thin sections (etched with HF) were ex-

amined under the SEM, after being coated with an Au-Pd conductor. While the morphology of these samples was examined under the SEM, semiquantitative elemental chemical analyses were obtained by XES. XES data for individual elements were also obtained in the form of line scans and abundance maps.

Chemical analyses of the weathering rinds and of the associated fresh rocks were made by laboratories of the U.S. Geological Survey. Where the thickness of the weathering rind permitted, samples for chemical analysis were obtained from several layers of the rind. Most samples were analyzed by "rapid-rock" (wet-chemical) methods, but a few were analyzed by a combination of X-ray fluorescence (XRF) and atomic absorption (AA) techniques.

Differential thermal analysis (DTA) was performed on the samples in an oxygen atmosphere. Precalcined alumina, which was used as the inert material, was heated along with the samples at a rate of 10°C/min.

MINERALOGIC ALTERATIONS IN BASALT AND ANDESITE WEATHERING

Several topics will be discussed in this section, including: (1) stages of mineral alteration, (2) products of weathering, (3) relative stabilities of primary minerals, (4) relation of weathering stages to time, and (5) relation between weathering and soil clay-mineral formation. These closely related topics are difficult to discuss separately. Because all conclusions concerning the weathering of basalts and andesites are based on data and observations for individual minerals, the details of the stages and products of the alteration of each major mineral group will be discussed first.

STAGES AND PRODUCTS OF MINERAL ALTERATION

GENERAL OBSERVATIONS

This section is a combined discussion of the observed sequence of events that occurred during the weathering of each of the major minerals in basalts and andesites and of the resulting weathering products. The observed alterations appear to be due almost entirely to the degradation of the primary minerals, rather than to the formation of distinct new mineral species. Early alteration products appear to result from the destruction of the primary mineral structure, but some crystallinity is preserved and most of the products are in optical continuity with remnants of the primary mineral. As the intensity or duration of weathering increases, the products become finer grained and less crystalline and lose this optical continuity. Chemical data, discussed in detail in a later section, indicate continuous depletion of all elements (except perhaps titanium) relative to the amounts in the unaltered rock.

Alteration appears to proceed more rapidly in the fine-grained matrix than in the phenocryst grains, presumably because of the larger surface area of the matrix constituents. However, where large phenocrysts have abundant fractures, localized weathering along the fractures may alter them more rapidly than it would alter smaller, less fractured minerals. Regardless of grain size, however, early stages of alteration are mostly localized along grain boundaries and fractures. Exceptions are glass and some pyroxene grains, which commonly display uniform alteration throughout, although most pyroxenes are preferentially altered along grain margins and fractures.

Control of weathering by mineral structure was not observed. The cockscomb terminations of weathered pyroxene and amphibole, which are often observed in sediments and soils (Birkeland, 1974, p. 160) and in volcanic ash (Hay, 1959, pl. 2), were not found in basalts or andesites in this study. The absence of these features may be due to the fact that most weathered minerals in rinds are encased in a rim of their alteration products. The boundary between the mineral and the alteration product commonly is smooth and regular.

Compositional variation in minerals appears to affect the location and the rate of weathering. Many of the rocks examined contain plagioclase that has normal, reversed, or oscillatory zonation; the more calcic zones in these minerals altered first and more rapidly. In pyroxenes, varying degrees of alteration due to compositional variation were only rarely observed. Compositional zonation in olivine, if present, did not affect the location or the rate of weathering.

As time passes or as weathering becomes more severe, minerals become encased in an increasingly thick sheath of weathering products. Hence, in time this sheath may impede the movement of weathering solutions to and from the remnants of primary minerals. In extremely weathered portions of some weathering rinds, nearly fresh remnants of primary minerals appear to be protected in this manner by sheaths of weathering products.

Examples of the preceding general observations are given in the next section.

WEATHERING STAGES FOR INDIVIDUAL MINERALS

The products of weathering described here primarily result from degradational rather than from formative processes. Therefore, they do not have distinct crystal

structures or readily determinable properties, and few have been described in the literature as distinct species. For this reason, weathering products are given arbitrary symbols such as 2a, 3c, and 5, and will be referred to as such. The descriptive properties of each weathering product are based on thin-section examinations, SEM-XES data, and XRD data (table 2).

The numbering scheme for weathering products (table 2) is based on the division of the products for each mineral (or glass) into stages (table 3). The stages are arbitrary, and are abstractions of the sequence of alteration of each mineral; the stages are numbered from I for the unaltered mineral to V for the completely weathered product. Because the stages are defined *for each mineral*, a given stage of weathering for one mineral is not necessarily associated either in time or in space with that same stage of a different mineral. For example, olivine stage IV (product 4a) is commonly found in less weathered portions of rocks than is plagioclase stage IV (product 4b). These mineral weathering stages are arbitrary; they serve only to organize the descriptions of the weathering products and to facilitate comparisons.

END PRODUCTS OF WEATHERING

The fate of all minerals in the weathering observed in the rinds is weathering product 5 (table 2). Different minerals approach product 5 through different series of weathering products, but eventually, all vestiges of the primary mineral structure are lost; this loss results in the fuzzy, indistinct masses of product 5. Considerable data were gathered on the properties of product 5, and it will be discussed first and in detail prior to discussing the sequence of other weathering products for each mineral phase.

Weathering product 5, which is very hydrated and X-ray amorphous, is composed primarily of Si, Al, and Fe; it has some Ti and little if any bases (Mg, Ca, Na, and K). Abundant oxidized iron imparts a reddish to yellowish-orange color to product 5; the Munsell colors of the dry, pulverized outer portions of rinds that contain abundant product 5 are typically 10*YR* 6/5 to 5/4.

Weathering product 5 constitutes the major portion of the clay-size fraction of the weathering rinds; the clay-size fraction is significant in many rinds, especially in those from deposits older than about 10^5 yr. Although no quantitative data were collected on the proportion of clay-size material in the rinds, it appears to increase with time.

XRD data indicate that the clay-size fraction of weathering rinds is X-ray amorphous (fig. 2). In contrast, samples of the soil matrix immediately adjacent to the rinds have well-defined clay-mineral peaks on X-ray diffractograms (fig. 2). Some very highly weathered portions of weathering rinds from old deposits show broad, ill-defined diffraction bands around 7 to 8 Å, suggesting possible incipient halloysite formation. The absence of clear X-ray clay-mineral peaks for weathering-rind samples was quite unexpected, and repeated attempts using a variety of sample preparations (section on "Analytical procedures"), including citrate-dithionite iron removal, failed to produce clay-mineral peaks on X-ray diffractograms of rinds. Identical techniques produced well-defined clay-mineral peaks for samples of adjacent soil matrices. The X-ray-amorphous character of the clay-size fraction of weathering rinds is supported by the few XRD observations that have been previously made for rinds. Crandell (1963) did not find XRD evidence of clay minerals in weathering rinds on andesites from Wingate Hill deposits near Mt. Rainier; Birkeland (written commun., 1976) also obtained negative XRD results for weathering rinds on andesites from Donner Lake deposits near Truckee.

XRD data were also collected for randomly oriented powders of some of the rinds. A few of the diffractograms showed a very small, poorly defined peak at about 19.9° 2θ. This peak might represent the 4.45 Å peak caused by diffraction off the (110) spacing of layer silicates. However, the poor definition of this peak makes such a conclusion tenuous.

The presence of abundant X-ray-amorphous, clay-size material in the weathering rinds immediately suggests that a major portion of this material is allophane. This term has been commonly applied to such material since Ross and Kerr (1934) originally defined allophane as "amorphous [to X-rays] material composed of variable amounts of silica, alumina, and water." Since then, much work has shown that allophane has distinct but variable X-ray, morphological, chemical, infrared absorption, and differential thermal properties. Much of this work is summarized by Fieldes (1966) and Fieldes and Furkert (1966). Depending on composition, allophane properties vary considerably (Fieldes, 1966), and the continuous series from completely amorphous Si-Al gels to well-crystallized kaolin minerals has been divided into as many as four intermediate stages: allophane B ("pro-allophane"), allophane A, "imogalite" B, and "imogalite" A (Tan, 1969).

In addition to the X-ray-amorphous character of the clay-size fraction of weathering product 5, its morphology suggests a major allophane component. The morphology of the clay-size fraction of weathering rinds, as determined under the SEM, consists of irregular, spongelike masses and globules (fig. 3). These observations are similar to those made for allophane

TABLE 2.—*Weathering products observed in andesites and basalts*

Symbol	Properties				Tentative identification
	Plane light	Crossed polarizers	Principal elements from XES[1]	Clay-size XRD[2]	
1	Unaltered	Unaltered	Variable	—	Fresh mineral.
2a	Clear, brown to yellow to orange.	Optically isotropic	---do	—	Stained glass.
2b[3]	Translucent, yellow to reddish brown; around olivine boundaries and fractures.	Yellowish, microcrystalline, in colloform bands, simultaneous to undulatory extinction.	Si, Mg, Fe	—	"Iddingsite."
2c[3]	Opaque.	Opaque	Fe	—	Fe-oxides.
2d	Clear, yellow-green.	Very fine grained, normal extinction.	Si, Al, Fe (Ca, Mg, Na, K).	—	Chlorophaeite or chlorite.
2e[3]	Speckly yellow, around plagioclase boundaries and fractures.	Microcrystalline, speckled, normal extinction.	Si, Al, Ca (Na, Mg, Fe).	—	Unknown.
3a	Clear, yellow to yellow-green.	Microcrystalline, speckled to fibrous, sometimes radiating, normal extinction.	Si, Al, Fe (Ca, Mg, Na, K).	—	"Altered chlorophaeite."
3b	Clear to translucent, yellow to orange.	Microcrystalline, speckled to fibrous, vague undulatory extinction.	Si, Al, Fe (Ca, Mg).	Amorphous	Palagonite(?).
3c	Massive, clear to gray	Microcrystalline, very low birefringence, normal extinction.	Si, Al, Ca (K, Mg, Fe, Na).	—	Unknown.
4a	Clear to translucent, orange to red.	Massive, vague undulatory extinction.	Fe, Al, Si	Amorphous	Unknown.
4b	Massive, clear to gray	Massive, optically isotropic	Si, Al, Ca (Fe).	Amorphous	Allophane.
4c	Opaque, white (light bluish gray) in reflected light.	Opaque	Fe	—	Hematite (maghemite).
5	Gray- to reddish-brown, indistinct masses.	Indistinct masses, does not go to extinction.	Si, Al, Fe (Ti).	Amorphous	Allophane and iron oxide-hydroxide.

[1]( ), elements present in subordinate amounts.

[2]X-ray diffraction (XRD) patterns determined for the clay-size fraction of the weathering rinds showed all such material to be X-ray amorphous. Weathering products larger than clay-size are shown as leaders (—); where it is uncertain whether the material was of clay size or larger, the entry is queried.

[3]These products result from the alteration of only part of the original mineral, commonly along grain boundaries and fractures; alteration proceeds inward from these zones toward the core.

TABLE 3.—*Mineral-weathering stages and weathering products*

[( ), product commonly absent; leaders (—), not observed]

Mineral[1]	Stages				
	I Fresh mineral[2]	II Slightly weathered	III Moderately weathered	IV Extensively weathered	V Completely weathered
Glass	1, (2a)	(2a), (2d)	3a, 3b	4a	5
Olivine	1, 2b	2b	—	4a	5
Pyroxene	1	(2c), 2d	3a, 3b	(4a)	5
Plagioclase	1	2e	3c	4b	5
Amphibole	1, 2c	1, 2c	2c, 3b	—	2c, 5
K-feldspar	1	—	3c	—	5
Opaques	1	—	—	4c	5

[1]Includes mineraloids (glass, some opaques).

[2]Fresh minerals, those found in the unweathered core of the rock, may include products of deuteric alteration, such as Fe-oxides and "iddingsite".

by Hay (1960), DeKimpe and others (1961), Bates (1962), Aomine and Wada (1962), Roberson (1963), and Wada (1967). No evidence was observed of the long, threadlike forms of "imogalite" (Wada, 1967; Yoshinaga and others, 1968), the tubelike forms of halloysite (Grim, 1968, p. 168), nor the hexagonal forms of kaolinite (Grim, 1968, p. 171).

A chemical test for the presence of allophane was developed by Fieldes and Perrott (1966). The method is based on the fact that aqueous solutions of fluoride react with the hydroxy-aluminum sites in certain types of materials, including cracking catalysts and allophane; this reaction causes the release of hydroxide ions and an increase in pH. Fieldes and Perrott (1966)

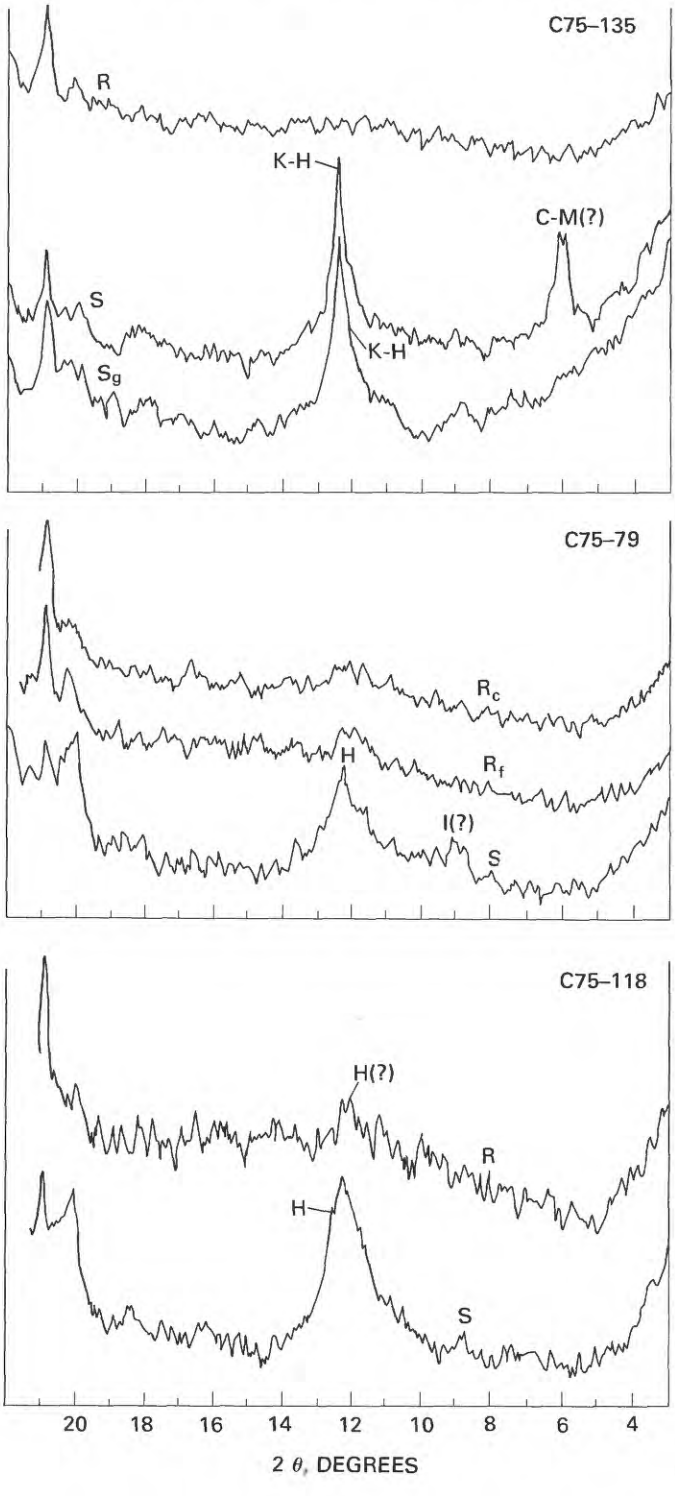

FIGURE 2.—Typical X-ray diffractograms of the clay-size fraction of weathering rinds and of associated soil matrices. Numbers in upper right corner are sample numbers. R, weathering rind; c, coarse-grained rock type; f, fine-grained rock type; S, soil matrix; g, glycolated; K, kaolinite; H, halloysite; C, chlorite; M, smectite (montmorillonite(?)); I, illite. Ni-filtered CuKα radiation. Peaks above 20° are from the ceramic sample holder.

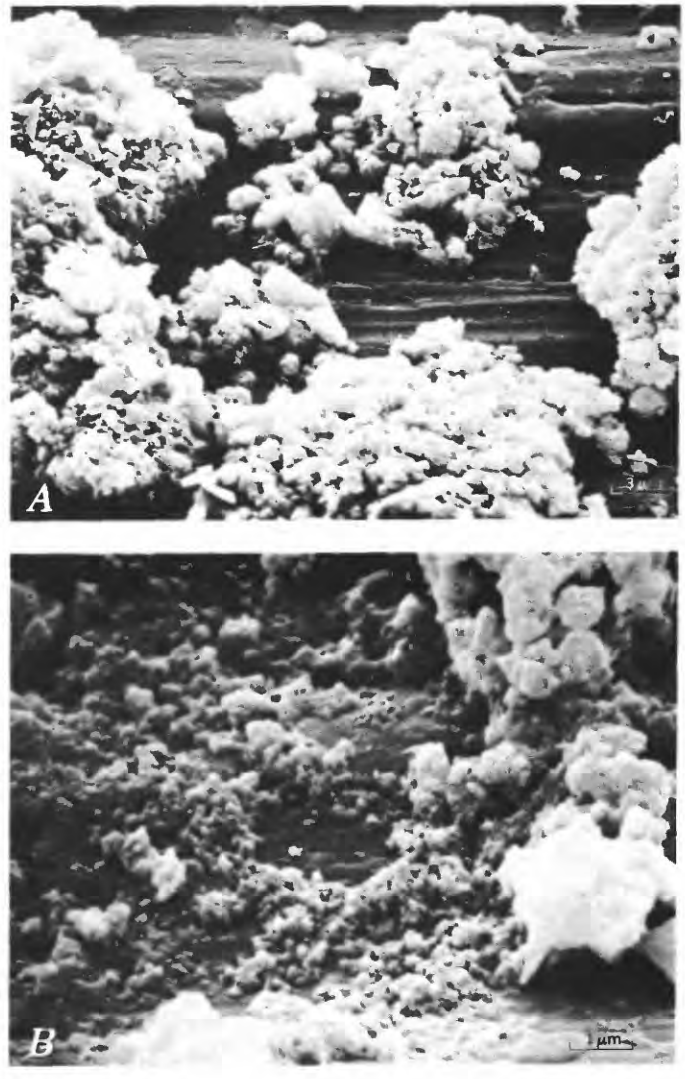

FIGURE 3.—SEM photomicrographs of samples of the clay-size fraction separated from weathering rinds. *A*, sample 140; *B*, sample 79. This material is mostly weathering product 5 (table 2). Note the irregular, spongelike masses and globules. Background is the metal surface of the sample holder.

found that by using suitable NaF and soil solutions, the pH of allophanic soils subjected to the treatment rose rapidly, generally to more than 9.0, but the pH of soils without allophane generally remained below 8.0. Results of the fluoride test on samples of weathering rinds and on the associated soil matrices (table 4) indicate the presence of allophane in all samples tested. The rapid rise in pH to values considerably above 9.0 in some samples suggests abundant allophane.

The only convincing evidence of clay minerals in weathering rinds is found in differential thermal analysis (DTA) data (fig. 4). In general, DTA profiles of the clay-size fraction of weathering rinds have the follow-

TABLE 4.—*pH results of NaF test for allophane*

[Results are for samples weighing about 2 g in 100 mL of 1M NaF solution (pH 7.5), except for the 1:1 soil-water mixtures. Clay-size fraction of outer weathering rind is mostly weathering product 5]

Sample No.	Soil matrix				Clay-size fraction of outer weathering rind		
	1:1 soil-water	After 10 min	After 30 min	After 75 min	After 10 min	After 30 min	After 75 min
118	5.5	8.9	9.0	9.2	8.4	8.9	9.1
120	5.4	8.7	9.1	9.2	8.2	8.7	8.7
121	5.6	9.0	9.1	9.2	8.4	8.8	8.8
102	5.7	8.9	9.0	9.3	9.1	9.1	9.1
105	6.1	8.7	9.2	9.2	8.9	9.5	9.5
109	5.6	9.0	9.2	9.2	9.0	9.1	9.2
86	6.1	9.1	9.4	9.6	9.4	9.8	10.3
79	6.4	9.0	9.4	9.5	9.0	9.1	9.2
134	6.2	8.9	9.0	9.0	8.3	8.4	8.5

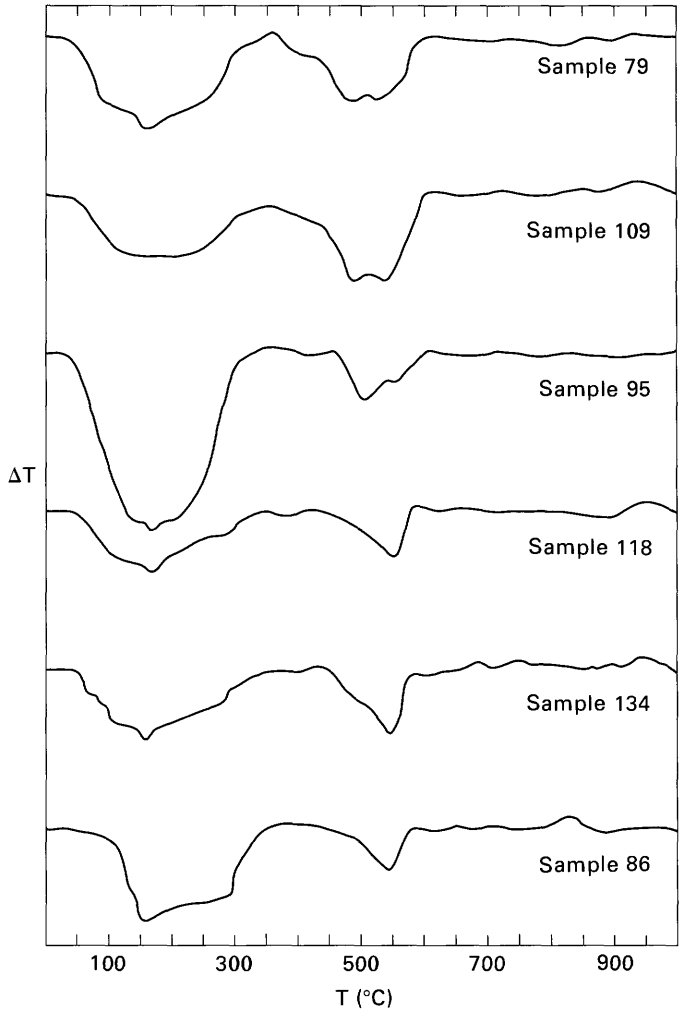

FIGURE 4.—Differential thermal curves for samples of the clay-size fraction of weathering rinds. Sample numbers for curves are given at right. Vertical scale is relative.

ing features: (1) A large, broad, complex endothermic peak occurs between about 50°C and 350°C. This peak commonly is centered at about 160°C and (or) has an additional individual peak at about 160°C. (2) A moderately sharp endothermic peak of variable size occurs at about 540°-560°C. This peak commonly includes a secondary peak, or at least a shoulder, at about 480°-490°C. (3) A slightly variable, but generally featureless curve occurs above 570°C, and commonly has a weak exothermic peak at about 935°-940°C.

The broad, low-temperature endothermic peak is characteristic of allophane (Holdridge and Vaughan, 1957). This peak is due to the low-temperature loss of weakly held water; the average peak temperature for allophane is 160°C (Holdridge and Vaughan, 1957, table 5).

Endothermic peaks between 400°C and 650°C are characteristic of clay minerals, but identification of individual minerals from DTA data is difficult, especially for mixtures of clay minerals. The 540°-560°C peak is slightly low for typical halloysite (Holdridge and Vaughan, 1957, table 5), but some mixtures of dioctahedral smectites and kaolin minerals have DTA curves similar to those in figure 4 (Greene-Kelly, 1957). The exothermic peak between 900°C and 950°C is characteristic of allophane and of a variety of clay minerals.

Elemental X-ray energy spectrometry (XES) obtained on the SEM for samples of the clay-size fraction of the weathering rinds (fig. 5) indicates that Si, Al, and Fe are the principal elements in the clay-size fraction. The small amounts of Ti and bases (Mg, Ca, Na, and K) present are probably from small remnants of primary minerals in the clay-size fraction. XES data

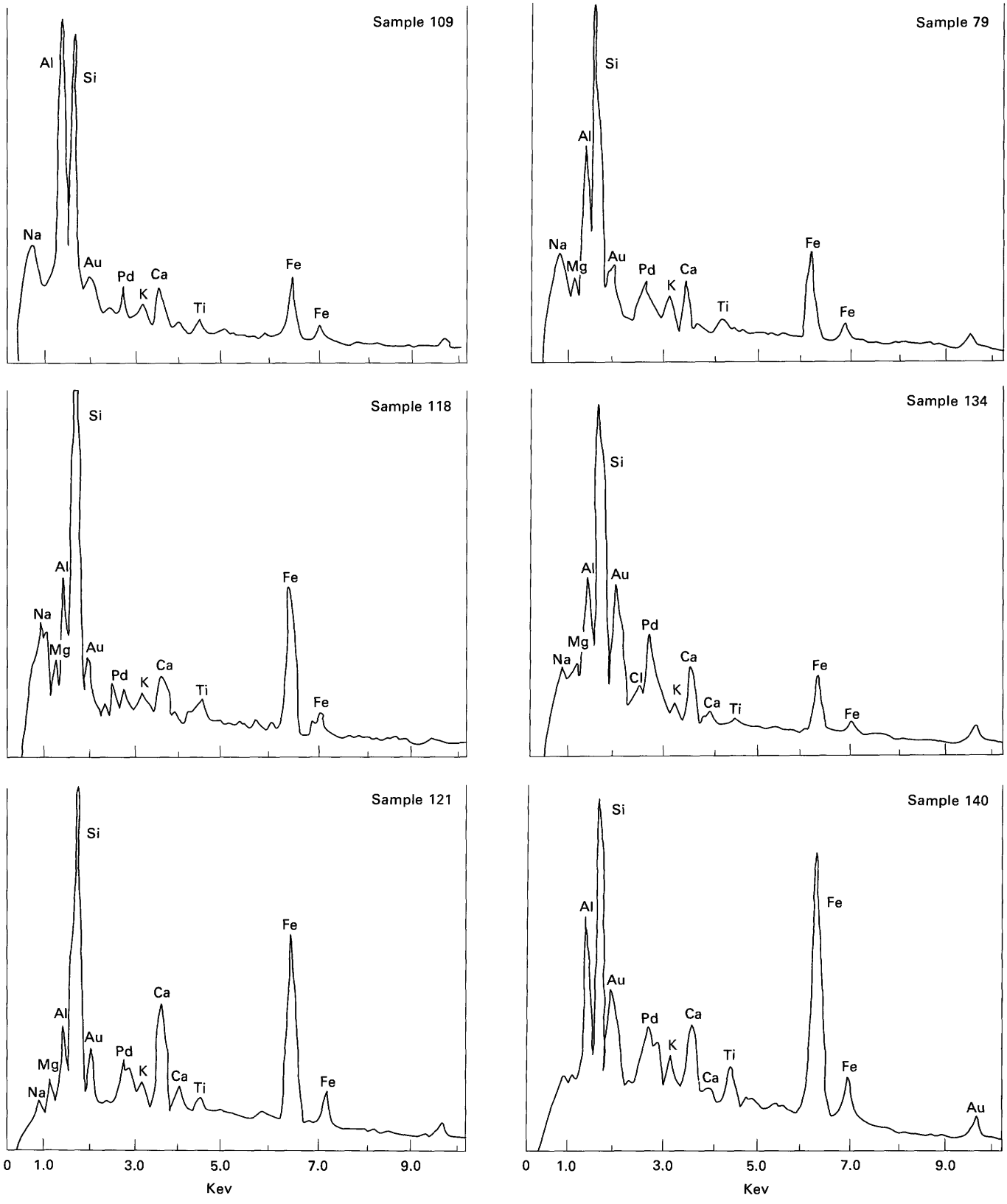

FIGURE 5.—X-ray energy spectrometry for samples of the clay-size fraction of weathering rinds. This material is mostly weathering product 5. Peak heights indicate relative abundance. Au and Pd are from the conductive sample coating; some Na is from the dispersing agent, sodium pyrophosphate. Sample numbers are given at right.

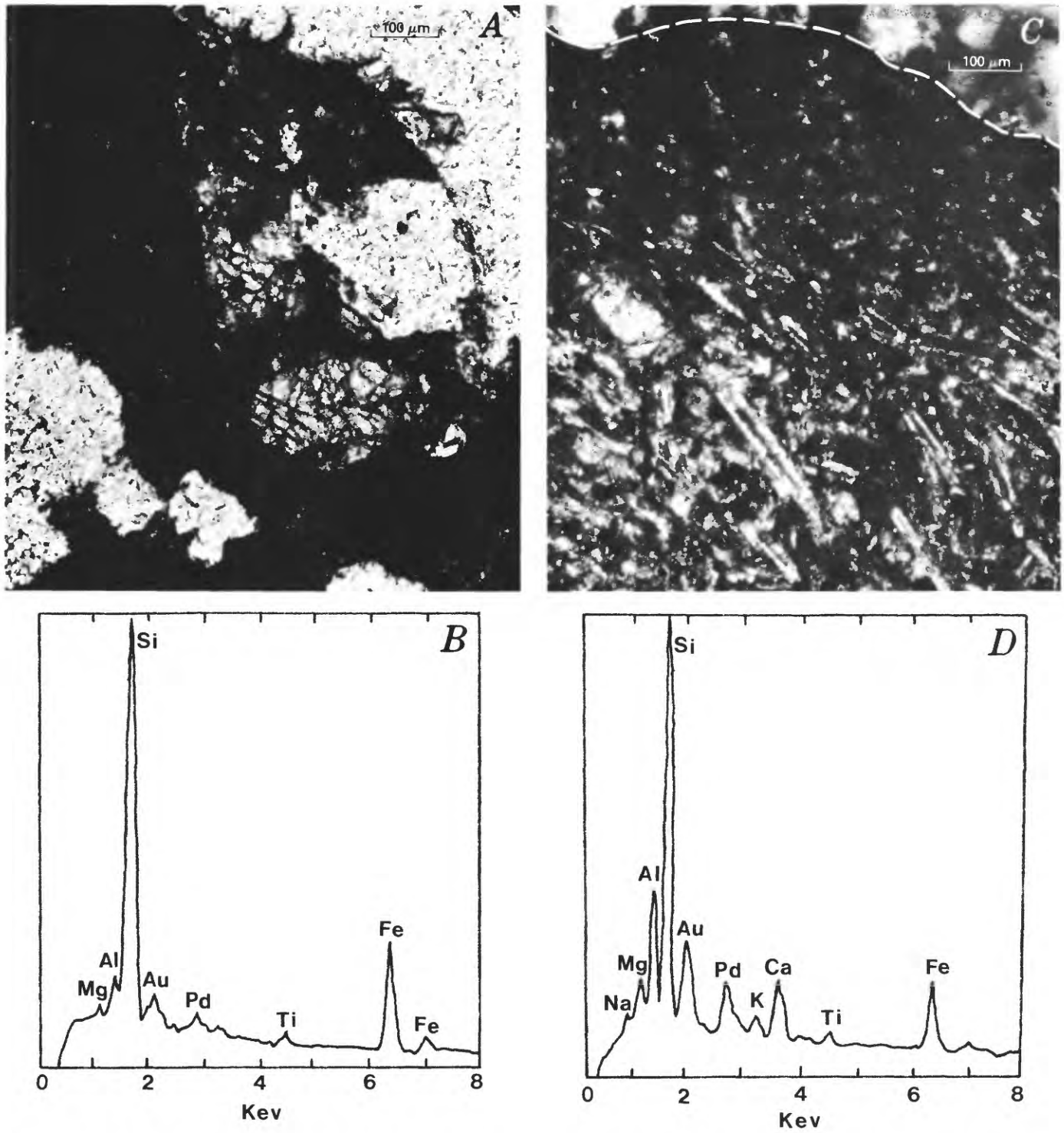

FIGURE 6.—Photomicrographs and XES data for weathering product 5. Au and Pd are from the conductive sample coating. *A*, Photomicrograph (plane light) of andesite matrix weathered mostly to product 5 (dark). Sample 118–a. *B*, XES data for product 5 in *A*; note low Al content. Peak heights indicate relative abundance. *C*, Photomicrograph (crossed polars) of basalt, altered mostly to product 5 below stone surface (dashed line). Sample 135–a. *D*, XES data for product 5 in *C*. Peak heights indicate relative abundance.

for in-place product 5 (fig. 6) indicate the presence of only minor amounts of bases, and the low concentration of Al in some samples (fig. 6) suggests depletion of this element.

The predominance of Si and Al in the clay-size fraction is consistent with the presence of abundant allophane. XES data demonstrate that Fe is also an abundant element in the clay-size fraction. Although

XRD and DTA data do not show evidence of secondary iron minerals, the Fe in the clay-size fraction of rinds may occur as very fine grained or poorly crystalline minerals.

In summary, weathering product 5 comprises most of the clay-size fraction of weathering rinds; it is composed mostly of allophane, and of lesser amounts of iron oxide-hydroxides and poorly developed clay minerals. The poor development of clay minerals may be due either to (1) very fine grain size, (2) poor crystallinity, or to (3) very low concentrations, but likely results from all three conditions. The clay minerals present are X-ray amorphous and yield only moderately defined DTA peaks. Together the XRD, DTA, SEM, and chemical data suggest not only that the clay minerals are a minor constituent of weathering rinds, but also that they are very fine grained and poorly crystalline. Allophane-rich weathering product 5 appears to be the end product of the intensities and durations of weathering observed in this study.

DESCRIPTIONS OF THE ALTERATION OF INDIVIDUAL MINERALS

ALTERATION OF GLASS

Glass is an abundant constituent of most of the rocks sampled in this study (Appendix 1); it is also the least stable. Evidence of altered glass in the otherwise unaltered part of a few of the rocks suggests deuteric alteration. In weathering rinds from young deposits (about 20,000 yr old or less), alteration of glass and olivine is primarily responsible for the discoloration that defines the weathering rind.

In the early stages of weathering, glass shows a variety of weathering products. Alteration generally proceeds throughout the entire mass, but some glass alters inward from edges and fractures. Alteration of some glass produces only stained glass (product 2a), which results from the yellow, orange, or brown colors produced by iron oxidation. Product 2a is identical in every other respect to the unaltered glass.

In other samples, the glass alters to a clear, yellow-green material that is very fine grained; it shows normal extinction under crossed polars (product 2d). This material is very similar to chlorophaeite as defined by Peacock and Fuller (1928), although it resembles chlorite in a few samples. XES data for this material (fig. 7), compared with that for the unaltered glass in the core of the rock, suggest little or no leaching of major elements. Further alteration of the chlorophaeite to a more yellow material suggests some oxidation of iron;

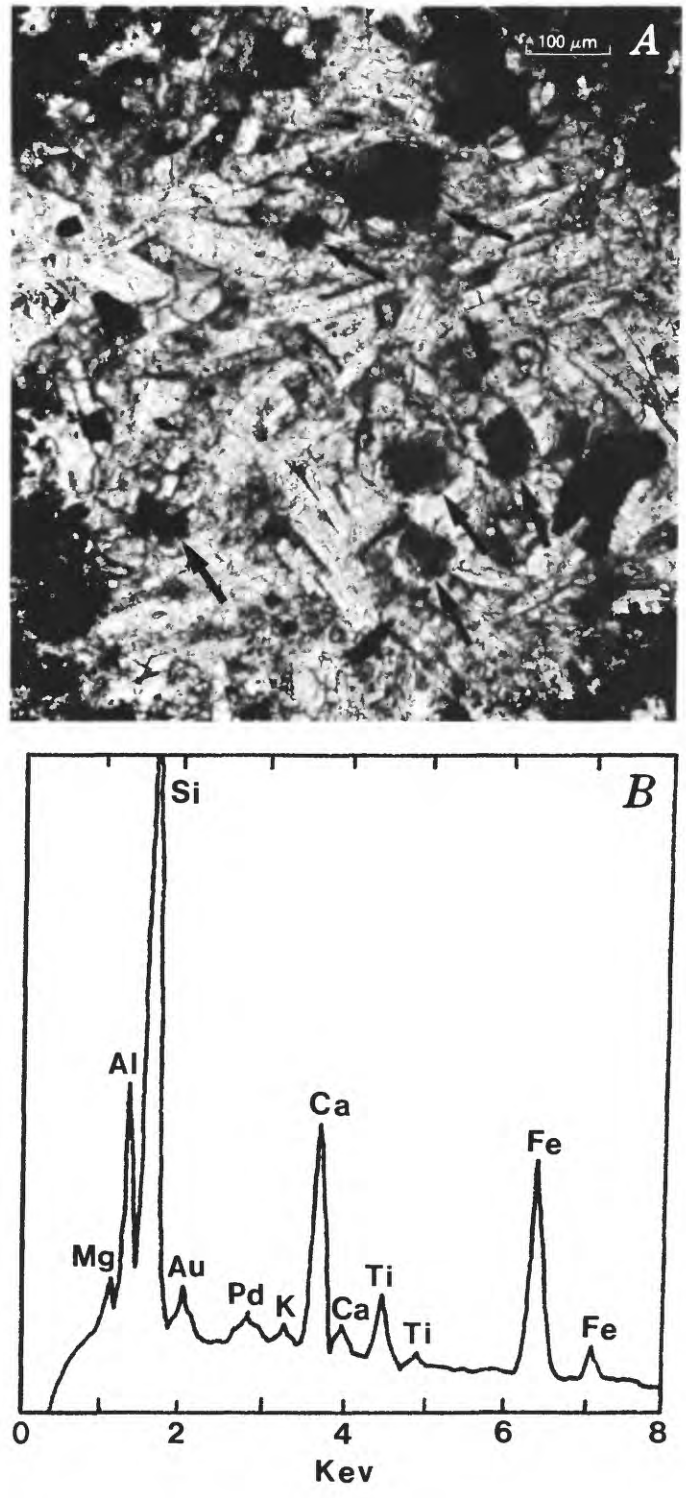

FIGURE 7.—Photomicrograph and XES data for glass altered to chlorophaeite (weathering product 2d). *A*, Photomicrograph (plane light) of altered glass (arrows). *B*, XES data for one of the glass grains marked in *A*. Au and Pd are from the conductive sample coating. Peak heights indicate relative abundance.

under crossed polars this material appears speckly to fibrous. These changes suggest increased alteration, but because the resulting material (product 3a) probably still fits the definition of chlorophaeite, it is called "altered chlorophaeite" here.

Because the altered glass eventually becomes yellow-orange and is commonly translucent, continuing oxidation of iron is suggested. This material (product 3b) is speckly to fibrous under crossed polars, but shows weak undulatory extinction throughout the grain. Product 3b was probably included in the X-ray samples of the clay-size fraction of the weathering rinds and hence is amorphous to X-rays. Product 3b appears to fit the descriptions of palagonite, as defined by Peacock and Fuller (1928) and Hay and Iijima (1968).

Continued alteration of product 3b produces a material that is redder and more translucent (product 4a). Under crossed polars this material is no longer fibrous or speckly, but is massive and shows vague, undulatory extinction. XES data (fig. 8) for product 4a suggest a loss of silica and bases (Mg, Ca, Na, and K) and a concentration of iron. Product 4a was probably included in the X-ray samples of the clay-size fraction of the weathering rinds and is therefore X-ray amorphous. A description of a distinct species with properties similar to those of product 4a was not found in the literature. Product 4a eventually alters to product 5.

ALTERATION OF OLIVINE

Olivine, like glass, is one of the least stable constituents of the rocks examined in this study, and, in some rocks, it shows evidence of deuteric alteration. Olivine was always observed to alter first along grain fractures and around margins. Inward from these zones toward the cores of olivine, unaltered remnants persist for long periods of time considering the initial instability of olivine. Compositional zonation, if present, had no observable effect on the alteration.

The initial weathering product formed around the edges and along the fractures of olivine grains is translucent and yellowish to reddish brown (product 2b). Under crossed polars it is yellowish and microcrystalline and shows simultaneous to undulatory extinction; XES data (fig. 9*C*) indicate that it is composed primarily of Si, Mg, and Fe. Product 2b is "iddingsite," as defined by Gay and LaMaitre (1961).

"Iddingsite" can apparently form without losing much of the major elements present in the unaltered mineral. Oxidation of iron and destruction of the olivine structure are evident in thin section in the formation of "iddingsite" (fig. 9*A*), but XES data for some samples indicate little or no differential loss of Si or Mg (fig. 9*B*). In other examples of the alteration of olivine to "iddingsite" (fig. 10), significant depletion of Si and Mg has occurred along fractures, and some of these elements have been depleted along the grain margins (fig. 10*B*).

As weathering increases, "iddingsite" becomes redder and massive and shows vague, undulatory extinction under crossed polars. It appears to alter to weathering product 4a and then to weathering product 5.

ALTERATION OF PYROXENE

Pyroxene appears to weather through a series of products very similar to those described for glass. Like glass, some pyroxenes are weathered throughout the grain; however, other pyroxenes weather progressively inward from grain edges and fractures. In addition, some alterations of pyroxene produce finely disseminated opaque grains, presumably iron oxide. Pyroxene initially alters directly to product 2d (chlorophaeite) along grain edges and fractures, or to product 3b throughout the grain. From there, alteration proceeds through the same sequence as that outlined for glass (2d→3a→3b→4a→5).

XES line scans for Ca, Mg, and Si on pyroxene grains weathered along fractures and edges (fig. 11) show concordant, localized decreases in abundance of these elements, whereas line scans for Fe (fig. 11) are discordant with those of other elements. These data suggest that Ca, Mg, and Si are lost along grain fractures and margins, but that most Fe remains immobile. In contrast, pyroxenes that are altered mostly to product 3b throughout the grain (fig. 12) show little if any localized depletion of Ca, Mg, Si, or Fe. This alteration appears to be due primarily to the disintegration of the pyroxene structure and to the discoloration caused by iron oxidation.

ALTERATION OF PLAGIOCLASE

The weathering of plagioclase is controlled by primary chemical zonation and by fractures and grain boundaries. Much of the plagioclase examined, especially phenocrysts in andesite, is compositionally zoned, and the zoning may be either normal, reversed, or oscillatory. It appears that the more calcic zones, most of which are in the cores of the plagioclase grains, are more susceptible to alteration than are the less calcic zones. Plagioclase alteration is also concentrated along

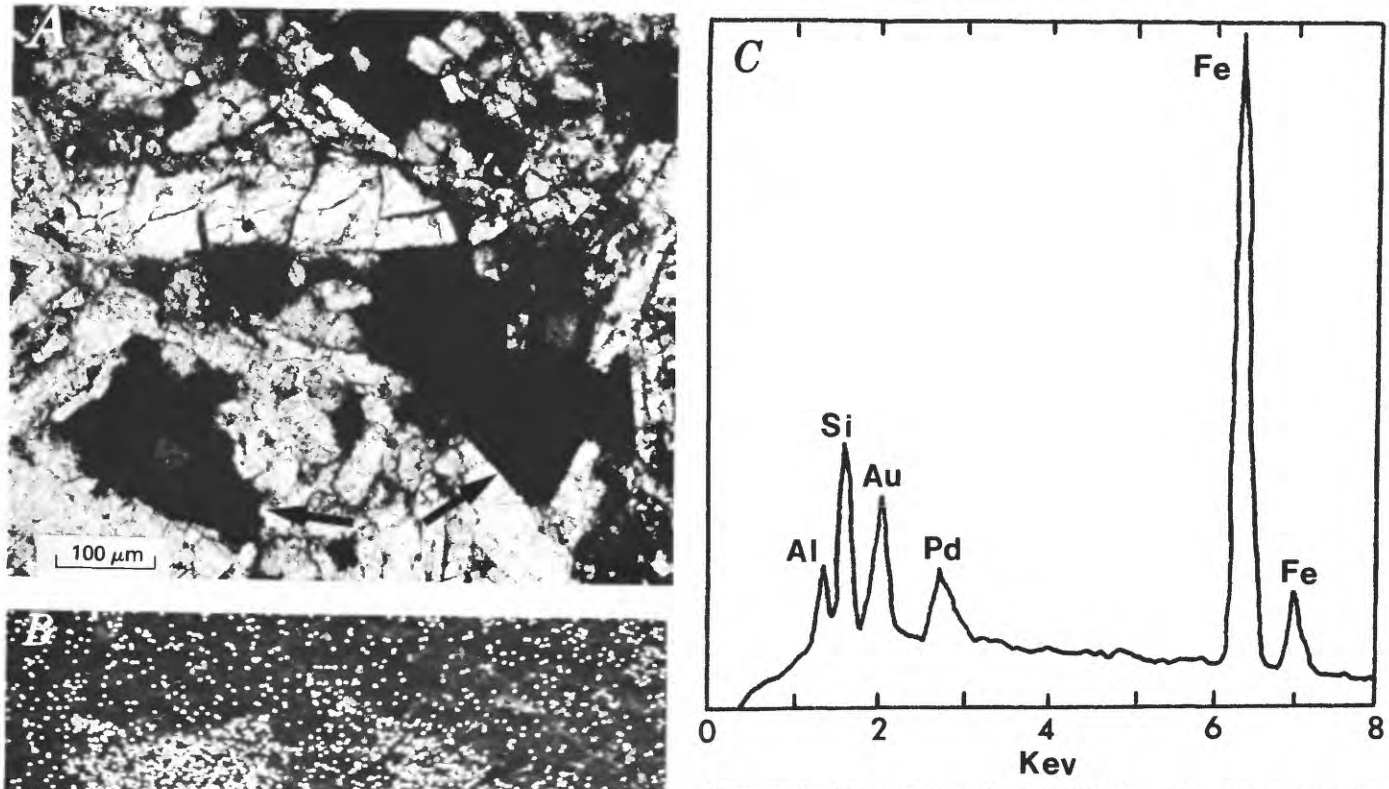

FIGURE 8.—Photomicrograph and XES data for glass altered to weathering product 4a. *A*, Photomicrograph (plane light) of two large glass grains (arrows) stained by iron oxidation. *B*, XES dot map of iron for the two altered glass grains in *A*. Density of dots is proportional to iron concentration. *C*, XES data for glass grain on right in *A*. Au and Pd are from the conductive sample coating. Peak heights indicate relative abundance.

grain fractures and boundaries. In no sample does plagioclase show uniform, or nearly uniform, weathering throughout the grain.

The initial weathering product of the alteration of plagioclase is a yellow, speckly material (product 2e); it is microcrystalline and speckly and has normal extinction under crossed polars. This material is found along grain fractures and boundaries, or in the most calcic zones of the mineral grain. XES data (fig. 13) indicate that product 2e is composed mostly of Si, Al, and Ca. In some samples small amounts of Fe, K, and Mg are incorporated into product 2e, which also contains small amounts of Na. Compared to the composition of the unaltered plagioclase grain, product 2e is largely depleted in Na, Ca, and Si. A description of a distinct species with properties similar to those of product 2e was not found in the literature.

As alteration increases, product 2e is transformed into product 3c, which commonly appears light gray and massive. Under crossed polars it is microcrystalline and has normal extinction and very low birefringence. XES data (fig. 14) indicate that Ca is present in small amounts, suggesting that it has been largely depleted, compared to amounts that were probably originally present. Si and Al are the principal constituents of product 3c. Na has been virtually eliminated, and very small amounts of Mg and K, and some Fe have been incorporated. Whether product 3c was included with the X-ray samples of the clay-size fraction is uncertain, and so product 3c may or may not be X-ray amorphous. A description of a distinct species with properties similar to product 3c was not found in the literature.

In highly weathered samples, parts of plagioclase grains have altered to product 4b, either in their cores (fig. 15) or around their edges (fig. 16). This material is massive and optically isotropic, and it is typically gray. Product 4b was probably included in the X-ray samples of the clay-size fraction and hence is amorphous to X-rays. XES data (figs. 15, 16) indicate that

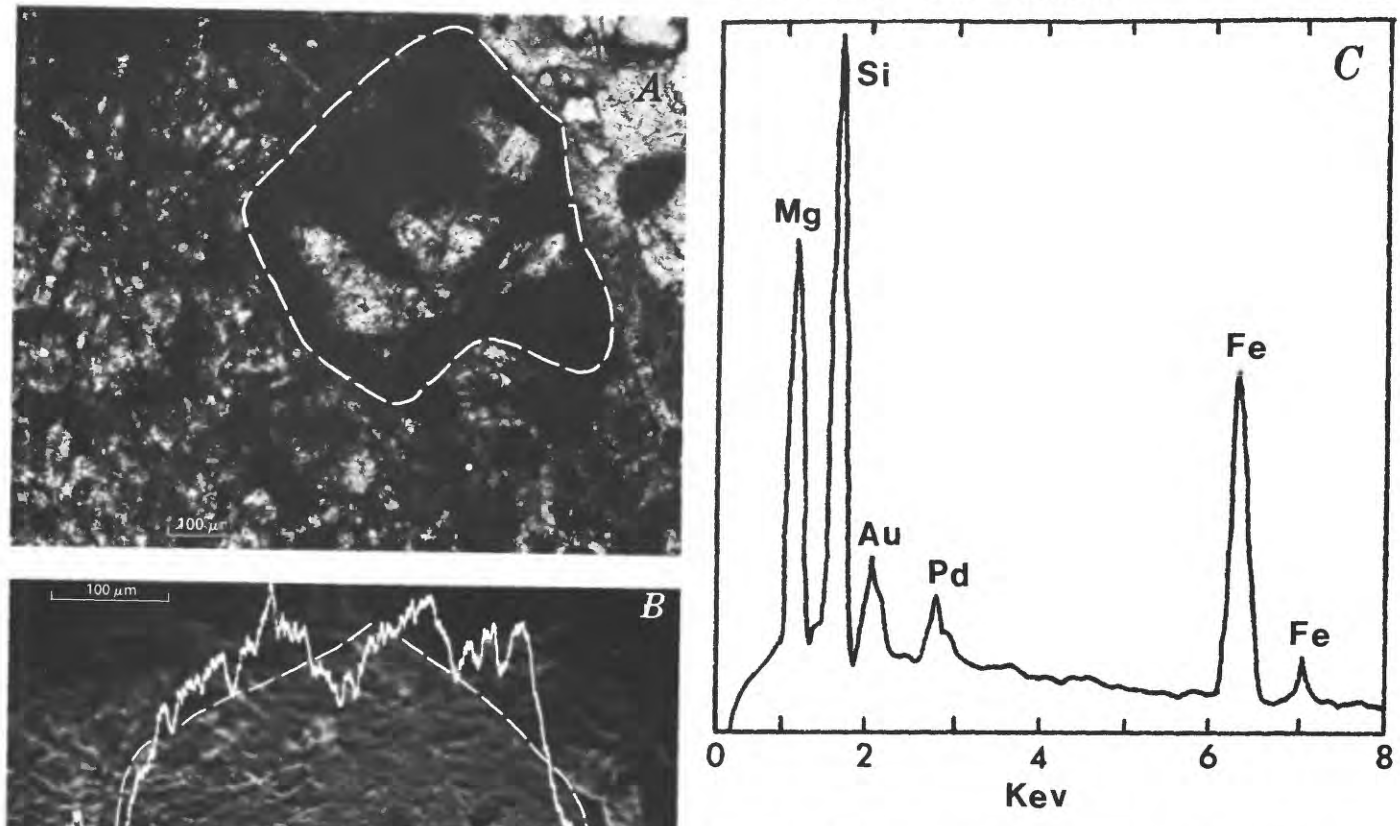

FIGURE 9.—Photomicrographs and XES data for olivine altered to "iddingsite" (weathering product 2b). *A*, Photomicrograph (plane light) of olivine grain altered to "iddingsite" along edges and fractures (dashed line outside grain edges). *B*, SEM photomicrograph of olivine grain in *A* (outlined by dashed line) and XES line scans for Fe and Mg. Line scans show relative abundances along horizontal line. *C*, XES data for "iddingsite" in *A*. Au and Pd are from the conductive sample coating. Peak heights indicate relative abundance.

product 4b is composed primarily of Si and Al and has much smaller amounts of Ca. Na has been almost entirely removed; Si and Ca have been depleted, Ca severely, compared to the composition of the unaltered plagioclase. The only other cations present are Fe and some small amounts of K, which are probably incorporated from sources outside the plagioclase grain. These data suggest that product 4b is allophane, and that it differs from product 5 only in its isolation as a discrete replacement of plagioclase and its low Fe oxide-hydroxide content. Eventually, entire plagioclase grains are altered to allophane (product 4b), which then combines with amorphous iron oxide-hydroxides to form product 5.

ALTERATION OF AMPHIBOLE AND POTASSIUM FELDSPAR

Amphibole and potassium feldspar are rare in the rocks examined in this study; consequently, generalizations concerning the stages involved in their weathering are tentative at best. Amphibole phenocrysts commonly have reaction rims of fine-grained opaques, presumably iron oxide, which are in part the result of deuteric alteration. As weathering increases, these rims become thicker, and the interiors of the grains begin to alter to weathering product 3b, especially along fractures. Other intermediate products between the unweathered mineral and product 5 were not observed.

Small amounts of potassium feldspar, probably from xenoliths, were observed in clusters in a few samples. These minerals appeared to be quite resistant to alteration, but altered to materials resembling product 3b and eventually to product 5.

ALTERATION OF OPAQUE MINERALS

Opaque minerals, primarily titanomagnetites (fig. 17), proved to be extremely resistant to alteration during the weathering of the rocks studied. In well-

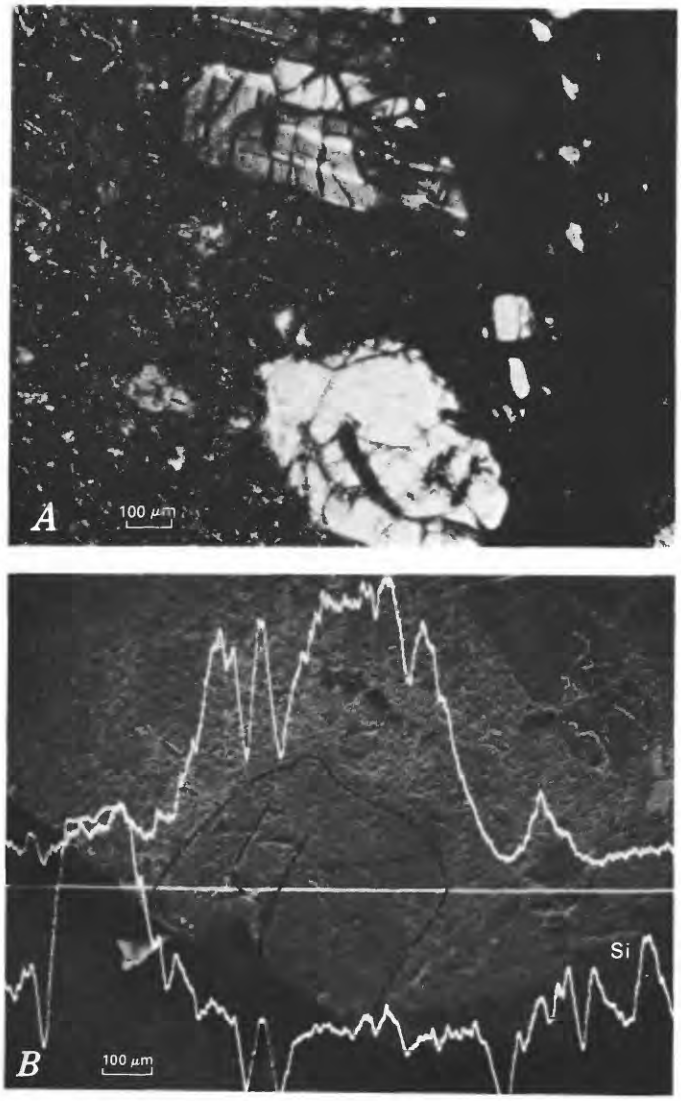

FIGURE 10.—Photomicrographs and XES data for olivine altered along grain margins and fractures. *A*, Photomicrograph (crossed polars) of olivine grain (bottom). Note prominent fractures within the grain. *B*, SEM photomicrograph and XES line scans for Mg and Si of olivine grain in *A*. Dashed lines, grain boundaries and major fractures. Line scans show relative abundances along horizontal lines; note depletion of Si and Mg along grain fractures and margins.

developed weathering rinds, small amounts of hematite, mostly along (111) planes, and maghemite along fractures (products 4c) were observed under reflected light in oil immersion. In the most advanced stages of weathering, some opaques appear to have been altered around their edges to a material resembling product 5.

STABILITY OF PRIMARY MINERALS

Weathering rinds provide two useful ways of comparing relative mineral stabilities. First, adjacent grains of different minerals can be compared in the same portion of a weathering rind, where they have been subjected to the same environment throughout their weathering history. Second, outer portions of the rinds on stones from deposits of different ages can be compared to provide a mineral-weathering sequence through time. These comparisons are valid because rinds beneath the ground surface are not subject to physical erosion or detrital contamination, and they begin to weather immediately after deposition of the stones.

The comparisons described above provide a basis for ranking minerals according to their stabilities (fig. 18). Volcanic glass and olivine are the least stable materials in the rocks examined. Pyroxene and plagioclase have intermediate stabilities, which vary with chemical composition. The composition of these minerals was estimated from optical properties, whole-rock chemical analyses (Appendix 2, table 9), some previous work (Appendix 1), and certain accessory minerals that were present (such as calcite). The relative stabilities of amphibole and potassium feldspar are tenuous because of the scarcity of these minerals in the rocks examined. Opaque minerals, primarily titanomagnetites, proved to be remarkably stable in the rocks and environments studied.

Of particular importance for weathering rinds on basalts and andesites is the inherent instability of volcanic glass and olivine. The rapid alteration of these materials imparts oxidation colors to the weathered portion of the rock soon after deposition and largely defines the early stages of rind development.

The stability of opaque minerals (primarily iron oxides in the rocks examined) has not been considered in many previous stability schemes. Opaque minerals are relatively abundant in basalts and andesites compared to other lithologies and they appear to be the most persistent minerals in weathering rinds on basalts and andesites. In the unaltered rocks, the opaques are mostly titanomagnetites, which partly alter to hematite and maghemite in the weathering rinds. In extremely weathered portions of weathering rinds, the opaques are often the only identifiable primary minerals that remain. This observation is consistent with the work of Abbott (1958), who noted the persistence of opaque minerals in weathered basalt in Hawaii.

Of the numerous mineral-stability schemes that have been previously formulated (table 5), few are based on extensive, direct observations of weathered minerals. The classic study by Goldich (1938) of the Morton Gneiss is one of the few exceptions. Most of the schemes presented are based on concepts such as bonding energies (Keller, 1954; Gruner, 1950), packing indices (Fairbairn, 1943), bulk chemistry (Reiche, 1943;

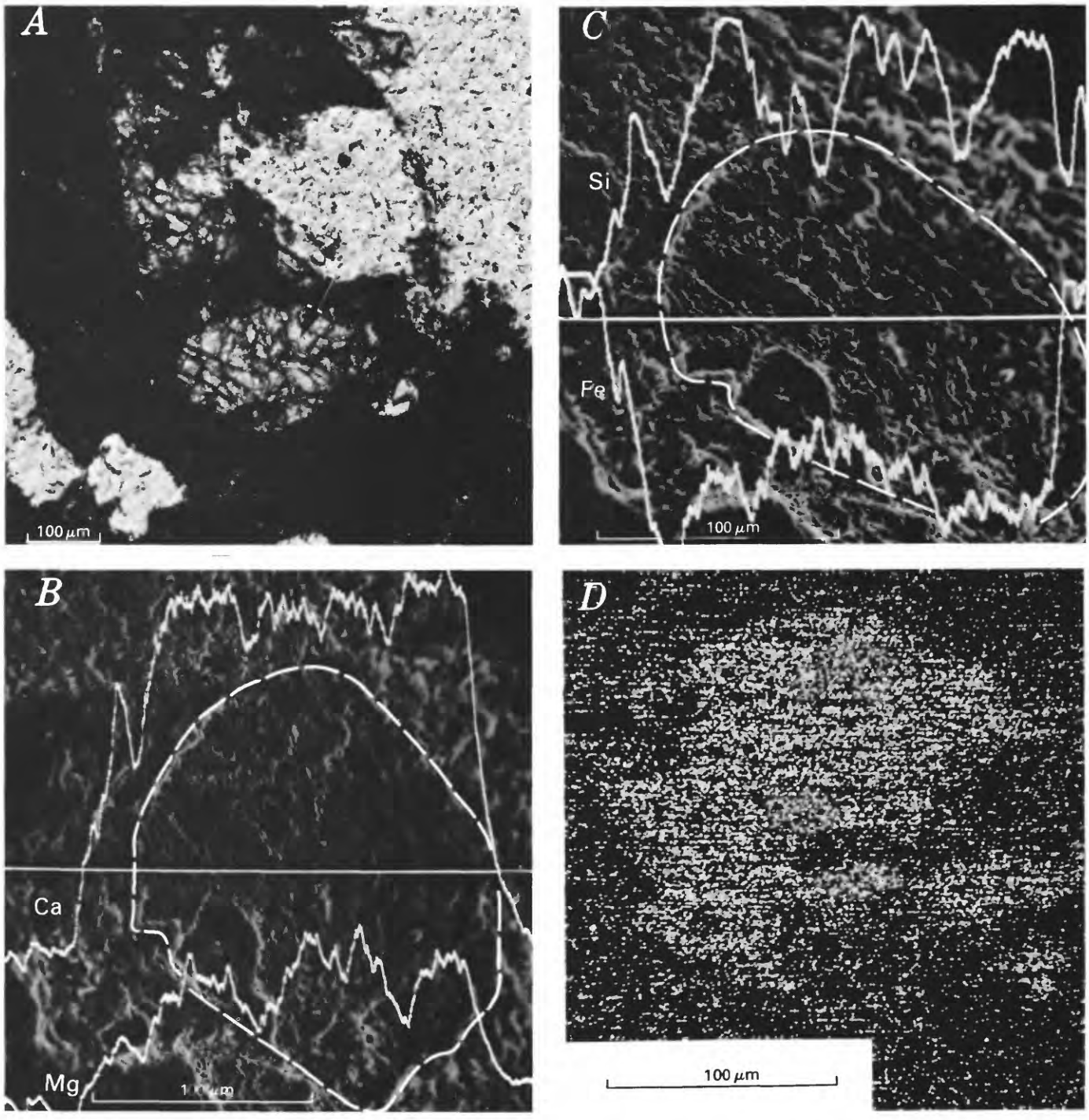

FIGURE 11.—Photomicrographs and XES data for pyroxene altered along grain margins and fractures. *A*, Photomicrograph (plane light) of pyroxene grain (arrow). *B*, SEM photomicrograph of pyroxene grain in *A* (dashed outline) and XES line scans for Ca and Mg. *C*, SEM photomicrograph of pyroxene grain in *A* (dashed outline) and XES line scans for Si and Fe. Note concordant, localized depletion of Ca, Mg, and Si, probably along fractures. Line scans show relative abundances along horizontal line. *D*, XES dot map for Ca; density of dots is proportional to Ca content. Dot map suggests little overall depletion of Ca in the pyroxene grain.

1950), reaction with H^+ clay (Jackson and Sherman, 1953), and abrasion pH (Stevens and Carron, 1948).

The stability sequences proposed by the above authors are, in general, consistent among themselves, with Goldich's (1938) sequence, and with the sequence proposed in this study. However, several differences in

TABLE 5.—*Estimates of relative stability for selected minerals*

[Stability increases downward in each list. Olv, olivine; Prx, pyroxene; Plg, plagioclase; Amp, amphibole; Fd, feldspar; Opq, opaques; Gl, glass; Aug, augite; Hor, hornblende; Ens, enstatite; Hyp, hypersthene; Qtz, quartz; Mag, magnetite; Ilm, ilmenite; Lab, labradite; Hem, hematite; Ort, orthoclase]

This study[1]	Goldich (1938)[2]	Jackson and Sherman (1953)[3]	Pettijohn (1941)[4]	Reiche (1943)[5]	Fairbairn (1943)[6]	Gruner (1950)[7]	Keller (1954)[8]	Stevens and Carron (1948)[9]
Gl	Olv	Olv	Olv	Olv 54	Aug 5.9	Olv 1.28	Olv 29,800	Olv 10–11
Olv	Aug	CaPlg	Hyp	Ens 50	Hyp 5.9	Aug 1.35	Aug 30,700	Aug 10
Prx	Lab	Aug	Aug	Aug 39	Olv 5.7–5.9	Ens 1.40	Hor 31,900	Hor 10
Plg	Hor	CaNaPlg	Hor	Hor 36	Hor 5.7	Hor 1.45	Ens 32,300	Lab 8–9
Amp	KFd	Hor	Mag	Lab 20	Qtz 5.2	Lab 1.46	Lab 33,500	Ort 8
KFd	Qtz	NaKFd	Ilm	Ort 12	Ort 5.0	Ort 1.48	Ort 34,300	Qtz 6–7
Opq	—	Qtz	—	Qtz 0	—	Qtz 1.80	Qtz 37,300	Hem 6

[1]Based on observations of minerals in weathering rinds on basalts and andesites.
[2]Based on observations of minerals in weathered gneiss, diabase, and amphibolite.
[3]Based on reaction of minerals with H^+ clay; measured as mineral cations are exchanged for H^+ ions on the clay.
[4]Based on persistence of minerals in sediments calculated from abundances in deposits of different ages.
[5]Based on Weathering Potential Index; calculated from chemical analyses.
[6]Based on a packing index for elements in the mineral lattice.
[7]Based on an energy index calculated from electronegativities and types of bonding in each mineral.
[8]Based on bonding energies (kcal) of the cations in each mineral associated with 24 oxygens.
[9]Based on abrasion pH; measured as hydrolysis releases cations from each mineral and H^+ ions are consumed.

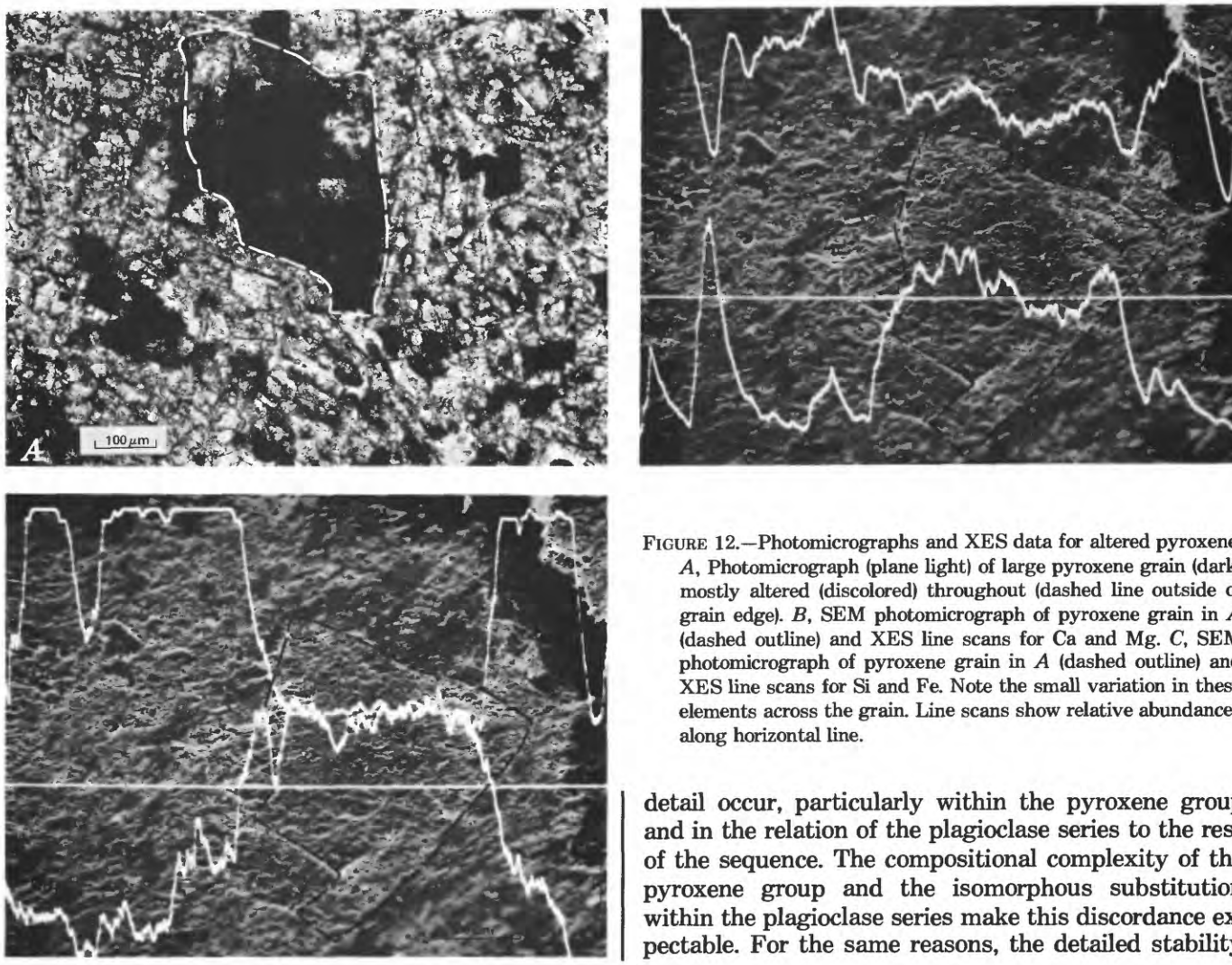

FIGURE 12.—Photomicrographs and XES data for altered pyroxene. *A*, Photomicrograph (plane light) of large pyroxene grain (dark) mostly altered (discolored) throughout (dashed line outside of grain edge). *B*, SEM photomicrograph of pyroxene grain in *A* (dashed outline) and XES line scans for Ca and Mg. *C*, SEM photomicrograph of pyroxene grain in *A* (dashed outline) and XES line scans for Si and Fe. Note the small variation in these elements across the grain. Line scans show relative abundances along horizontal line.

detail occur, particularly within the pyroxene group and in the relation of the plagioclase series to the rest of the sequence. The compositional complexity of the pyroxene group and the isomorphous substitution within the plagioclase series make this discordance expectable. For the same reasons, the detailed stability

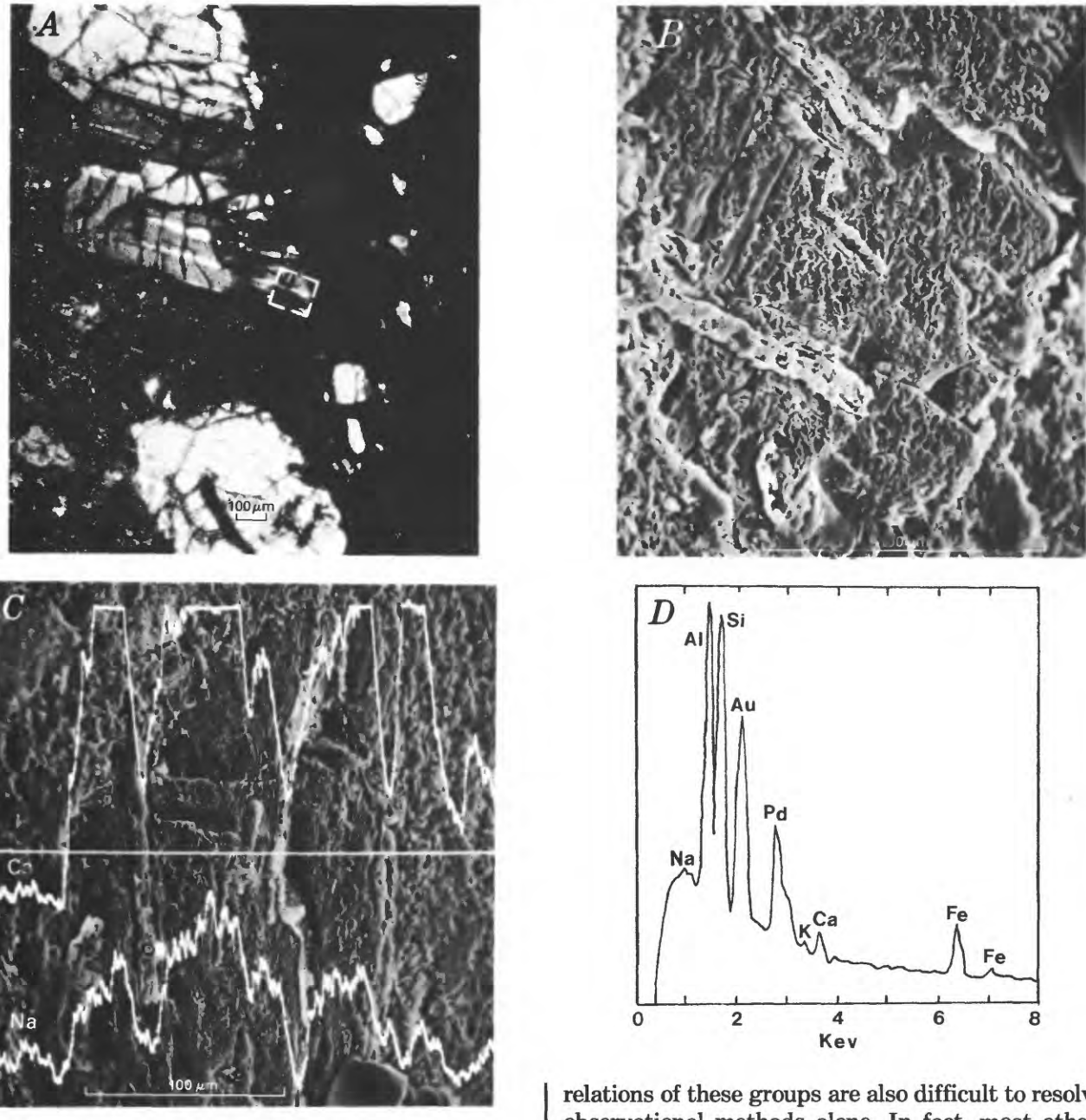

FIGURE 13.—Photomicrographs and XES data for plagioclase altered along fractures to weathering product 2e. *A*, Photomicrograph (crossed polars) of large plagioclase grain. General area of *B* and *C* outlined by dashed lines. *B*, SEM photomicrograph of the area outlined in *A*, showing relief (after etching with HF) of weathering product 2e along fractures. *C*, SEM photomicrograph of area outlined in *A* and XES line scans for Ca and Na. Note the depletion of these elements in weathering product 2e along fractures. Line scans show relative abundances along horizonal line. Circle, area of data in *D*. *D*, XES data for weathering product 2e at small circle in *C*. Au and Pd are from the conductive sample coating. Peak heights indicate relative abundance.

relations of these groups are also difficult to resolve by observational methods alone. In fact, most other observational stability schemes (Abbott, 1958; Tiller, 1958; Hendricks and Whittig, 1968; Hay and Jones, 1972) that are based on the examination of specific lithologies are quite different.

However, observational data have the advantage of physically demonstrating actual occurrences of stability differences among different minerals, an advantage not shared by laboratory or theoretical methods. This is particularly true for observations of weathering rinds, where variations in alteration among minerals can be observed both in time and in space.

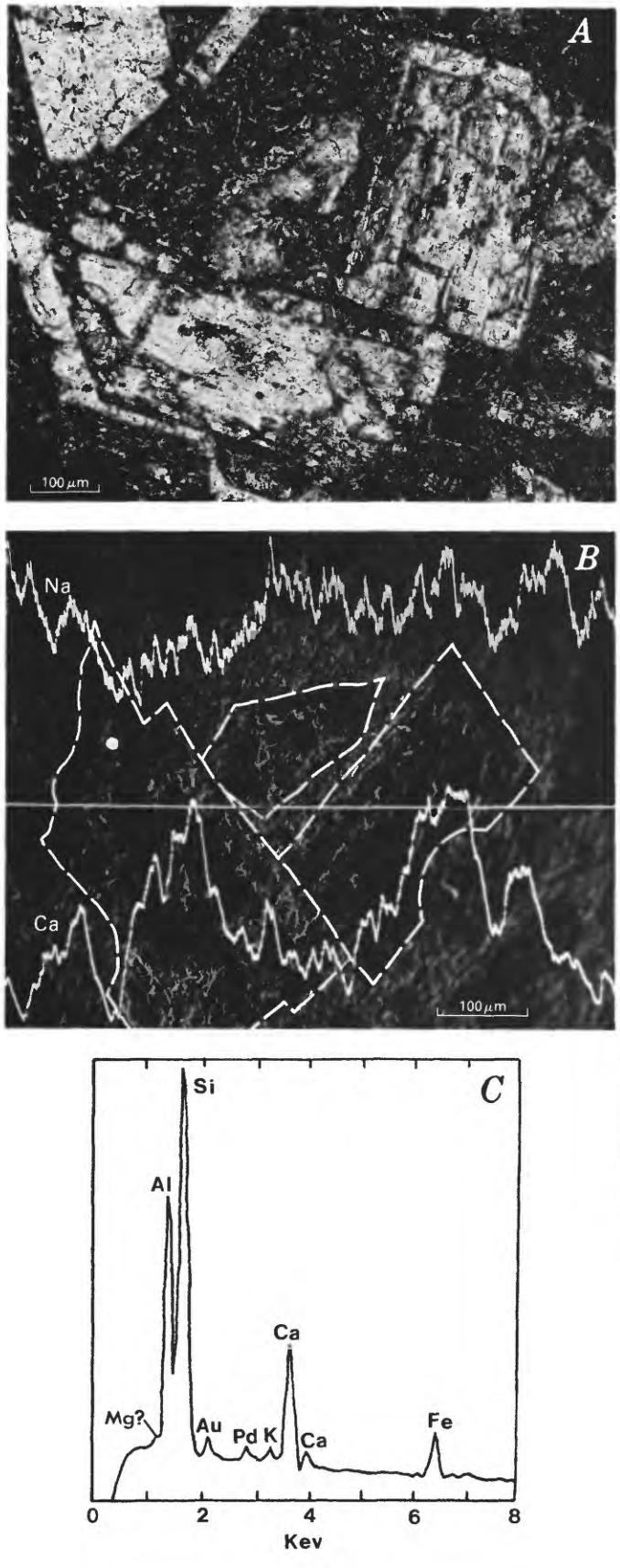

ROCK-WEATHERING STAGES

Because different minerals have different stabilities and alter at different rates (fig. 18), minerals in equal *mineral*-weathering stages (table 3) are not necessarily found together. Therefore, *rock*-weathering stages are defined by combinations of weathering products (table 2) associated with different *mineral*-weathering stages. Rock-weathering stages were defined for weathering rinds (table 6) on an arbitrary scale of one (A) for the unaltered rock to five (E) for the completely weathered rock. The products listed for a given stage of rock alteration are those that are associated in time or space; that is, those that are found together in individual rinds or in rinds subjected to similar duration or intensity of weathering. The arbitrary subdivision of alteration into stages is mainly a convenience for subdividing the observed sequence of weathering. Transitions between stages probably do not represent equal durations or equal intensities of weathering.

ROCK AND MINERAL ALTERATION WITH TIME

Weathering rinds offer two ways of examining mineralogic changes in rocks that occur through time: (1) the transition between fresh and weathered rock in individual rinds, and (2) the outer portions of rinds (maximum weathering) from deposits of different ages. These two approaches make weathering rinds particularly useful for studying weathering that occurs through time.

In weathering rinds on basalts and andesites, the boundary between altered and unaltered rock (the "weathering front") is commonly well defined, and the transition typically occurs over a distance of less than 0.2 mm. Because weathering-rind thickness is a function of time (Colman and Pierce, 1981), the weathering front migrates continuously from the surface of the stone toward the core. Therefore, the length of time that a given point in the rock has been subjected to weathering decreases with its distance from the stone surface.

FIGURE 14.—Photomicrographs and XES data for zoned plagioclase altered to weathering product 3c. *A*, Photomicrograph (plane light) of plagioclase grains with calcic(?) zones weathered to product 3c. *B*, SEM photomicrograph of plagioclase grains in *A* (dashed lines) and XES line scans for Na and Ca. Note generally low Na content in the altered zones, which probably were originally more calcic, and sharp depletion of Ca in these zones. Line scans show relative abundances along horizontal line. *C*, XES data for spot in weathered zone shown by small circle in *B*. Au and Pd are from conductive sample coating. Peak heights indicate relative abundance.

TABLE 6.—*Rock-weathering stages and weathering products*
[Weathering products (2a, 3b, 5, and others) defined in table 2; ( ), product commonly absent]

Mineral[1]	Stages				
	A Fresh rock[2]	B Slightly weathered	C Moderately weathered	D Extensively weathered	E Completely weathered
Glass	1,(2a)	(2a,2d),3a	3b,4a	5	5
Olivine	1,2b	2b	4a	5	5
Pyroxene	1	(2d)	3a,3b	(4a)	5
Plagioclase	1	2e	3c	4b	5
Amphibole	1,2c	1,2c	2c,3b	3b	3b,5
K-feldspar	1	1	1,3b	3b	3b,5
Opaques	1	1	1,4c	1,4c	1,4c,5

[1]Includes mineraloids (glass, some opaques).
[2]Some fresh rock (unweathered core) contains products of deuteric alteration, such as Fe-oxides or "iddingsite."

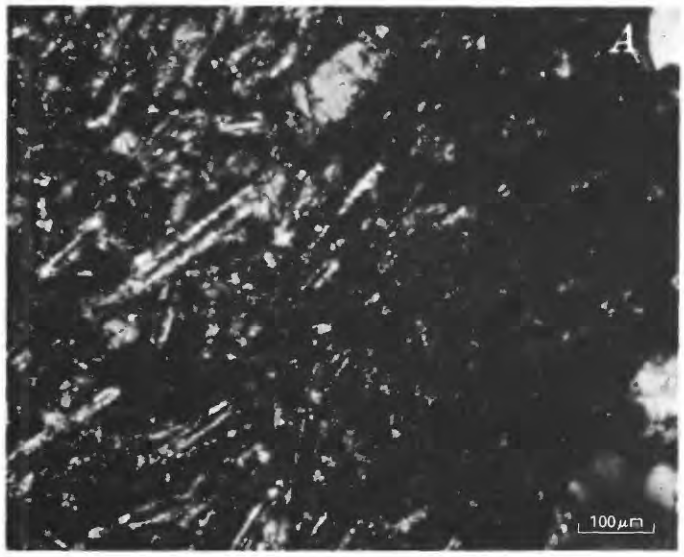

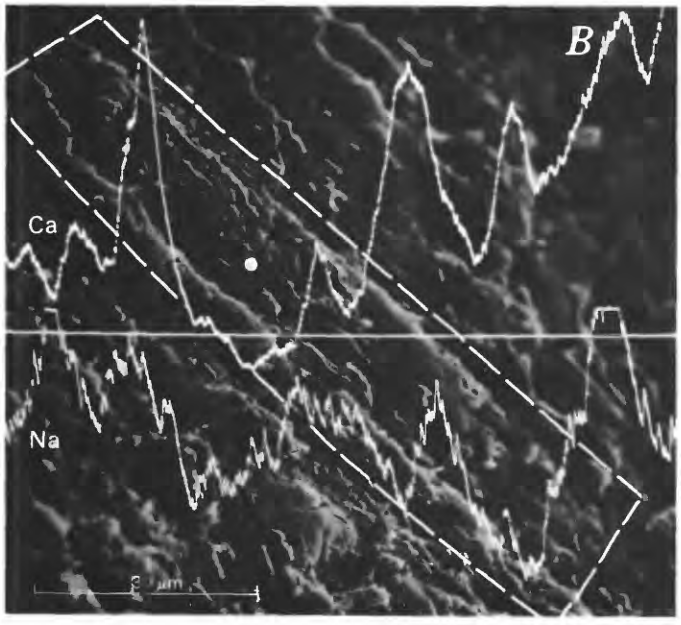

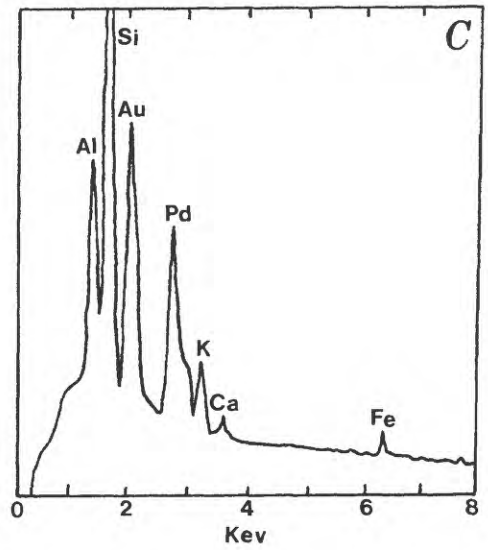

FIGURE 15.—Photomicrographs and XES data for plagioclase microlites altered to weathering product 4b in their cores. *A*, Photomicrograph (crossed polars) of several small plagioclase laths with altered cores. *B*, SEM photomicrographs of one of the plagioclase laths in *A* (dashed lines) and XES line scans for Ca and Na. Line scans show relative abundances along horizontal line. *C*, XES data for spot shown by small circle in *B*. Au and Pd are from the conductive sample coating. Peak heights indicate relative abundance.

As expected, mineral alteration in weathering rinds decreased with distance from the stone surface. For any given rind, arbitrary layers can be defined on the basis of the rock-weathering stages in table 6. The weathering stages typically decrease in a regular progression from the stone surface to the unaltered rock. Therefore, it can be demonstrated that weathering stages migrate continuously from the stone surface toward the core.

However, several problems hamper the determination either of the rates of migration of weathering

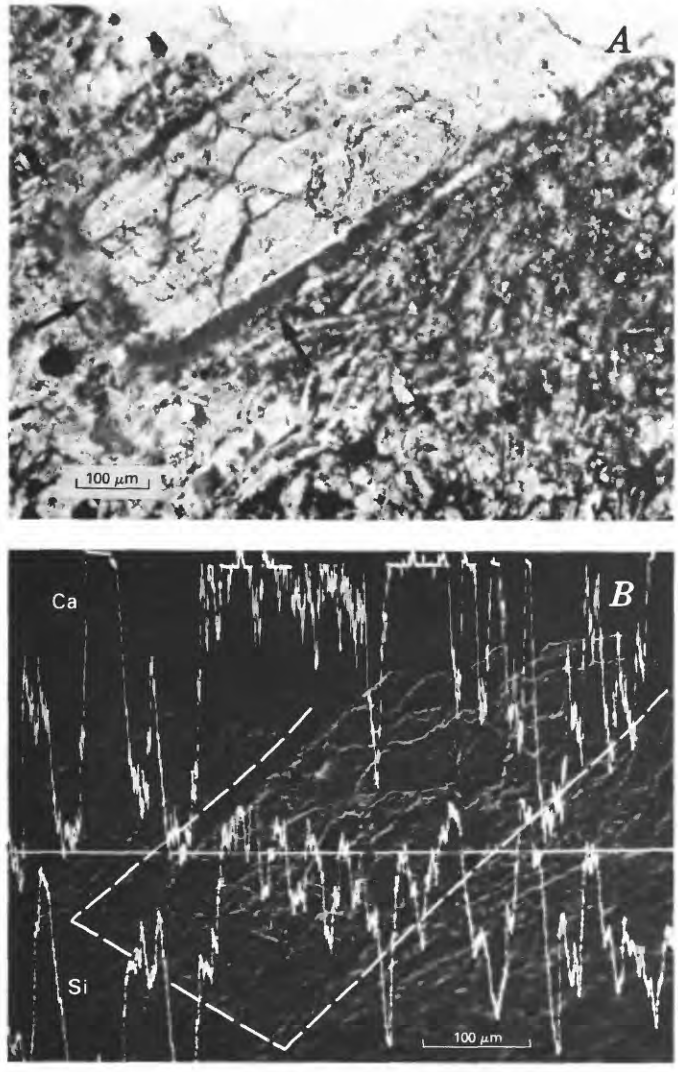

stages or of the time necessary for the transition from one stage to another. These problems include: (1) Rind thickness is not a simple function of time, but a logarithmic one (Colman and Pierce, 1981); (2) transitions between weathering stages probably do not represent equal durations or intensities of weathering; and (3) variations in rock type affect the rate of alteration. Because of these difficulties, the data in this study are insufficient to determine rates of mineral alteration from observations of progressive alteration in individual weathering rinds.

A more direct method of examining mineral alteration that occurs through time is to compare the maximum alteration in weathering rinds from different ages of deposits. Comparisons are facilitated by the fact that most stones are unweathered when deposited; thus, the duration of weathering to which the outer part of the stones has been subjected is about the same as the age of the deposit (Colman and Pierce, 1981). In addition, the outer part of the stones invariably contains the greatest degree of mineral alteration.

The rock-weathering stages in the outer part of the weathering rinds that were examined (table 7) show the expected progression with deposit age. Stages B and C in table 6 appear to be attained rather quickly; stage C is commonly found in deposits of late Wisconsin age. The transition from stage C to stage D appears to take more time, and stage D is uncommon in deposits younger than pre-Wisconsin. Thus, more than 10^5 yr are generally required to reach stage D. Stage E is predominant only in deposits that probably are at least several hundred thousand years old.

Both the stages defined in table 6 and the observations presented in table 7 are generalizations, and variations in weathering stages exist among rinds from the same deposit as suggested by entries of more than one stage in table 7. In general, however, rock weathering stages follow a regular age progression for all the sampled areas.

The time necessary to form the weathering products characteristic of each weathering stage is important to the conclusions based on the presence of each product.

FIGURE 16.—Photomicrographs and XES data for plagioclase altered to weathering product 4b around its edges (arrows). *A*, Photomicrograph (plane light) of large plagioclase grain with altered rim. *B*, SEM photomicrograph of plagioclase grain in *A* (dashed lines) and XES line scans for Ca and Si. Line scans show relative abundances along horizontal lines. *C*, XES data for the altered rim of the plagioclase in *A*. Au and Pd are from conductive sample coating. Peak heights indicate relative abundance.

TABLE 7.—*Rock weathering stages for each age of deposit*

[Rock stages for the outer part of rinds, as defined in table 6; ( ), less common; leaders (—), data not obtained. West Yellowstone, McCall, and Yakima Valley data are for basalts; other data for andesites]

Area	Deposit	Rock weathering stage
W. Yellowstone	Deckard Flats	—
	Pinedale	B-(C)
	Bull Lake	C-D
McCall	Pinedale	B-C
	Intermediate	—
	Bull Lake	D-E
Yakima Valley	Domerie	—
	Ronald	C-(D)
	Bullfrog	C-(D)
	Indian John	C-D
	Swauk Prarie	D-E
	Thorp	E
Mt. Rainier	Evans Creek	B-(C)
	Hayden Creek	—
	Wingate Hill	D-E
	Logan Hill	E
Lassen Peak	Tioga	B-C
	"early" Tioga	—
	Tahoe	C-D
	pre-Tahoe	E
Truckee	Tioga	B
	Tahoe	B-(C)
	Donner Lake	D-(E)

This consideration is particularly true for weathering product 5 (table 6, stages D and E), which is composed of allophane, iron oxide-hydroxide, and poorly developed clay minerals, and which apparently takes more than 10^5 yr to form in the rocks and environments examined in this study. The destruction of most primary minerals in basalts and andesites (stage E) takes several hundred thousand years under these conditions.

IMPLICATIONS OF THE CLAY MINERALOGY OF WEATHERING RINDS

It is generally assumed, either explicitly or implicitly, that clay minerals in well-developed soils are produced at least in part by weathering of primary minerals (Morrison, 1967, p. 6; Birkeland, 1974, p. 100). Therefore, the observed poor development of clay minerals (see section on "End products of weathering") in weathering rinds, which are produced solely by weathering processes, is unexpected, particularly in soils with well-developed argillic B horizons. Because of this apparent conflict, a brief review of previous studies of clay minerals formed by weathering of basic volcanic rocks and a short summary of several hypotheses for clay-mineral formation will be presented, followed by an attempt to resolve the problem on the basis of data from this and other studies.

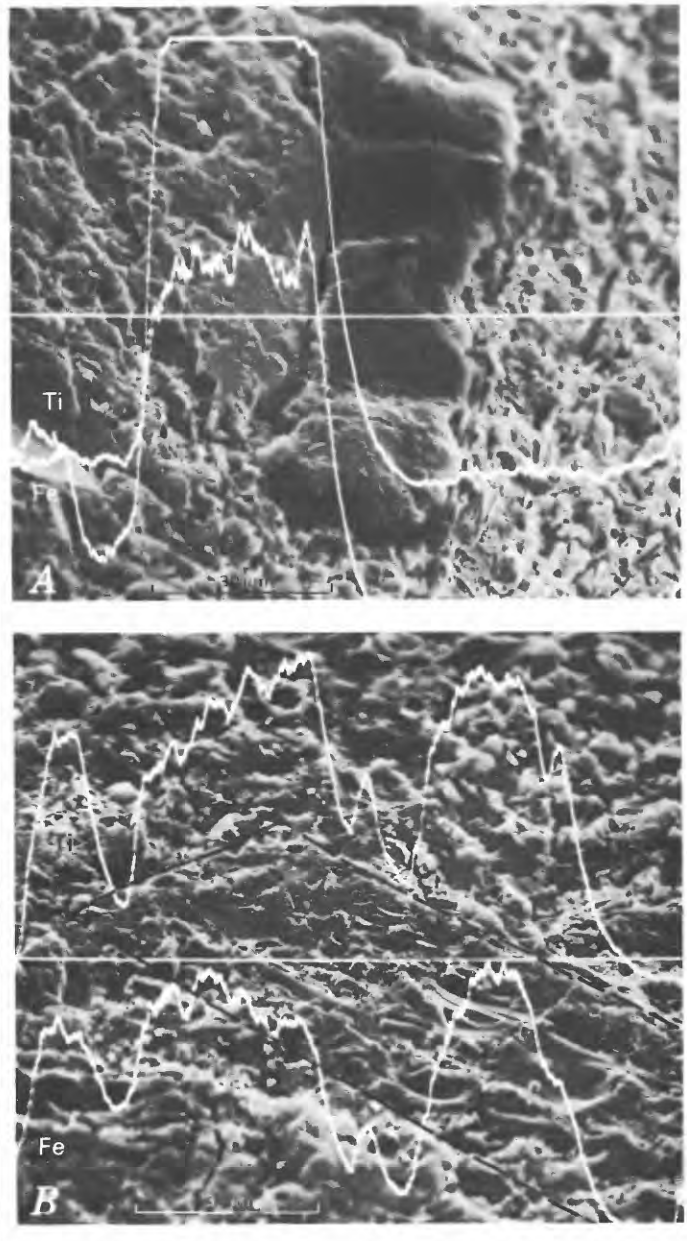

FIGURE 17.—SEM photomicrographs and XES data for titanomagnetite grains in weathering rinds. Analyzed grain in *A* stands in relief; analyzed grain in *B* shown by dashed outline. XES line scans are for Ti and Fe. They show relative abundances along horizontal line. The precise concordance of the two line scans in *B* suggests that the lower contents of Ti and Fe in the core of the grain are due to compositional zoning rather than to depletion by weathering.

Numerous workers have found clay minerals that are associated with weathered basalt and (or) andesite or

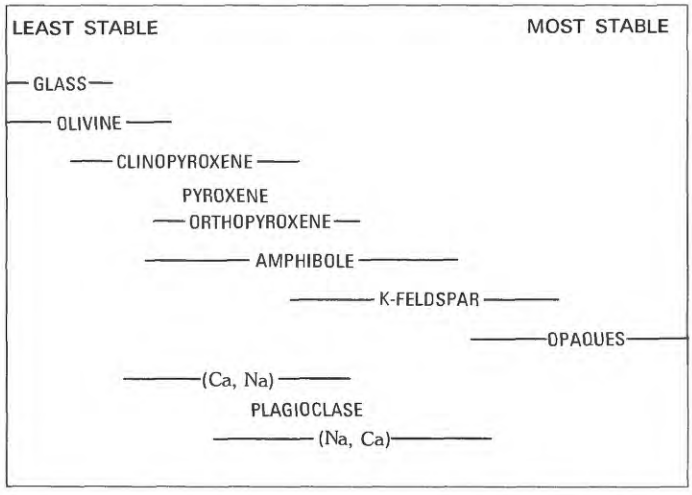

FIGURE 18.—Relative stabilities of minerals and glass in basalts and andesites. Ranking is based on observations of adjacent minerals in weathering rinds, or of outer portions of rinds subjected to varying intensities or durations of weathering.

with residual soils developed from these lithologies (Hough and Byers, 1937; Hardy and Rodrigues, 1939; Hanlon, 1944; Carroll and Woof, 1951; Eyles, 1952; Butler, 1954; Hutton and Stephens, 1956; Nichols and Tucker, 1956; Sherman and Uehara, 1956; Abbott, 1958; Tiller, 1958; Hay, 1960; Hay and Jones, 1972; Bates, 1962; Carroll and Hathaway, 1963; Craig and Loughnan, 1964; Swinedale, 1966; Hendricks and Whittig, 1968; and Loughnan, 1969). However, almost all of these studies were in intense weathering environments, commonly in tropical or semitropical climates, or were concerned with very old soils (as old as early Tertiary). In addition, most of these studies examined residual soil profiles rather than the weathered rock itself; exceptions include Abbott (1958) and Hendricks and Whittig (1968).

Carroll and Hathaway (1963) reviewed a number of these studies and concluded that the general sequence of alteration is: fresh mineral→montmorillonite→halloysite→kaolinite→gibbsite. Not all members of the sequence are always present, and the full sequence appears most common during the weathering of ferromagnesian minerals. Plagioclase may alter directly to halloysite (Bates, 1962), or to gibbsite (Abbott, 1958; Swinedale, 1966). The sequence of alteration and clay mineralogy is probably also a function of climate (Barshad, 1966; Hay and Jones, 1972; Birkeland, 1974, p. 226).

Most early workers were unaware of the presence of allophane, or they suggested that allophane resulted from the degradation of clay minerals (Hough and Byers, 1937). Modern consensus seems to be that allophane is abundant in soils formed from weathered basic volcanic rocks and that it represents an early stage in the transition from primary minerals to clay minerals (Fieldes, 1966). Swinedale (1966) concurred, but implied that primary minerals can also alter directly to clay minerals.

Theories of clay-mineral formation can be divided into three general categories: (1) precipitation from solution (Millot, 1970, p. 91), (2) condensation and crystallization of Si-Al colloids (Siffert, 1967; Barshad, 1964), and (3) direct alteration of primary silicates, including phyllosilicates (Krauskopf, 1967, p. 188; Grim, 1968, p. 522). These mechanisms are very difficult to document specifically (Birkeland, 1974, p. 90) and may not be mutually exclusive; different mechanisms may be dominant in individual instances.

Differences of opinion exist concerning the role of allophane in mechanisms of clay-mineral formation. Millot (1970, p. 91) concluded that allophane is the end product of degradation and leaching of primary *or* secondary silicates, and that its eventual fate, except for alumina, is dissolution. Accordingly, clays are formed in the weathering environment by precipitation of ions from solution in contact with residual alumina, rather than by crystallization of allophane.

In contrast, numerous studies of the weathering of basic volcanic rocks and other rock types have shown allophane to be an intermediate step in the transformation of primary minerals to clay minerals, commonly to halloysite or kaolinite (Birrell and Fieldes, 1952; Fieldes and Swinedale, 1954; Bates, 1959; Hay, 1960; Aomine and Wada, 1962; Roberson, 1963; Swinedale, 1966; Wada, 1967; Tan, 1969; and Nixon, 1979). Fieldes (1966, p. 601) stated unequivocably: "Allophanes are formed at an early stage of weathering of basic silicate minerals in basalt or ultrabasic rock." These studies suggest a continuous sequence between random-structured allophane and crystalline clay minerals. Much of the degradation of primary minerals is by hydrolysis and solution, and the residue, as well as the precipitate from the weathering solutions, consists mostly of allophane (Fieldes, 1966). These observations support the theory of clay-mineral formation by dehydration and crystallization of allophane.

Direct alteration of primary minerals to clay minerals occurs without the formation of allophane as an intermediate step. Because of the abundance of allophane and because of the poor development of clay minerals in weathering rinds on basalts and andesites, this mechanism does not appear to be significant in the alteration of these rocks. This conclusion does not pertain to the transformation of primary phyllosilicates—not present in the rocks observed—to clay minerals; such transformations have been well documented (Grim, 1968, p. 520–521).

Thus, on the basis of this and past studies of basic volcanic rocks, the mechanism of condensation and crystallization of allophane (or silica-alumina colloids) appears to be the most likely mechanism of clay-mineral formation in these lithologies. This mechanism is supported by: (1) the fact that allophane appears to be a common early alteration product in these rocks, (2) the fact that clay minerals do eventually form from these rocks, and (3) the fact that continuous gradation between random-structured allophane and crystalline clay minerals is observed in many weathering studies. The conclusion that the condensation-crystallization mechanism is dominant does not exclude simultaneous subsidiary roles of other mechanisms, and as Grim (1968, p. 520) pointed out, all changes from primary to clay minerals do not take place in the same way.

A number of observations concerning the conditions affecting the stability of allophane are pertinent here. Much of the alumina in allophane appears to be in fourfold coordination (Fieldes, 1966); to become part of a layer silicate, the alumina must be in sixfold coordination (DeKimpe and others, 1961; Wada, 1967, Linares and Huertas, 1971). Sixfold coordination of alumina is favored by low Si:Al ratios (DeKimpe and others, 1961), by pH's less than about 5.0 (Wada, 1967; DeKimpe and others, 1961), and by fulvic acids (Linares and Huertas, 1971). The converse of these conditions, therefore, favors the fourfold coordination of alumina and the persistence of allophane.

Because of its hydrated nature, allophane is also favored by continuously wet conditions (Fieldes, 1966). Other conditions that appear to contribute to high allophane contents in soils are high organic matter contents (Mitchell and Farmer, 1962; Kanno, 1959)—but not fulvic acids (Linares and Huertas, 1971)—and rapid weathering, weathered volcanic glass, and extreme comminution (Fieldes, 1966).

Concerning the problem of the poor development of clay minerals in weathering rinds on basalt and andesite, the fact remains that the rinds examined in this study contain abundant allophane and iron oxide-hydroxide, but only very fine grained and poorly crystalline clay minerals. Samples of the adjacent soil matrix, many of which were part of well-developed argillic B horizons, contain clear evidence of crystalline clay minerals (fig. 2). These soil and rind samples are from deposits of about 15,000 to at least several hundred thousand years old. This contrast leads to one or both of the following conclusions: (1) The clay minerals in the soil matrix were not formed by weathering of material in the soil, but were derived from other sources. Possible sources include overlying eolian deposits, aerosolic dust, suspended particles in precipitation, and the original clay-mineral component of the soil parent-material. (2) Conditions for crystallization of clay minerals in weathering rinds differ markedly from those in the adjacent soil.

The available evidence is not sufficient to evaluate the relative merits of these two alternatives. However, several arguments suggest that physical or chemical differences between the rinds and the soil matrix are probably not the only reason for the poor development of clay minerals in the rinds. First, previous studies of weathered andesite and basalt, rather than soil profiles developed over these lithologies, demonstrate that the weathering of these rock types in place does produce clay minerals (Abbott, 1958; Hendricks and Whittig, 1968), given sufficient time and (or) weathering intensity. This relation suggests that clay minerals will probably eventually form in the weathering rinds, but that they form much more slowly than is commonly assumed for environments sampled in this study.

Second, mineralogic observations indicate a large degree of weathering in the rinds and that, in many samples, almost all of the primary minerals have been destroyed. Chemical data, discussed in the section "Chemistry of basalt and andesite weathering," indicate thorough leaching of the weathering rinds. Weathering rinds are therefore weathered to a degree that commonly would be expected to include well-developed clay minerals as weathering products.

In summary, the fact that clay minerals are only poorly developed in the weathering rinds examined in this study suggests that clay minerals in associated argillic B horizons may be at least partly derived from sources other than the weathering of primary minerals. These sources include the original clay mineral component of the soil parent material, overlying eolian deposits, aerosolic dust, and suspended particles in precipitation. Differences in environmental conditions cannot be completely ruled out as an explanation for the difference between the rinds and the soils, and indeed they may have played a significant role. But it appears unlikely that all clay minerals have formed by weathering of primary minerals in the soils examined in this study.

These conclusions have important implications concerning the rates of formation, the sources, and the controls of both soil clay minerals and argillic B horizons. In many soils, especially in those with argillic B horizons, the clay-mineral component is commonly assumed to have resulted from the weathering of primary minerals. On the basis of this assumption, and because many soils about 10^5 yr old or older in the Western United States have argillic B horizons (Birkeland, 1974, p. 164–165), clay minerals should form within this length of time. However, the conclusions here suggest that the weathering of primary

minerals in the deposits examined in this study has produced only poorly developed clay minerals.

Therefore, at least for basaltic and andesitic materials in temperate climates, weathering appears to produce clay minerals much more slowly than is commonly assumed. This conclusion suggests that well-developed argillic B horizons may form at least partly by translocation of clays from extraneous sources, or by translocation of the original clay component of the parent material; this formation requires little or no contribution of clay minerals from the weathering of primary minerals. If this be true, then climate influences the clay mineralogy of these soils only in the transformation of inherited, or extraneous, clay minerals to clay minerals that are more in equilibrium with the soil environment.

CHEMISTRY OF BASALT AND ANDESITE WEATHERING

Chemical changes accompanying rock weathering have received much attention. (See, for example, reviews by Loughnan, 1969, p. 32–64; Ollier, 1969; Carroll, 1970, p. 69–71; and Birkeland, 1974, p. 52–77.) A number of workers have examined weathered basalt, including Hough and Byers (1937), Tiller (1958), Craig and Loughnan (1964), Lifshitz-Rottman (1971), and Hay and Jones (1972), and weathered andesite, including Hardy and Rodrigues (1939), and Hendricks and Whittig (1968). The climatic regimes in most of these studies were different from that in this study, and most of the workers did not examine the complete spectrum of basalt or andesite weathering, particularly the early stages. Of the above studies, that of Hendricks and Whittig (1968) is most comparable to the present study; their data and conclusions will be extensively cited in the following discussion.

Chemical analyses were determined for selected stones and their weathering rinds from deposits of different ages (table 1), as described in the "Methods" section. Where rinds were sufficiently thick, they were sampled and analyzed in layers, and so chemical gradients from the outer surface to the unweathered rock could be determined. The data were first calculated in the form of weight percentage (actual analyses, Appendix 2, table 9); and then they were recalculated as molecular percentages (table 10), molecular ratios (table 11), standard-cell cations (table 12), weights per unit-volume (table 13), and weights assuming TiO_2 constant (table 14).

WEATHERING INDICES

Several ways of presenting chemical-weathering data exist, and many have been reviewed by Reiche (1943). Most of these methods recast the analyses in terms of one or two indices, which summarize and condense the cumbersome array of raw data. Most indices are calculated from the molecular-percentage data, because the stoichiometric proportions of various elements are commonly more informative in weathering studies than are weight percentages (Reiche, 1943; Jenny, 1941, p. 26). Weathering indices that will be considered here are: (1) SiO_2:R_2O_3 and bases:R_2O_3, which are similar to the ratios used by Jenny (1941, p. 26), (2) silica-bases-R_2O_3 triangular diagrams (Reiche, 1943), (3) Parker's (1970) weathering index, (4) weathering potential index (WPI) versus product index (PI) (Reiche, 1943; 1950), (5) Fe_2O_3:FeO ratio, and (6) molecular percentage of water. For these indices, Mg, Ca, Na, and K were grouped as total bases; and Al_2O_3, Fe_2O_3, and TiO_2 were grouped as R_2O_3. TiO_2 was grouped with Al_2O_3 and Fe_2O_3 because of its apparently similar immobility (Loughnan, 1969, p. 44).

One minor problem, which was probably due to sampling procedures, became apparent in almost all of the weathering indices. In some sampling areas, especially at Truckee and at Lassen Peak, the two youngest deposits are close in age; the weathering indices for these deposits suggested a greater degree of weathering, but to a shallower depth in the stone, for the youngest deposit than for the next older deposit. Rinds from both ages of deposits were thin, and only one sample of the rind was obtainable. Thus, the sample from the youngest deposit contained only the most weathered portion of the rind, whereas the sample from the next older deposit contained both the outermost weathered part of the rind and the inner, less weathered part. Therefore, the relation (for young deposits) of more intense weathering to a shallower depth in the stone for the youngest deposit, compared to the weathering in the next older deposit, is considered to be consistent with the general trend of increasing weathering with deposit age.

Ratios of SiO_2:R_2O_3 and bases:R_2O_3 were plotted with distance from the stone surface (figs. 19 and 20). These ratios indicate the mobility of SiO_2 and bases relative to R_2O_3, which is generally considered stable (Loughnan, 1969, p. 52). To the degree to which R_2O_3 remains immobile these indices approach measures of absolute changes.

The SiO_2:R_2O_3 ratio changes systematically with the ages of the deposits sampled (fig. 19). The sequences for the McCall, West Yellowstone, and Mt. Rainier areas show particularly good progression with age. These data indicate that SiO_2 is systematically depleted with time relative to R_2O_3. Such depletion can exceed 50 percent, and it is commonly more than 20 percent for deposits older than about 10^5 yr. In ad-

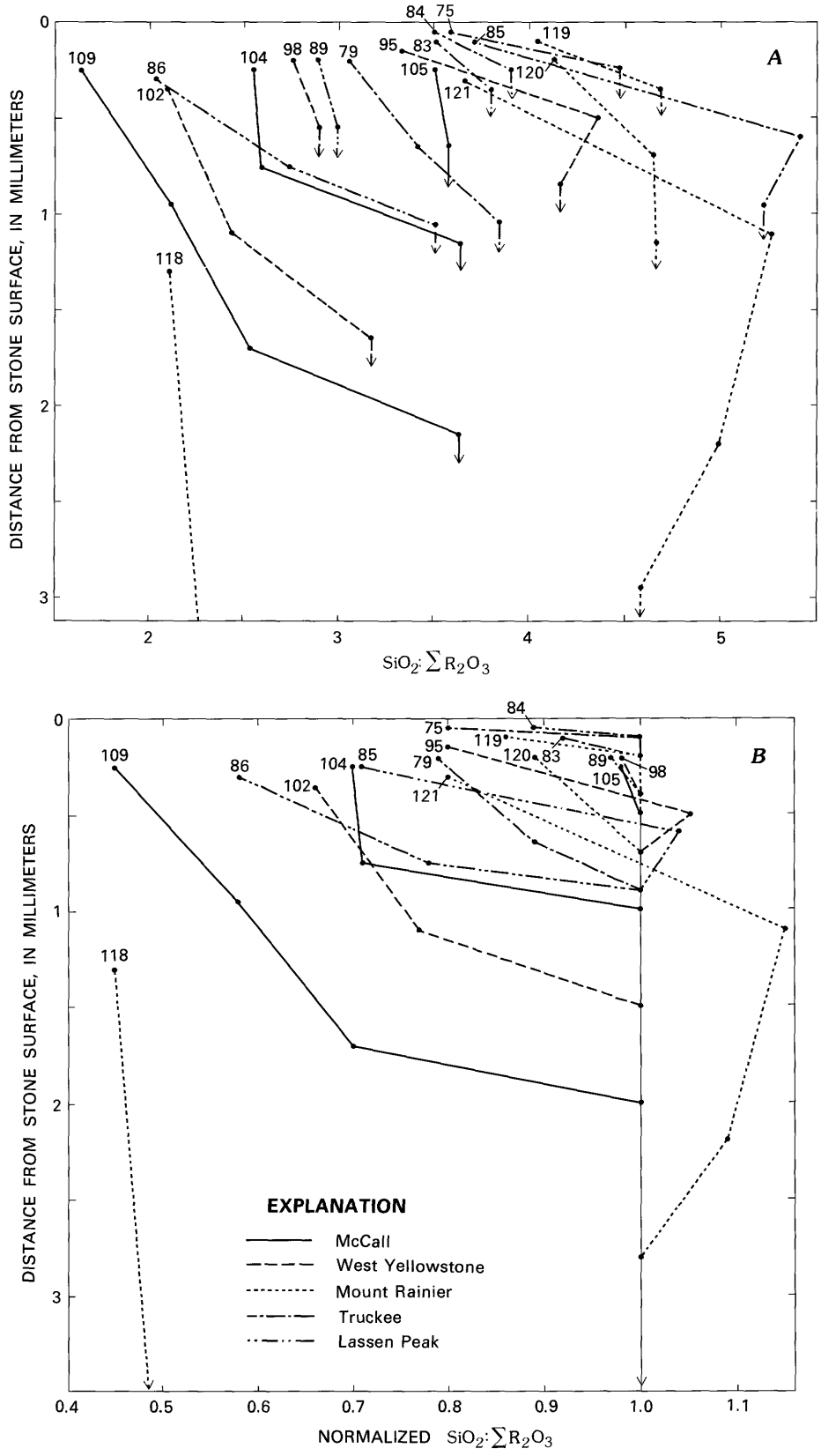

FIGURE 19.—Plots of SiO_2:R_2O_3 with distance from the stone surface. *A*, SiO_2:R_2O_3 raw molecular ratios (table 11). *B*, Data in *A* normalized to the value in the unaltered rock (table 15). Data points represent the midpoint of channel samples over the sampling interval given in table 9. Arrows indicate that the sample above them is from unaltered rock. See table 1 for the deposit and lithology of each sample (numbers).

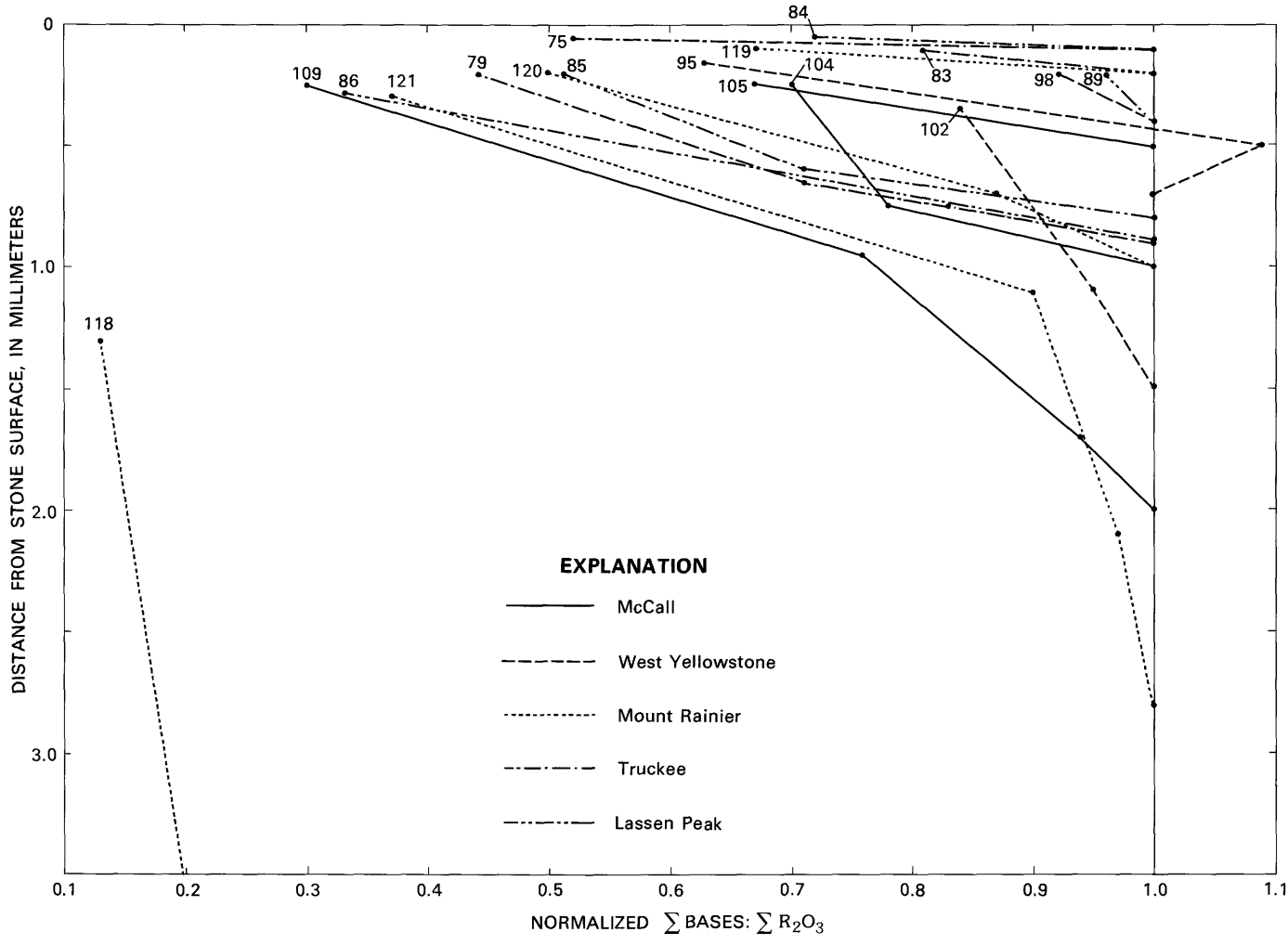

FIGURE 20.—Plots of bases:R_2O_3 with distance from the stone surface. Data are normalized to the value in the unaltered rock (table 15). Data points represent the midpoint of channel samples over the sampling interval given in table 9. Arrows indicate that the sample above them is from unaltered rock. See table 1 for the deposit and lithology of each sample (numbers).

dition, with minor exceptions, the SiO_2:R_2O_3 ratio decreases regularly from the fresh interior of a stone to its weathered outside surface.

The bases:R_2O_3 ratio (fig. 20) has trends similar to the SiO_2:R_2O_3 ratio, but the depletion of bases relative to R_2O_3 is greater than that of SiO_2. In all sampling areas, the bases:R_2O_3 ratio decreases with the age of the deposit. In addition, with one minor exception, the bases:R_2O_3 ratio decreases regularly from the unaltered rock interior to the weathered surface for all samples. These data indicate that bases are lost relatively rapidly from weathering rinds compared to the rate of loss of other elements. In fact, the small change in the bases:R_2O_3 ratio for the outer portions of sample 118 suggests that the outer portion of the rind has reached a small limiting value of bases. In samples from deposits more than about 10^5 yr old, the value of the bases:R_2O_3 ratio has commonly decreased to 30–50 percent or less of its value in the unaltered rock.

Parker's (1970) weathering index, which is also a measure of the loss of bases during weathering, was plotted against distance from the stone surface for the weathering-rind samples (fig. 21). The index is defined as:

$$100(K/0.25+Na/0.35+Ca/0.7+Mg/0.9),$$

where the denominators represent measures of the strengths of the cation-oxygen bond. The index is not referenced to R_2O_3 or to any other stable constituent, so different samples (that have different initial compositions) are not directly comparable. However, the index changes rapidly as bases are lost, so it is a sensitive indicator of early stages of weathering in a given

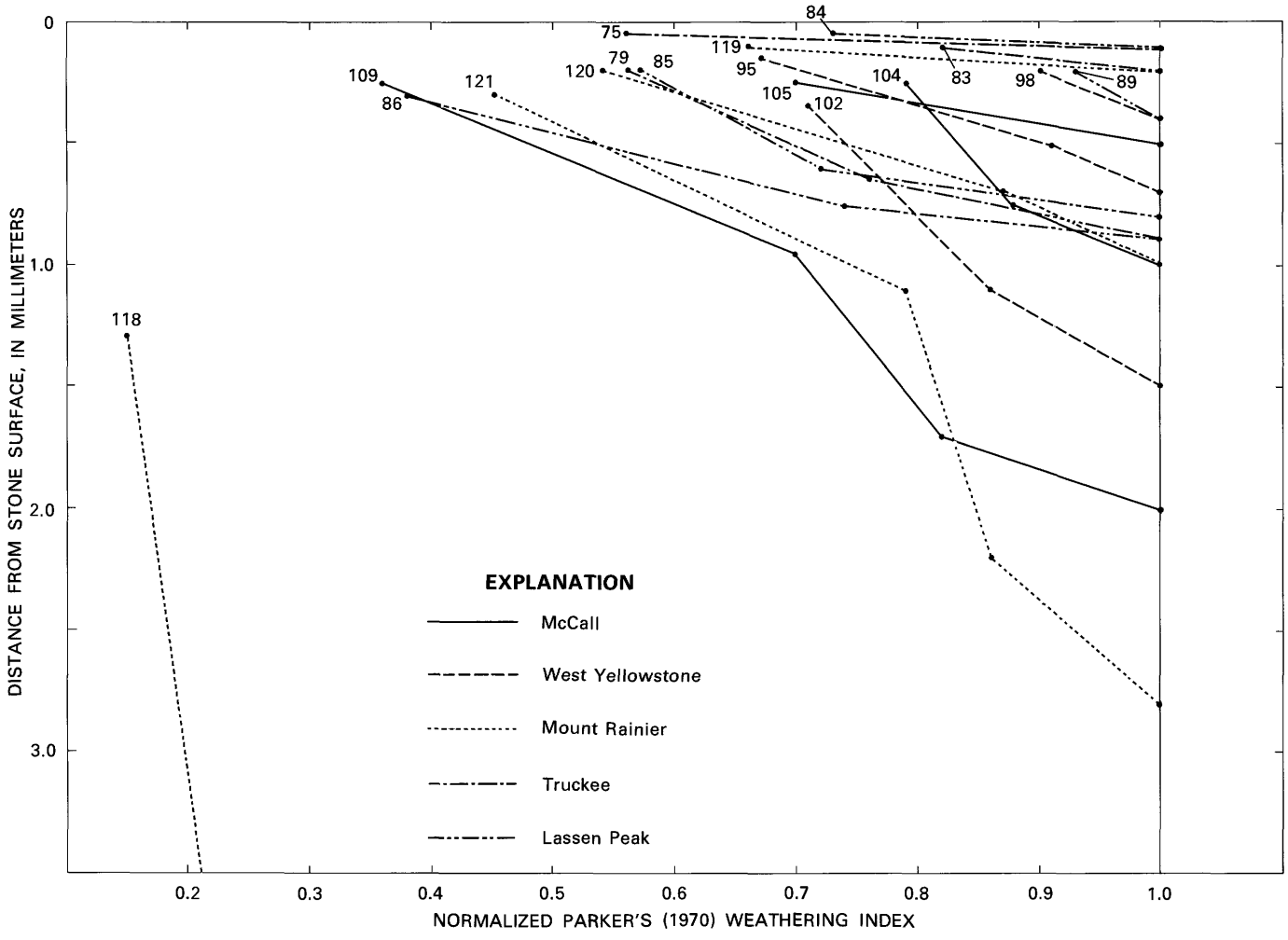

FIGURE 21.—Plots of Parker's (1970) weathering index with distance from the stone surface. Data are normalized to the value in the unaltered rock (table 15). Data points represent the midpoint of channel samples over the sampling interval given in table 9. Arrows indicate that the sample above them is from unaltered rock. See table 1 for the deposit and lithology of each sample (numbers).

sample. As weathering advances and bases are depleted (sample 118), the minimal changes that occur in the index suggest that the index asymptotically approaches a small limiting value. The index shows regular decreases, both with the age of the deposit sampled in each area and with the distance of the sample from the unaltered rock in individual rinds.

The amount of water incorporated in the rinds as a result of weathering appears to be a sensitive measure of weathering (fig. 22). Molecular percentages of water were calculated from the analyses of water released above 110°C (H_2O^+) in the "Rapid-Rock" analyses and from the difference of the total-weight percentage from 100 percent in the XRF analyses. The samples were air dried before analysis, and the amount of water released below 110°C (H_2O^-) commonly was small (table 9). Thus, most of the water incorporated in the weathering rinds is released only above 110°C, and it is therefore either included in crystal lattices or bound to hydrated cations. Because the development of new mineral species was minimal in the weathering rinds (see "End products of weathering" section), the latter source is considered to be dominant.

Water is rapidly incorporated in the rinds as weathering progresses, and in highly weathered material (sample 118) the molecular percentage of water exceeded 50 percent (fig. 22). Rinds from deposits more than 10^5 yr old commonly contain 20–40 molecular-percent water. The changes in water content increased as deposit age increases in each area, and water content increases regularly from the unaltered rock to the weathered surface.

The Fe_2O_3:FeO ratio is a measure of the oxidation that occurs during weathering (fig. 23); it is particu-

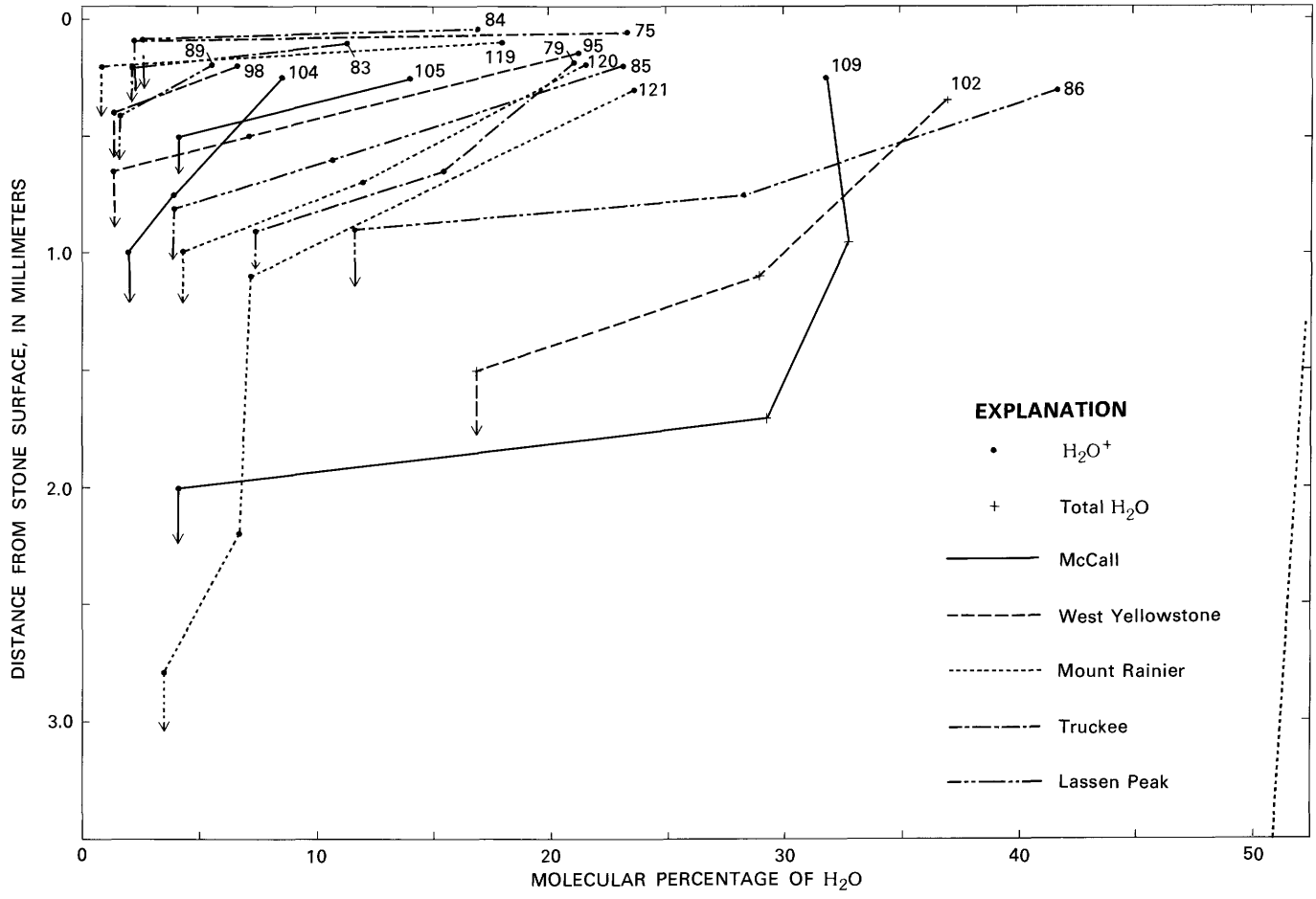

FIGURE 22.—Plots of molecular percentage of water with distance from the stone surface. Data are from table 10. Data points represent the midpoint of channel samples over the sampling interval given in table 9. Arrows indicate that the sample above them is from unaltered rock. See table 1 for the deposit and lithology of each sample (numbers).

larly important for weathering rinds, which are defined largely by color. Fe_2O_3 is generally stable in most weathering environments (Loughnan, 1969, p. 52), but any depletion of Fe_2O_3 and the potential mobility of FeO may affect the Fe_2O_3:FeO ratio as a measure of oxidation. The Fe_2O_3:FeO ratio tends to increase with age in each area and toward the outside of each rind, but several irregularities exist (fig. 23). In addition to potential losses of Fe_2O_3 or FeO, other complicating factors may affect the Fe_2O_3:FeO ratio. For example, rinds from McCall are much more oxidized than are those from West Yellowstone. The fact that the rinds from McCall have incorporated more water than have those from West Yellowstone (fig. 22) may account for the difference in oxidation. The difference in oxidation is also observed in the colors of the rinds, which are much redder and brighter in those from McCall. The redness and brightness of the rinds generally increase with deposit age within each sampling area, but colors are not comparable from area to area because of differences in rock type and climate.

Reiche (1943; 1950) devised two indices that incorporate almost all of the major elements involved in weathering. They are based on molecular percentages and are called the weathering potential index (WPI) and the product index (PI), which are defined as:

$$WPI = 100(\Sigma bases - H_2O)/(\Sigma bases + SiO_2 + \Sigma R_2O_3)$$
$$PI = 100(SiO_2)/(SiO_2 + \Sigma R_2O_3).$$

The amount of weathering in each weathering-rind sample is clearly shown by plots of these two indices against each other (fig. 24). In unaltered igneous rocks, these indices have high values; as weathering progresses, WPI decreases rapidly as bases are lost and as water is gained, and PI decreases more slowly as silica is lost. R_2O_3 functions as a reference constituent in the indices.

Because the WPI-PI plot combines all the major elements involved in weathering (bases, silica, R_2O_3, and water), it is probably the optimum two-dimensional portrayal of chemical weathering. However, it has the

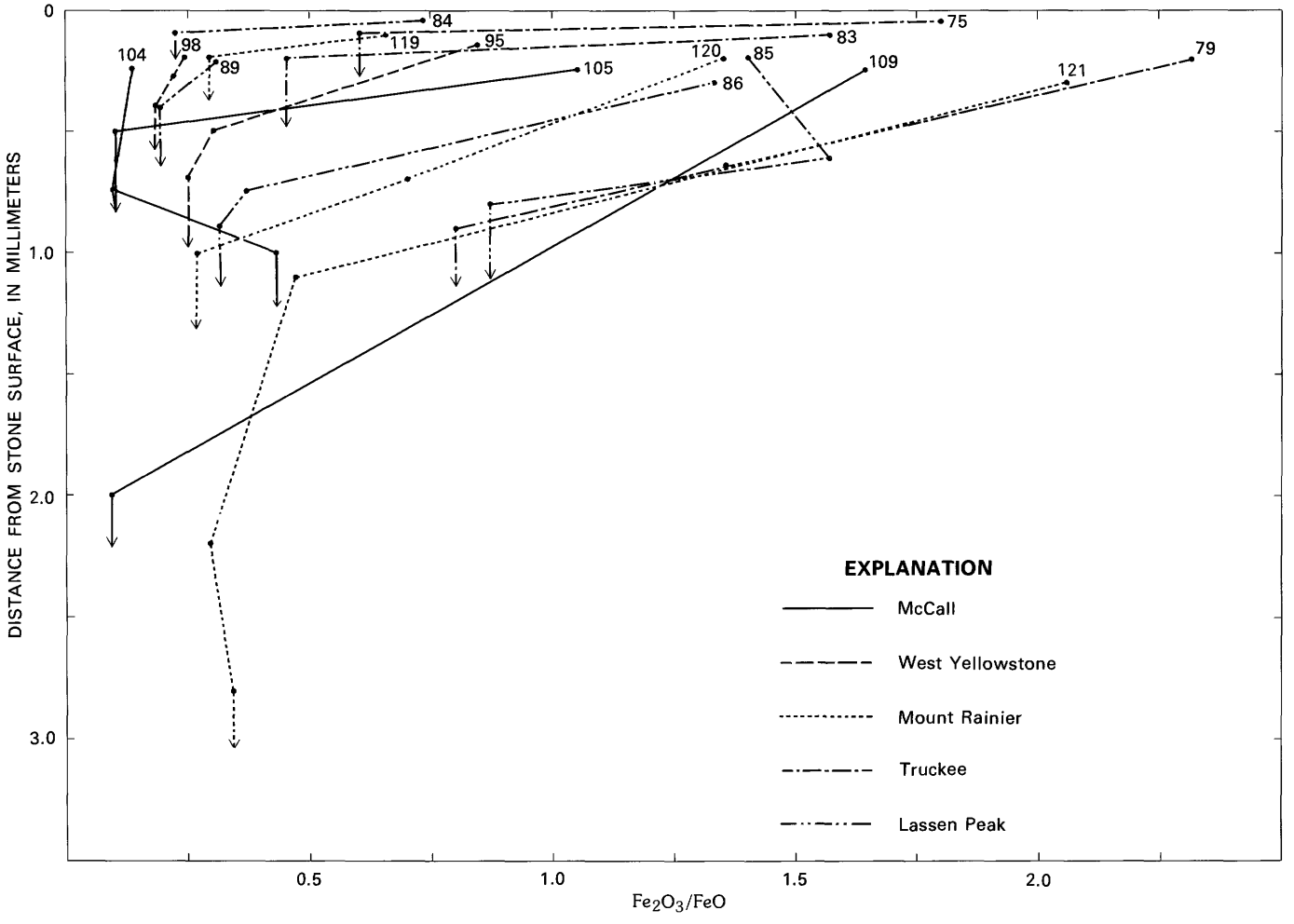

FIGURE 23.—Plots of Fe_2O_3:FeO ratio with distance from the stone surface. Data are from table 11. Data points represent the midpoint of channel samples over the sampling interval given in table 9. Arrows indicate that the sample above them is from unaltered rock. See table 1 for the deposit and lithology of each sample (numbers).

disadvantage of not showing changes in individual elements, and because it is based on percentage data, it does not account for compensating (relative) changes in elements or groups of elements. However, the WPI-PI plot shows that weathering-rind samples all change in order of increasing age in each area, and that the changes within rinds are all systematic. In addition, some samples (109, 86, and 118) approach or exceed the stability fields of kaolinite and halloysite (fig. 24).

Another method of portraying overall chemical changes occurring during weathering is a triangular diagram of molecular percentages that has silica, bases, and R_2O_3 as the three coordinates (fig. 25). This plot shows that the general tendencies during weathering-rind formation are concentration of R_2O_3; depletion of bases; and small, irregular changes in SiO_2. Although the plot is useful for illustrating general weathering trends, it has the disadvantage inherent in all percentage data that the changes shown in elements or groups of elements are relative. Concentration of R_2O_3 is more likely due to depletion of other elements than to actual increases in R_2O_3. Also, more silica is probably lost than that indicated, but it is compensated for by the greater depletion of bases.

The weathering indices discussed above have several disadvantages. First, because they are based on molecular percentages, all changes in a given element are relative to changes in other elements. Second, in an effort to present the data in one or two indices (dimensions), changes in individual elements are obscured, and compensating changes in grouped elements are not apparent. However, they are useful in that they condense and summarize the data and illustrate general weathering trends.

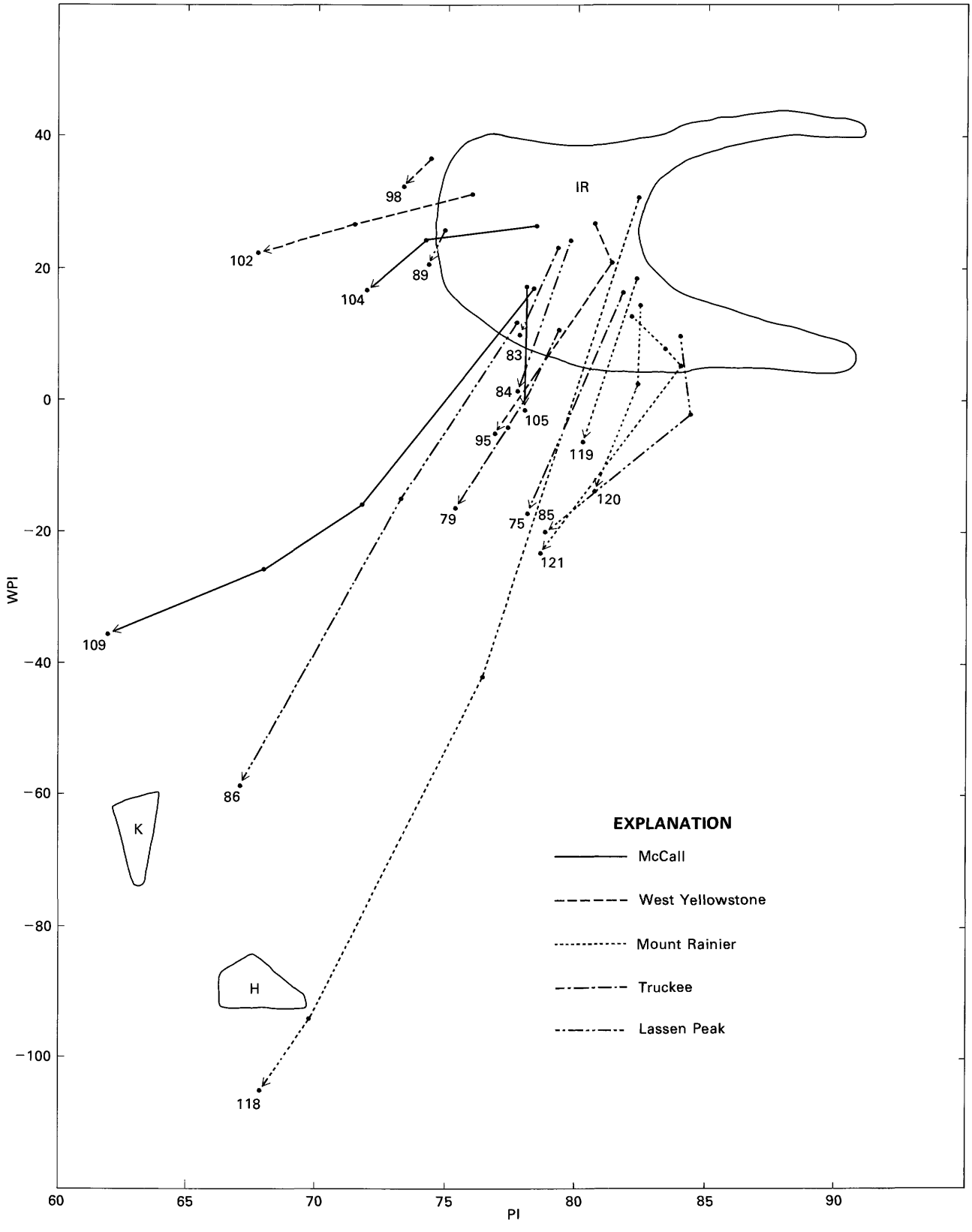

FIGURE 24.—Plots of weathering potential index (WPI) versus product index (PI) for weathering-rind data. $WPI=100(\Sigma bases-H_2O)/(\Sigma bases+SiO_2+\Sigma R_2O_3)$; $PI=100(SiO_2)/(SiO_2+\Sigma R_2O_3)$ (Reiche, 1943; 1950). Enclosed areas are the fields of igneous rocks (IR), kaolinite (K), and halloysite (H) (Reiche, 1943). Arrows indicate the trend from unaltered to weathered rock. Data from table 11. See table 1 for the deposit and lithology of each sample (numbers).

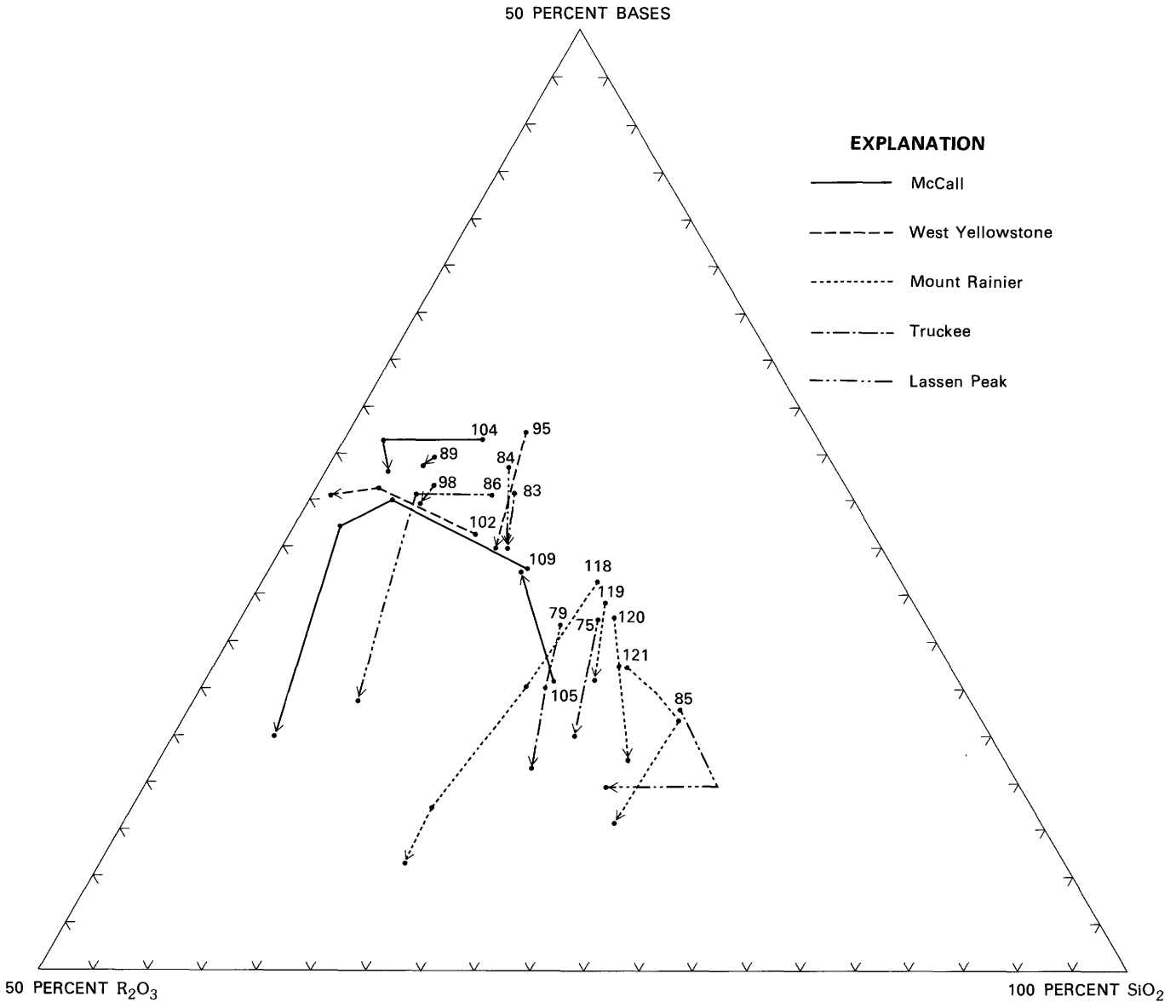

FIGURE 25.—Triangular plots of SiO_2, R_2O_3, and bases ($MgO+CaO+Na_2O+K_2O$) for weathering-rind data. Arrows indicate the trend from unaltered to weathered rock. Calculated from data in table 11. See table 1 for the deposit and lithology of each sample (numbers).

The weathering indices indicate that the most important chemical processes occurring during weathering-rind formation are: (1) rapid depletion of bases, (2) rapid incorporation of water, (3) slower loss of silica, (4) concentration of sesquioxides, and (5) oxidation of iron. Reiche's (1943; 1950) WPI-PI indices appear to be the most useful, because they include all the major elements involved in the weathering processes. In general, all the indices show a trend of increasing weathering as the age of the sampled deposit increases and a trend of increasing weathering toward the outside of the stone or rind.

ABSOLUTE CHEMICAL CHANGES

In detailed weathering studies, changes in the quantities of individual elements are important for assessing degrees and processes of weathering. These changes are most useful if they are determined on an absolute scale, rather than on the relative scale inherent in percentage data. Variation in individual elements on an absolute scale not only determines the order of mobility of the elements but also suggests conclusions about the solubility of individual elements within the weathered materials and about the composition of the weathering products.

Three general methods are available for calculating changes in elemental abundances on an absolute scale, using the relative weight-percentage data; each of these methods involves at least one major assumption. One method, which requires only the assumption that alteration has proceeded without volume change, was developed by Barth (1948); it is based on the cations associated with a theoretical standard cell containing 160 oxygens. If the alteration is isovolumetric, the number of oxygens remains constant, and the number of cations of each element can be calculated from molecular percentages.

A second method, which also requires the isovolumetric alteration assumption, is based on the weight of each elemental oxide in a unit-volume of rock. To convert the weight-percentage data to weight per unit-volume, bulk density must be measured for each sample. If volume changes have not occurred, the weights of a given element in unit-volumes of material in each stage of weathering are directly comparable. This method has been infrequently used, but Hendricks and Whittig (1968) obtained reasonable results for andesite weathered to saprolite, a case in which isovolumetric weathering could be substantiated.

A third method, which is most commonly used in weathering studies, is based on the assumption that at least one element remains constant, or immobile, during weathering (Reiche, 1943; Loughnan, 1969, p. 89; Birkeland, 1974, p. 69). This method does not require isovolumetric weathering; it only assumes the immobility of a reference constituent. Al_2O_3, Fe_2O_3, and TiO_2 are commonly used as reference constituents; these elements are only slightly soluble in most weathering environments (Loughnan, 1969, p. 52). The quantities of each elemental oxide are calculated directly from the weight-percentage data by multiplying the weight percentage by the ratio of the amount of the reference constituent in the fresh rock to that in the weathered material. The resulting values are equivalent to the amounts remaining after the weathering of 100 g of fresh rock.

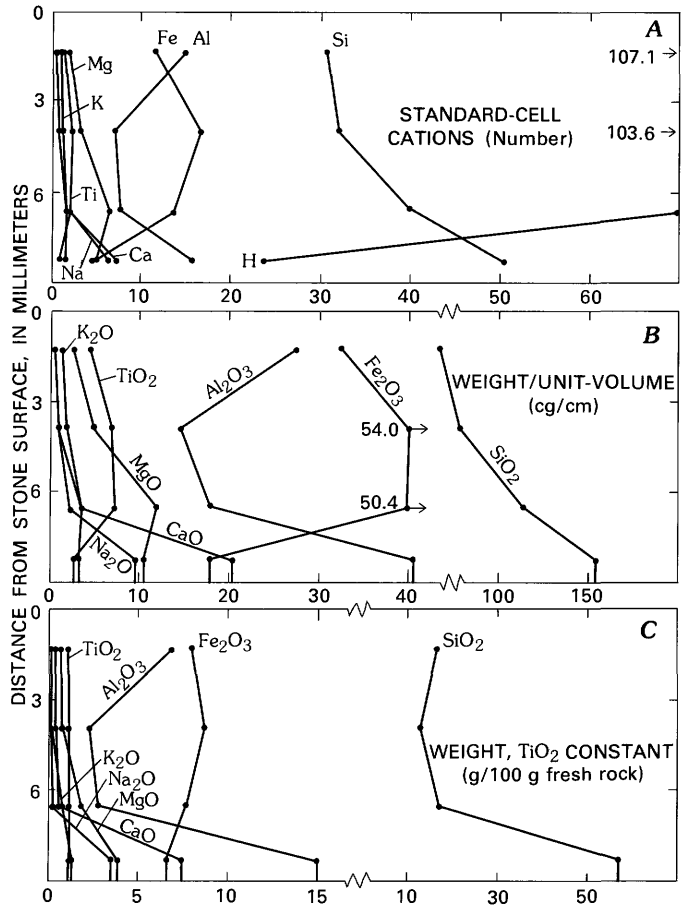

FIGURE 26.—Three methods of calculating chemical changes on an absolute scale, using profile of sample 118 as an example. *A*, Number of cations in a standard cell containing 160 oxygens, calculated by Barth's (1948) methods, assuming isovolumetric alteration. *B*, Weight per unit-volume, calculated from weight percentages and bulk density, assuming isovolumetric weathering. *C*, Weight resulting from the weathering of 100 g of fresh rock, assuming TiO_2 constant.

STANDARD-CELL-CATIONS METHOD

The data for the number of cations in a standard cell (table 12; fig. 26*A*), calculated by the methods of Barth (1948) for the weathering-rind samples, contain some unexpected results. Silica remains nearly constant for samples from young deposits and decreases only slightly for those from older deposits. Alumina, iron, and titanium tend to increase significantly compared to the amounts in the fresh rock. Base cations (Mg, Ca, Na, and K) show a general tendency to decrease with weathering, but the trend is often erratic and K and Mg increase in some samples compared to the amounts in the fresh rock. Some K and Mg could be incorporated into clay minerals, but considering the poor development of clay minerals in the rinds this is not believed to be an important mechanism.

If weathering proceeds mainly by depletion, and if it is isovolumetric, no element should increase to more than the amount present in the unaltered rock. Therefore, the observed increase in standard cell cations must be due either to: (1) additions in solution from extraneous sources, (2) preferential concentration of elements mobilized from within the rock, or (3) volume decrease during alteration. Additions in solution from outside sources and preferential concentration are considered unlikely, particularly because of the low solubilities of Al, Fe, and Ti at Eh-pH conditions of normal

weathering environments (Loughnan, 1969, p. 52). In addition, for most samples in this study, concentration gradients should be *away* from the fresh rock and toward the stone surface, especially those for Fe, Mg, and Ca. There is also little reason to expect that the gradients of pH, or of other factors affecting cation solubility, would be irregular enough to produce zones of concentration of elements within the rinds.

If the addition of elements from extraneous sources and the preferential concentration of elements in zones are insignificant, then a volume decrease must have accompanied the weathering observed in this study. However, no evidence of volume reduction was observed in thin section, in terms either of textures, distribution of minerals, or of collapse of minerals with weathered cores. These properties may not be sensitive measures of volume changes, but large volume decreases should be evident.

Because volume reduction may have accompanied the weathering observed, the basic assumption of the standard-cell method is questionable. Values calculated by the standard-cell method for elemental abundances in the weathered portion of the rock are therefore overestimates, by the amount of volume reduction, of the abundances resulting from the weathering of the fresh rock. If neither the addition of elements nor the preferential concentration of elements has occurred in the rinds, the volume decrease can be estimated if one element has remained immobile during weathering. Using this assumption for TiO_2 (an assumption discussed in the section on the "TiO_2–constant method"), the outer portion of the rind in sample 109, for example, has undergone more than a 50-percent decrease in volume, because Ti, calculated by the standard-cell method (table 12), has more than doubled. This seems to be an excessive volume decrease to go undetected in the physical properties of the rinds.

Despite the anomalous elemental variations calculated by the standard-cell method, elements that are mineralogically associated behave consistently. For example, Fe and Mg show similar trends, as do Ca and Na. Therefore, it appears that the process that has produced the anomalous elemental variations has affected all the elements proportionately. This relation is consistent with an overall volume reduction, rather than with the addition of elements in solution from extraneous sources or the preferential concentration within the rind. However, neither alternative is attractive, and both volume reduction and additions or preferential concentration may have operated within the rinds. Analytical error, especially in TiO_2 amounts, would also explain some of the anomalies.

WEIGHT-PER-UNIT-VOLUME METHOD

The weight-per-unit-volume method of determining absolute changes in elemental abundances uses bulk density to convert percentage data to weight per unit-volume. However, to compare a given volume of weathered material directly with an equal volume of fresh rock, one must assume that the alteration takes place without volume change. Hendricks and Whittig (1968) used this method to calculate changes accompanying the alteration of andesitic rocks to saprolite. Preservation of the original fabric and structure of the rock suggested to them that minimal volume changes had occurred. Bulk densities measured for the saprolite were very low, as low as 1.1.

An attempt was made to measure bulk densities for the weathering-rind samples in this study. However, the small size of the samples (on the order of 0.1 mm^3), their lack of coherence, and their rather high porosity prevented consistent results using either Jolly balance, air-comparison picnometer, or direct-measurement methods. Consequently, bulk densities were estimated by comparing chemical analyses with the data for similar rock types from Hendricks and Whittig (1968); that is, the ratios of Al_2O_3 and TiO_2 in the fresh rock to those in the weathered rock for samples in this study were compared with those of Hendricks and Whittig's (1968) samples for which bulk densities were known. Changes in bulk density in the weathering rinds, which were deliberately estimated conservatively, are thought to be accurate within about 10–20 percent.

Weights per unit-volume of each elemental oxide were calculated for the weathering-rind samples using the weight-percentage data and the estimated bulk densities (table 13 and fig. 26*B*). The weight-per-unit-volume data appear to be somewhat more reasonable than the standard-cell data, because more elements show a tendency to decrease, rather than to increase. Decreases in Si are consistent with the duration of weathering for each deposit; for example, more than 50 percent for sample 118. The behavior of Al and Fe is somewhat erratic, but they tend to decrease and increase, respectively, with the degree of weathering. All base cations tend to decrease with increasing alteration, although Mg and K increase slightly in some samples. The amount of Ti has a strong tendency to increase with increasing weathering.

Using the same arguments presented in the discussion of the standard-cell method (previous section), all elements should decrease in abundance during the formation of weathering rinds; most of the apparent increases in elemental abundances are probably due to volume decrease during alteration. Therefore, both the

standard-cell and the weight-per-unit-volume data indicate a volume decrease during weathering. Both methods depend on the isovolumetric assumption; if contradicted, the calculated values of elemental abundances in the rinds become overestimates of the amounts resulting from the weathering of the original rock. The fact that mineralogically associated elements behave consistently in both methods adds support to the conclusion that volume decreases during weathering.

The reason that the weight-per-unit-volume data appear to be more reasonable than the standard-cell data is probably due to the conservative estimates of bulk-density changes. If TiO_2 is assumed to remain constant during weathering, the volume decrease for the outer part of the profile of sample 109 is estimated to be less than 40 percent using the weight-per-unit-volume data (table 13), compared to more than 50 percent using the standard-cell data. The difference is probably due to the conservative estimates of bulk-density changes compensating for some of the volume decrease.

TiO_2-CONSTANT METHOD

The third and most widely used method for calculating changes in elemental abundances is based on the assumption that some reference constituent remains constant, or immobile, during weathering. Although this assumption is impossible to prove independently, it can commonly be strongly supported. In addition, the method is not affected by volume changes. The most commonly used reference constituent is Al_2O_3; but Fe_2O_3, TiO_2, and a combination of the three elements are also used (Loughnan, 1969, p. 89; Birkeland, 1974, p. 69).

TiO_2 was used as the reference constituent in this study for several reasons: First, elements that are immobile or nearly immobile during weathering should increase in weight percentage during weathering because of the relative depletion of other elements. Inspection of table 9 indicates that Al_2O_3 and Fe_2O_3 (or total iron) commonly *decrease* with weathering rather than increase. These decreases in weight percentage indicate that alumina and iron are not suitable reference constituents for the samples in this study. On the other hand, TiO_2 increases in weight percentage in the weathering rinds, compared to amounts in the unaltered rocks, in almost every sample.

Second, TiO_2 is virtually insoluble above pH 2.5, and $Ti(OH)_4$ is soluble only below pH 5 (Loughnan, 1969, p. 44). Thus, if titanium is in the dioxide form, it is immobile in virtually all weathering environments. Alumina is immobile in the pH range of 4.5–9.5; iron is immobile in normal oxidizing conditions, but is mobile under reducing conditions (Loughnan, 1969, p. 52). Both alumina and iron can be mobilized by chelating agents in normal weathering environments (Loughnan, 1969, p. 48). Therefore, titanium is potentially the most immobile constituent in basic volcanic rocks, especially if it is released in the dioxide form. Even if titanium is released as $Ti(OH)_4$, it is insoluble above pH 5, and may dehydrate to one of the insoluble crystalline polymorphs of TiO_2 (for instance, anatase; Loughnan, 1969, p. 44).

Loughnan (1969, p. 45) showed a weathered profile on basalt in which there has been differential movement of titanium relative to alumina. He inferred from this relation that titanium has been released as $Ti(OH)_4$ from magnetite and augite and has been mobilized. This conclusion, however, that alumina has remained immobile as a reference is based on an unproved assumption. The converse, that alumina has moved relative to titanium, seems equally likely.

The third reason TiO_2 was used as a reference constituent is that titanium is relatively abundant in the rocks examined in this study and that most of it appears to be concentrated in titanomagnetite. As discussed earlier (fig. 17), this mineral appears to be remarkably stable in the weathering rinds, and it experiences only partial alteration to hematite and maghemite in highly weathered samples. XES data suggest that pyroxene grains in the rocks examined contain little or no titanium. Thus, it appears that most of the titanium tends to be retained in resistant, primary-mineral grains and that the titanium released probably remains immobile.

Assuming that TiO_2 remains immobile, the weight of each elemental oxide in the weathering-rind samples was calculated by multiplying its weight percentage by the ratio of the weight percentage of TiO_2 in the fresh rock to that in the weathered sample (table 14; figs. 26*C*, 27). The calculated values are equivalent to the amounts remaining after the weathering of 100 g of fresh rock. These data appear to be more reasonable than the data calculated using the standard-cell or weight-per-unit-volume methods, because most elements decrease in abundance as weathering increases. However, one cannot rule out the possibility of small losses of titanium during weathering. If some titanium has been lost, the elemental abundances calculated in table 14 are overestimates by the percentage of loss. In some of the rinds for which multiple layers were sampled, TiO_2 weight percentage decreased slightly in the outermost part of the rind compared to that in the next layer inward; this decrease suggests the possibility of slight depletion of TiO_2 in the outermost part of the rind. Such depletion would account for the small increases in Al_2O_3 and SiO_2 in the outermost parts of

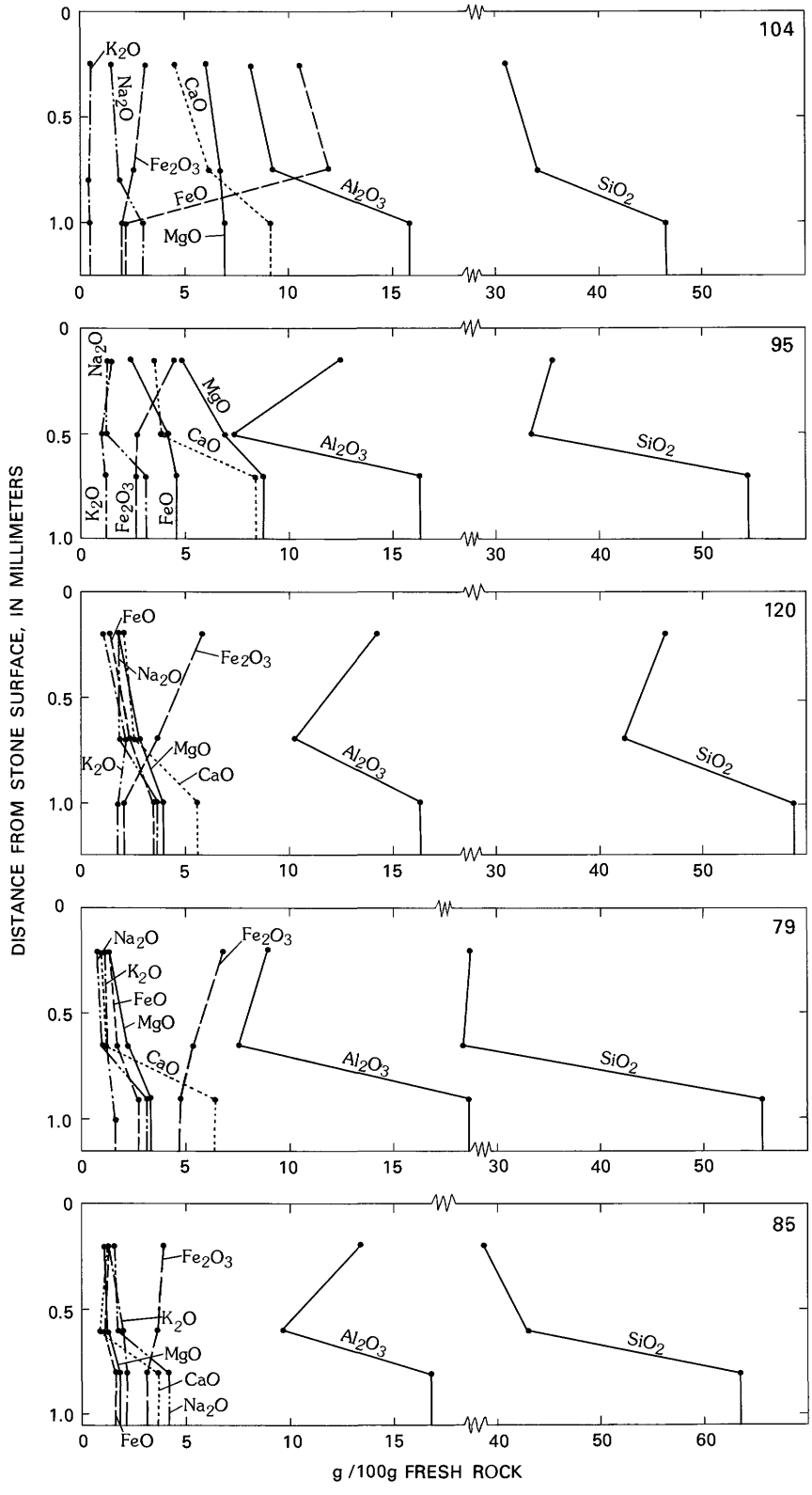

FIGURE 27.—Changes in elemental abundances, calculated assuming TiO_2 constant, for selected weathering-rind samples. Data are from table 14. Data for sample 118 are in figure 26*C*. See table 1 for the deposit and lithology of each sample (numbers).

those rinds in the data calculated assuming TiO_2 constant (fig. 27). Some of the TiO_2 variation could also be due to analytical error.

The observed decreases in abundance are consistent with what appear to be almost entirely degradational processes responsible for forming weathering rinds, and with the poor development of secondary-mineral species (see section on "End products of weathering"). Decreases of more than 50 percent in Al_2O_3 are somewhat unexpected, but Hendricks and Whittig (1968) also showed significant losses of alumina during weathering of similar rock types; such losses could be explained by the influence of chelating agents. The data in table 14 and figure 27 also indicate trends in losses of other elements that are similar to the losses shown by Hendricks and Whittig (1968).

The abundances of elements on an absolute scale can be used to estimate relative elemental mobilities. Because volume decrease affects all elements proportionately, all three methods of determining absolute changes can be used. That these methods yield essentially the same sequence lends further support to the conclusion that individual elements have not been added to the weathering rinds, but that an overall decrease in volume of the weathered material has occurred. The sequence of mobility, based on the abundance of each element in the weathering rinds compared to that in the unaltered rock (table 16), is:

$$Ca \geq Na > Mg > Si > Al \geq K > Fe > Ti.$$

This sequence agrees rather well, except for the position of K, with the general sequence:

$$Ca > Na > Mg > K > Si > Fe > Al,$$

which has been determined by several workers studying stream waters draining igneous rocks (Polynov, 1937; Feth and others, 1964) or the weathering of igneous rocks themselves (Goldich, 1938; Tiller, 1958). The small amount of K originally present may be fixed by incipient formation of halloysite or other kaolin minerals (see section on "End products of weathering").

CHEMICAL CHANGES WITH TIME

The most direct method of estimating chemical changes that occur with time is to compare the changes in rocks that have been subjected to weathering for different amounts of time. This method was used for the outer portions of weathering rinds from different ages of deposits in all the sampling areas. Chemical variation between rocks was accounted for by normalizing the elemental abundances in the weathering rinds by those in the unaltered rock. The weight-percentage data, assuming TiO_2 constant (table 14), were used. The method involves two primary assumptions: (1) that the factors that affect the rate of weathering are identical for sampling sites on different ages of deposits, and (2) that the rate of loss of an element is not significantly dependent on the amount originally present.

The results of these comparisons (table 8) show general trends of depletion of most elements, but many inconsistencies and contradictions exist. Iron, magnesium, and potassium amounts were particularly erratic, and the apparent relative mobility of the elements was inconsistent with that based on the sequences of changes in individual stones. Therefore the basic assumptions of the method appear to be unfounded. More consistent results could probably be obtained with a larger number of samples, which would better define the apparently large variation in the loss of elements within a given age of deposit.

Considering probable ages of deposits sampled (Colman and Pierce, 1981), table 8 suggests that the rate of loss of most elements decreases with time. The decreasing rate of loss of most of the elements is probably due to their rapid release as the primary minerals disintegrate, followed by slower loss as they reach low concentrations and as fine-grained weathering products impede the movement of water. The degree to which the weathering products are more stable than the primary minerals will also tend to slow the loss of elements that they contain. In the outer portions of the rinds in the oldest deposits in each area, the weathered material is composed mostly of allophane, amorphous iron oxide-hydroxide, and poorly developed clay minerals (see section on "End products of weathering"). This composition is consistent with the chemical data, which show that the extensively weathered material is composed primarily of Si, Al, and Fe.

SUMMARY AND CONCLUSIONS

Weathering rinds on basaltic and andesitic stones offer a number of advantages for studying the weathering of these lithologies. These advantages include certainty of the original composition of the weathered material, absence of detrital contamination, and physical preservation of the insoluble weathered material. Mineralogic changes in weathering rinds were observed with the scanning electron microscope combined with X-ray energy spectrometry, thin and polished sections, X-ray diffraction, and differential thermal analysis. Standard chemical analyses of the rocks and weathering rinds were obtained to document the chemical changes occurring during weathering.

The formation of weathering rinds on andesitic and

TABLE 8. —*Ratios of elements in the outermost parts of weathering rinds to that in the unaltered rock*

[Calculated from data assuming TiO_2 constant (table 14). Leaders (—), not analyzed]

Sample	SiO_2	Al_2O_3	Fe_2O_3	FeO	MgO	CaO	Na_2O	K_2O	H_2O^+
105	1.05	1.18	3.67	0.35	0.67	0.70	0.82	0.89	3.59
104	.66	.51	1.55	4.97	.87	.50	.49	.99	3.53
109	.30	.57	3.86	.21	.31	.18	.05	.15	3.63
98	.69	.60	1.00	.77	.73	.62	.58	1.02	3.45
95	.65	.77	1.72	.52	.57	.42	.42	1.18	11.71
102	.43	.40	.95	—	.89	.45	.18	.45	1.46
119	.83	.94	1.62	.71	.75	.53	.67	.71	18.88
120	.79	.87	1.94	.39	.45	.36	.53	.58	4.13
121	.63	.75	1.82	.30	.34	.16	.32	.78	5.12
118	.29	.45	1.22	—	.17	.02	.04	.25	2.16
75	.94	1.25	1.37	.46	.61	.56	.65	.87	12.14
83	.80	.80	1.60	.46	.78	.57	.69	.96	4.44
79	.49	.48	1.39	.48	.38	.13	.26	.74	1.57
84	.85	.95	1.77	.53	.72	.61	.78	.81	6.32
89	.84	.79	1.36	.85	.91	.79	.72	1.17	3.31
85	.61	.81	1.27	.79	.59	.34	.38	.61	4.53
86	.70	1.25	2.16	.50	.47	.26	.32	1.37	3.89

basaltic stones appears to be due largely to degradational processes. Each of the primary minerals alters at a different rate through a series of weathering products. A few of these weathering products have been previously described and named, including chlorophaeite and "iddingsite." But most of the weathering products described here are only arbitrarily defined stages in a continuous process of degradation of the primary minerals and have not been previously named or described. Grain size, degree of fracturing, and chemical zonation appear to be the most important lithologic controls on the variations in the alteration rate of individual minerals.

Volcanic glass and olivine are particularly unstable in the weathering environment, and their alteration quickly imparts oxidation colors to weathering rinds. Opaque minerals, primarily titanomagnetites, are remarkably stable; they exhibit only minor and partial alteration even in severely altered portions of weathering rinds. The stability of pyroxene and plagioclase, which is intermediate and variable, depends on the composition of these minerals. The location and rate of weathering in plagioclase are strongly controlled by chemical zonation.

The fate of all minerals observed in this study is alteration to an X-ray-amorphous mixture of allophane, iron oxide-hydroxide, and poorly developed clay minerals. The presence of allophane is confirmed by its X-ray diffraction, morphological, and chemical characteristics. Previous studies have shown that allophane is commonly an early stage in the transition of primary minerals to clay minerals, and that clay minerals eventually form during the alteration of basalt and andesite. The abundance of allophane in weathering rinds on basalts and andesites suggests that, in the alteration of these lithologies, clay minerals form by condensation and crystallization of the allophane.

Only very fine grained, poorly crystalline, X-ray-amorphous clay minerals were observed in samples of the weathering rinds; the associated soil matrices, however, are commonly part of argillic B horizons, and many contain clear X-ray evidence of crystalline-clay minerals. This relation suggests that the crystalline-clay minerals in the argillic B horizons may not have formed by weathering of primary minerals but may have been derived from extraneous sources. Given the probable ages of some of the deposits from which weathering rinds were sampled, clay-mineral formation by weathering processes in the rinds appears to occur more slowly than is commonly assumed, at least for the environments examined in this study.

Chemical analyses of the weathering rinds, particularly for different layers of the rinds, document the chemical changes accompanying weathering of basalts and andesites. A number of indices portray the alterations well, including the SiO_2:R_2O_3 ratio, bases:R_2O_3 ratio, Parker's (1970) index, Reiche's (1943; 1950) WPI and PI indices, molecular percentage of water, Fe_2O_3:FeO ratio, and SiO_2-R_2O_3-bases triangular plots. The general trends demonstrated by these indices are large losses of bases, some depletion of SiO_2, relative concentration of R_2O_3, oxidation of iron, and incorporation of water during weathering.

Three methods were used to estimate absolute changes in individual elements during weathering: (1) the standard-cell method (Barth, 1948), (2) the weight-per-unit-volume method using bulk densities, and (3) the method assuming an immobile reference

constituent (TiO_2). The first two methods assume that the alteration is isovolumetric; they underestimate chemical changes in weathering rinds, because volume reduction appears to have accompanied the alteration in weathering rinds. The relative elemental mobilities determined by the third method are:

$$Ca \geqslant Na > Mg > Si > Al \geqslant K > Fe > Ti.$$

All elements, except perhaps Ti, are continuously depleted during weathering.

Absolute chemical changes as functions of time are difficult to estimate because of variation in factors affecting the rate of weathering between deposits of different ages. However, the data suggest that the rate of loss of most elements decreases with time.

REFERENCES CITED

Abbott, A. T., 1958, Occurrence of gibbsite on the island of Kauai, Hawaiian Islands: Economic Geology, v. 53, p. 842–855.

Aomine, S., and Wada, K., 1962, Differential weathering of volcanic ash and pumice, resulting in the formation of hydrated halloysite: American Mineralogist, v. 47, p. 1024–1048.

Barshad, I., 1964, Chemistry of soil development, *in* Bear, F. E., ed., Chemistry of the soil: New York, Reinhold Publishing Corporation, p. 1–70.

_____1966, The effect of variation in precipitation on the nature of clay mineral formation in soils from acid and basic igneous rocks: International Clay Conference, Jerusalem, 1966, Proceedings, v. 1, p. 167–173.

Barth, T. W., 1948, Oxygen in rocks a basis for petrographic calculations: Journal of Geology, v. 56, p. 50–61.

Bates, T. F., 1959, Morphology and crystal chemistry of 1:1 layer lattice silicates: American Mineralogist, v. 44, p. 78–114.

_____1962, Halloysite and gibbsite formation in Hawaii: Proceedings of National Conference of Clays and Clay Minerals, v. 9, p. 307–314.

Birkeland, P. W., 1963, Pleistocene volcanism and deformation of the Truckee area, north of Lake Tahoe, California: Geological Society of America Bulletin, v. 74, p. 1453–1464.

_____1974, Pedology, weathering, and geomorphological research: New York, Oxford University Press, 285 p.

Birrell, K. S., and Fieldes, M., 1952, Allophane in volcanic ash soils: Journal of Soil Science, v. 3, p. 156–166.

Butler, J. R., 1954, The geochemistry and mineralogy of rock weathering, Part II, The Nordmarka area, Oslo: Geochimica Cosochimica Acta, v. 6, p. 268–281.

Carroll, D., 1970, Rock weathering: New York, Plenum Press, 203 p.

Carroll, D., and Hathaway, J. C., 1963, Mineralogy of selected soils from Guam: U.S. Geological Survey Professional Paper 403-F, 53 p.

Carroll, D., and Woof, M., 1951, Laterites developed on basalt of Inverall, New South Wales: Soil Science, v. 72, p. 87–99.

Christiansen, R. L., and Blank, H. R., Jr., Volcanic Stratigraphy of the Quaternary rhyolite plateau in Yellowstone National Park: U.S. Geological Survey Professional Paper 729-B, 18 p.

Colman, S. M., and Pierce, K. L., 1981, Weathering rinds on andesitic and basaltic stones as a Quaternary age indicator, Western United States: U.S. Geological Survey Professional Paper 1210, 56 p.

Craig, D. C., and Loughnan, F. C., 1964, Chemical and mineralogic transformations accompanying the weathering of basic volcanic rocks from New South Wales: Australian Journal of Soil Research, v. 2, p. 218–234.

Crandell, D. R., 1963, Surficial geology and geomorphology of the Lake Tapps quadrangle, Washington: U.S. Geological Survey Professional Paper 388-A, 84 p.

Dan, J., and Yaalon, D. H., 1971, On the origin and nature of the paleopedological formations in the coastal desert fringe areas of Israel, *in* Yaalon, D. H., ed., Paleopedology: Jerusalem, Israel University Press, p. 245–260.

DeKimpe, C., Gatusche, M. C., and Brindley, G. W., 1961, Ionic coordination in alumino-silica gels in relation to clay mineral formation: American Mineralogist, v. 46, p. 1370–1381.

Eyles, V. A., 1952, The composition and origin of Antrim laterites and bauxites: Geological Survey of Northern Ireland Memoir, 90 p.

Fairbairn, H. W., 1943, Packing in ionic minerals: Geological Society of America Bulletin, v. 54, p. 1305–1374.

Feth, J. H., Robertson, C. E., and Polzer, W. L., 1964, Sources of mineral constituents in water from granitic rocks, Sierra Nevada, California and Nevada: U.S. Geological Survey Water Supply Paper 1535-I, 70 p.

Fieldes, M., 1966, The nature of allophane in soils., Part 1, Significance of structural randomness in pedogenesis: New Zealand Journal of Science, v. 9, p. 599–607.

Fieldes, M., and Furkert, R. J., 1966, The nature of allophane in soils, Part 2, Differences in composition: New Zealand Journal of Science, v. 9, p. 608–622.

Fieldes, M., and Perrott, K. W., 1966, The nature of allophane in soils, Part 3, Rapid field and laboratory test for allophane: New Zealand Journal of Science, v. 9, p. 623–629.

Fieldes, M., and Swinedale, L. D., 1954, Chemical weathering of silicates in soil formation: Journal of Science Technology of New Zealand, v. 56, p. 140–154.

Fiske, R. S., Hopson, C. A., and Waters, A. C., 1963, Geology of Mount Rainier National Park, Washington: U.S. Geological Survey Professional Paper 444, 93 p.

Foster, R. J., 1958, The Teanaway dike swarm of central Washington: American Journal of Science, v. 256, p. 644–653.

Gay, P., and LeMaitre, R. W., 1961, Some observations on "iddingsite": American Mineralogist, v. 46, p. 92–111.

Gile, L. H., 1977, Holocene soils and soil-geomorphic relations in a semi-arid region of southern New Mexico: Quaternary Research, v. 7, p. 112–132.

Goldich, S. S., 1938, A study on rock weathering: Journal of Geology, v. 46, p. 17–58.

Greene-Kelly, R., 1957, The montmorillonite minerals (smectites), *in* MacKenzie, R. C., ed., Differential thermal investigation of clays: Oxford, Alden Press, p. 140–164.

Grim, R. E., 1968, Clay mineralogy: New York, McGraw-Hill, 596 p.

Gruner, J. W., 1950, An attempt to arrange silicates in order of reaction energies at relatively low temperatures: American Mineralogist, v. 35, p. 137–148.

Hanlon, F. N., 1944, The bauxites of New South Wales, their distribution, composition, and probable origin: Royal Society of New South Wales Journal and Proceedings, v. 78, p. 94–112.

Hardy, F., and Rodrigues, G., 1939, Soil genesis from andesite in Grenada, BWI: Soil Science, v. 48, p. 361–384.

Hay, R. L., 1959, Origin and weathering of late Pleistocene ash deposits on St. Vincent, BWI: Journal of Geology, v. 67, p. 65–87.

_____1960, Rate of clay formation and mineral alteration in a 4,000-year-old volcanic ash on St. Vincent, BWI: American Journal of Science, v. 258, p. 354-368.

Hay, R. L., and Iijima, A., 1968, Nature and origin of palagonite tuffs of the Honolulu Group on Oahu, Hawaii: Geological Society of America Memoir 116, p. 331-376.

Hay, R. L., and Jones, B. F., 1972, Weathering of basaltic tephra on the island of Hawaii: Geological Society of America Bulletin, v. 83, p. 317-332.

Hendricks, D. M., and Whittig, L. D., 1968, Andesite weathering, Part II, Geochemical changes from andesite to saprolite: Journal of Soil Science, v. 19, p. 147-153.

Holdridge, D. A., and Vaughan, F., 1957, The kaolin minerals (kandites), *in* MacKenzie, R. C., ed., Differential thermal investigation of clays: Oxford, Alden Press, p. 98-139.

Hough, G. J., and Byers, H. G., 1937, Chemical and physical studies of certain Hawaiian soil profiles: U.S. Department of Agriculture Technical Bulletin no. 584, 26 p.

Hutton, J. T., and Stephens, C. G., 1956, Paleopedology of Norfolk Island: Journal of Soil Science, v. 7, p. 255-267.

Jackson, M. L., and Sherman, G. D., 1953, Chemical weathering of minerals in soils: Advances in Agronomy, v. 5, p. 219-318.

Jenny, H., 1941, Factors of soil formation: New York, McGraw-Hill, 281 p.

Kanno, I., 1959, Clay minerals of Quaternary volcanic ash soils and pumices from Japan: Advances in Clay Science, v. 1, p. 213-233.

Keller, W. D., 1954, The energy factor in sedimentation: Journal of Sedimentation and Petrology, v. 24, p. 62-68.

Krauskopf, K. B., 1967, Introduction to geochemistry: New York, McGraw-Hill, 721 p.

Lifshitz-Rottman, H., 1971, Natural and experimental weathering of basalts: New Mexico Institute of Mining and Technology Ph.D. dissertation, 123 p.

Linares, J., and Huertas, F., 1971, Kaolinite: Synthesis at room temperatures: Science, v. 171, p. 896-897.

Loughnan, F. C., 1969, Chemical weathering of the silicate minerals: New York, American Elsevier Publishing Company, 154 p.

Mehra, O. P., and Jackson, M. L., 1960, Iron oxide removal from soils and clays by a dithionite-citrate system buffered with sodium bicarbonate: Clays and Clay Minerals, v. 7, p. 317-327.

Millot, G., 1970, Geology of clays: New York, Springer-Verlag, 429 p.

Mitchell, D. D., and Farmer, V. C., 1962, Amorphous clay minerals in some Scottish soil profiles: Clay Minerals Bulletin, v. 28, p. 128-144.

Morrison, R. B., 1967, Principles of Quaternary soil stratigraphy, *in* Morrison, R. B., and Wright, H. E., eds., Quaternary soils: INQUA Congress, VII, 1965, Proceedings, v. 9, p. 1-70.

Nichols, K. D., and Tucker, B. M., 1956, Pedology and chemistry of the basaltic soils of the Lismore District, New South Wales: Commonwealth Science Industry Research Organization of Australia, Soil Publication 7, 153 p.

Nixon, R. A., 1979, Formation of allophane from some granitic rocks: Geological Society of America, Abstracts with Programs, v. 11, no. 4, p. 207.

Ollier, C. D., 1969, Weathering: Edinburgh, Oliver and Boyd, 304 p.

Parker, A., 1970, An index of weathering for silicate rocks: Geology Magazine, v. 107, p. 501-504.

Peacock, M. A., and Fuller, R. E., 1928, Chlorophaeite, sideromelane, and palagonite from the Columbia River plateau: American Mineralogist, v. 13, p. 360-382.

Pettijohn, F. J., 1941, Persistence of heavy minerals and geologic age: Journal of Geology, v. 49, p. 610-625.

Polynov, B. B., 1937, The cycle of weathering: London, Murby, 220 p. (A. Muir transl.).

Reiche, P., 1943, Graphic representation of chemical weathering: Journal of Sedimentary Petrology, v. 13, p. 58-68.

_____1950, A survey of weathering processes and products: New Mexico University Publication in Geology, no. 3, 95 p.

Roberson, R. H. S., 1963, Allophanic soil from Trail Bridge, Oregon, with notes on mosaic growth in clay minerals: Clay Mineralogy Bulletin, v. 5, p. 237-247.

Ross, C. S., and Kerr, P. F., 1934, Halloysite and allophane: U.S. Geological Survey Professional Paper 185-G, p. 135-148.

Sherman, G. D., and Uehara, G., 1956, The weathering of olivine basalt in Hawaii and its pedogenic significance: Soil Science Society of America Proceedings, v. 20, p. 337-340.

Siffert, B., 1967, Some reactions of silica in solution—formation of clay: Jerusalem, Israel Program for Scientific Translations, 100 p.

Stevens, R. E., and Carron, M. K., 1948, Simple field test for distinguishing minerals by abrasion pH: American Mineralogist, v. 33, p. 31-49.

Swinedale, L. D., 1966, A mineralogic study of soils derived from basic and ultrabasic rocks in New Zealand: New Zealand Journal of Science, v. 9, p. 484-506.

Syers, J. K., Jackson, M. L., Berkheiser, V. E., Clayton, R. N., and Rex, R. W., 1969, Eolian sediment influence on pedogenesis during the Quaternary: Soil Science, v. 107, p. 421-427.

Tan, K. H., 1969, Chemical and thermal characteristics of allophanes in andosols of tropics: Soil Science Society of America Proceedings, v. 33, p. 469-472.

Tiller, K. G., 1958, Geochemistry of some basaltic materials—associated soils of southeastern South Australia: Journal of Soil Science, v. 9, p. 225-241.

Wada, K., 1967, A structural scheme of soil allophane: American Mineralogist, v. 52, p. 690-708.

Williams, H., 1932, Geology of Lassen Volcanic National Park, California: California University Department of Geology Science Bulletin, v. 21, no. 8, p. 195-385.

Yoshinaga, N., Yoisumoto, H., and Ibe, K., 1968, An electron microscopic study of soil allophane with an ordered structure: American Mineralogist, v. 53, p. 319-323.

APPENDIXES 1 and 2

APPENDIX 1.—GENERALIZED PETROGRAPHIC DESCRIPTIONS

The following are generalized petrographic descriptions of the rock types in each of the major study areas on which weathering rinds were measured.

BASALTS

WEST YELLOWSTONE

Basalts examined near West Yellowstone, Mont., are derived from the Pleistocene Madison River Basalt of Christiansen and Blank (1972). The rocks commonly contain scattered phenocrysts of plagioclase as much as 1 mm long and less commonly contain phenocrysts of olivine as much as 0.5 mm in diameter, locally forming glomeroporphyritic clusters. The matrix consists of plagioclase, in laths 0.1–0.2 mm long; crystals of clinopyroxene, olivine, and opaque minerals, about 0.05–0.1 mm in diameter; and irregular-shaped masses of basaltic glass and chlorophaeite. Matrix textures are mostly intergranular to intersertal and are less commonly subophitic. Visual estimates of the modal composition are: plagioclase, 45–55 percent; pyroxene, 25–30 percent; olivine, 5–10 percent; glass and chlorophaeite, 5–10 percent; and opaque minerals about 10 percent.

McCALL

Rocks examined near McCall, Idaho, are extremely uniform in texture and composition, and are probably derived from the upper part of the Miocene Yakima Basalt Subgroup of the Columbia River Basalt Group (John Bond, oral commun., 1976). The rocks, which are mostly aphanitic, contain plagioclase laths 0.1–0.2 mm long (and contain scattered microphenocrysts up to 0.5 mm long); crystals of clinopyroxene, olivine, and opaque minerals 0.05–0.01 mm in diameter; and masses of glass, chlorophaeite, and calcite of irregular shape. The textures are mostly intersertal to hyalo-ophitic and are less commonly intergranular to subophitic. Visual estimates of the modal composition are plagioclase, 45–55 percent; pyroxene, 20–30 percent; olivine, 0–5 percent; calcite, 0–5 percent; glass and chlorophaeite, 15–20 percent, and opaque minerals, 10–15 percent.

YAKIMA VALLEY

Rocks examined from the Yakima Valley, Wash., are derived from the Eocene Teanaway Basalt (Foster, 1958). They are mostly aphanitic, but some contain scattered phenocrysts of plagioclase or opaque minerals 0.3–0.5 mm in longest dimension. Grain size generally ranges between 0.05 and 0.2 mm, and textures are mostly intersertal; less commonly, textures are intergranular, hyalo-ophitic, and subophitic. Visual estimates of the modal composition are: plagioclase, some of which is zoned, 45–55 percent; clinopyroxene, 25–35 percent; olivine, 0–10 percent; opaque minerals, 5–10 percent; glass, chlorophaeite, and (or) chlorite, 10–20 percent; and rare (< 1 percent) potassium feldspar.

PUGET LOWLAND

The precise source of the basalt in the Puget Lowland drifts in Washington is not known, but it is probably mostly drived from the Eocene Crescent Formation in the Olympic Mountains. The basalt contains microphenocrysts of plagioclase, 0.5–0.8 mm long, and clinopyroxene, 0.3–0.5 mm in diameter. The matrix consists mostly of thin plagioclase laths 0.3–0.5 mm long; equant clinopyroxenes 0.05–0.1 mm in diameter; and masses of devitrified glass, chlorophaeite, and chlorite of irregular shape. Glass is rarely present. Textures are mostly intersertal and are less commonly hyalo-ophitic. Visual estimates of the modal composition are: plagioclase, 40–55 percent; clinopyroxene, 25–35 percent; olivine, 0–1 percent; opaque minerals, 5–10 percent; and altered glass and chlorite, 10–20 percent.

ANDESITES

Weathering rinds from sampling areas containing andesitic rocks were measured on two groups of stones: "coarse grained" and "fine grained." The two textural groups represent an arbitrary field classification based on phenocryst content and matrix texture.

MT. RAINIER

Most of the rocks examined from the Mt. Rainier area, Washington, are derived from the Quaternary Mt. Rainier Andesite of Fiske and others (1963), although some weathering rinds were measured on stones derived from older volcanic rocks. Mt. Rainier Andesite is a hypersthene andesite that is remarkably uniform in composition.

The fine-grained andesites contain scattered phenocrysts 0.5–1.5 mm in largest dimension, but microphenocrysts 0.1–0.3 mm long are more abundant.

Plagioclase is the most abundant phenocryst, with lesser amounts of pyroxene and a few crystals of amphibole and olivine. Both the plagioclase and the pyroxene are typically zoned, and the plagioclase shows a wide range in degree of zoning. Both ortho- and clinopyroxenes are present; slightly pleochroic orthopyroxene (hypersthene?) is more abundant. Amphiboles and some pyroxenes have reaction rims of iron oxides. The very fine grained matrix (0.01–0.05 mm) appears to consist mostly of plagioclase, pyroxene, opaques, and glass. Visual estimates of the modal composition are: plagioclase, 45–50 percent; pyroxene, 30–35 percent; opaques, 5–10 percent; glass, 5–10 percent; amphibole, 0–1 percent; and olivine 0–1 percent. Textures are primarily hyalopilitic.

Coarse-grained andesites are similar compositionally to fine-grained andesites. Grain size is highly bimodal; the rocks contain abundant, large (0.5–3.0 mm) phenocrysts of plagioclase and pyroxene, and rare phenocrysts of olivine and opaque minerals, in a very fine grained (0.01–0.03 mm) matrix. The pyroxene phenocrysts commonly occur in glomeroporphyritic clusters. Textures range from hyalopilitic to pilotaxitic.

LASSEN PEAK

Rocks examined from the Lassen Peak area, California, are derived from the andesitic flows that make up the volcanic complex around Lassen Peak (Williams, 1932). The mineralogy of these andesites is variable.

The fine-grained andesities are nonporphyritic to weakly porphyritic. Phenocrysts, if present, range from 0.3–1.5 mm in size; plagioclase, some of which is zoned, is generally the largest and most abundant phenocryst; phenocrysts of chino- or orthopyroxenes and olivine are less common. The matrix is typically fine grained (0.08–0.1 mm) and consists of plagioclase, pyroxene, opaque minerals and glass; it also contains rare calcite, potassium feldspar, and olivine. In rocks containing calcite or olivine, clinopyroxene is more abundant than is orthopyroxene. Textures are mainly pilotaxitic to intergranular. Visual estimates of the modal composition are: plagioclase, 40–60 percent; pyroxene, 25–40 percent; opaques, 5–10 percent; glass, 0–15 percent; potassium feldspar, 0–10 percent; calcite, 0–5 percent; and olivine, 0–15 percent.

The coarse-grained andesites have similar mineralogy, except that they contain very little glass. Phenocrysts are abundant; the most common is plagioclase (1.0–2.0 mm long), which is commonly zoned. Pyroxene and olivine phenocrysts range from 0.6–1.2 mm; phenocrysts of clinopyroxenes are more abundant than are those of orthopyxorenes. The matrix grain size is about 0.1–0.2 mm, and textures are mostly intergranular to pilotaxitic.

TRUCKEE

The rocks examined from near Truckee, Calif., are derived mostly from the late Tertiary andesites that are abundant in the area. A few basalt clasts (those without olivine phenocrysts) from the Pliocene and Pleistocene Lousetown Formation may have been included with the fine-grained andesites (Birkeland, 1963).

The fine-grained andesites contain microphenocrysts (0.1–0.3 mm) and a few scattered phenocrysts (as much as 2 mm). The phenocrysts are plagioclase, pyroxene, olivine, and amphibole in varying proportions; the microphenocrysts are plagioclase (more abundant) and pyroxene. A few of the plagioclase and pyroxene phenocysts are zoned. Clinopyroxene is commonly more abundant than orthopyroxene. The matrix is very fine grained (0.02–0.07 mm) and consists mostly of plagioclase, pyroxene, and opaque minerals. Glass is scarce. Visual estimates of the modal composition are: plagioclase, 50–65 percent; pyroxene, 20–35 percent; opaques, 5–10 percent; olivine, 0–10 percent; amphibole, 0–5 percent; glass, 0–5 percent. Textures are primarily pilotaxitic to trachytic.

The coarse-grained andesites are similar mineralogically and texturally to the fine-grained andesites. They contain abundant phenocrysts of plagioclase and pyroxene (0.5–2.0 mm) in a matrix whose grain size is generally 0.01–0.1 mm.

APPENDIX 2.—TABLES OF ANALYTICAL DATA

TABLE 9.—*Weight percentage, sample interval, and bulk density*

[For samples 109-a2, 109-a3, 102 (all), and 118 (all), Na_2O and MgO determined by atomic absorption; other elements determined by X-ray fluorescence; total Fe as Fe_2O_3. All other samples analyzed by "rapid rock" (wet-chemical) methods. Leaders (—), not analyzed]

Sample[1] No.	Interval[2]	Bulk density[3]	SiO_2	Al_2O_3	Fe_2O_3	FeO	MgO	CaO	Na_2O	K_2O	TiO_2	P_2O_5	MnO	CO_2	H_2O^+	H_2O^-	Sum
109-a1	0.0-0.5	2.1	35.6	17.6	16.0	4.4	2.8	3.2	0.30	0.50	4.8	0.40	0.20	0.10	9.5	3.4	98.8
109-a2	0.5-1.4	2.4	38.0	12.0	21.0	—	5.3	7.2	1.01	.81	3.9	<1	.18	.00	10.7	—	100.
109-a3	1.4-2.0	2.6	41.0	12.0	18.	—	5.3	8.3	1.84	.81	3.1	<1	.20	.00	9.5	—	100.
109-a4	>2.0	2.8	53.7	14.1	1.9	9.8	4.2	8.1	2.8	1.5	2.2	.40	.20	.10	1.2	.3	100.5
105-a1	0.0-0.5	2.7	53.6	16.8	7.0	3.0	2.7	5.4	2.2	1.1	2.0	.30	.20	.10	4.1	1.8	100.3
105-a2	>0.5	2.8	53.4	15.0	2.0	9.0	4.2	8.1	2.8	1.3	2.1	.40	.20	10	1.2	.5	100.3
104-a1	0.0-0.5	2.3	43.8	11.5	4.4	14.8	8.5	6.4	2.1	.70	3.4	.30	.20	.10	2.5	.3	99.5
104-a2	0.5-1.0	2.6	43.9	11.9	3.2	15.3	8.7	7.9	2.4	.50	3.1	.40	.20	.10	1.1	.1	98.8
104-a3	>1.0	2.8	46.5	15.8	2.0	2.1	6.9	9.1	3.0	.50	2.4	.30	.20	.10	.5	.2	99.6
102-a1	0.0-0.7	2.4	36.0	9.6	23.	—	6.40	6.6	.96	.74	3.8	<1	.26	.00	12.6	—	100.
102-a2	0.7-1.5	2.5	40.0	11.0	20.	—	6.05	7.7	1.76	.74	3.2	<1	.24	.00	9.3	—	100.
102-a3	>1.5	2.8	48.0	14.0	14.	—	4.18	8.5	3.05	.96	2.2	<1	.19	.00	5.0	—	100.
98-a1	0.0-0.4	2.5	46.1	13.2	5.5	10.5	6.5	7.9	2.3	.70	3.3	.30	.20	.10	1.9	.1	98.6
98-a2	>0.4	2.8	48.8	15.9	4.0	9.9	6.5	9.2	2.9	.50	2.4	.30	.20	.10	.4	.1	101.2
118-a1	0.0-2.6	1.7	39.0	16.	19.	—	1.6	.29	.31	.72	2.6	<1	.09	.00	20.4	—	100.
118-a2	2.6-5.2	2.0	39.0	7.2	27.	—	2.45	.49	.49	.95	3.4	<1	.09	.00	18.9	—	100.
118-a3	5.2-7.8	2.4	47.0	7.5	21.	—	4.98	1.5	.95	1.5	3.0	<1	.12	.00	12.4	—	100.
118-a4	>7.8	2.7	57.0	15.0	6.6	—	3.90	7.5	3.6	1.2	1.1	<1	.11	.00	4.0	—	100.
95-a1	0.0-0.3	2.4	47.6	16.8	6.0	3.2	6.6	4.7	1.8	1.9	1.1	.17	.23	.01	6.6	2.4	99.
95-a2	0.3-0.7	2.5	52.8	11.6	4.3	6.4	10.9	6.3	2.0	1.6	1.3	.11	.19	.01	2.2	1.1	101.
95-a3	>0.7	2.8	54.5	16.3	2.6	4.6	8.7	8.4	3.2	1.2	.82	.25	.13	.02	.42	.3	101.
119-a1	0.0-0.2	2.5	54.5	16.9	4.1	2.8	3.2	3.7	3.0	1.4	1.1	.41	.11	.02	5.4	3.0	100.
119-a2	>0.2	2.7	59.8	16.4	2.3	3.6	3.9	6.3	4.1	1.8	1.0	.35	.10	.02	.26	.2	100.
120-a1	0.0-0.4	2.3	57.9	17.8	5.1	1.7	2.2	2.5	2.4	1.3	1.2	.15	.09	.01	6.2	2.5	101.
120-a2	0.4-1.0	2.4	57.3	13.8	5.0	3.2	3.9	3.5	2.6	3.0	1.3	.14	.11	.03	3.5	1.2	99.
120-a3	>1.0	2.7	58.9	16.4	2.1	3.5	3.9	5.6	3.6	1.8	.96	.34	.10	.02	1.2	.45	99.
121-a1	0.0-0.6	2.1	55.9	19.3	6.4	1.4	1.4	1.2	1.8	1.6	1.2	.14	.07	.01	7.2	2.7	100.
121-a2	0.6-1.6	2.4	63.5	12.9	4.3	4.1	3.9	1.9	2.7	2.0	1.5	.08	.11	.02	2.1	.8	100.
121-a3	1.6-2.8	2.5	61.9	14.1	3.0	4.7	4.2	2.5	3.0	1.8	1.3	.10	.13	.01	1.9	1.1	100.
121-a4	>2.8	2.7	60.3	17.5	2.4	3.2	2.8	5.1	3.8	1.4	.82	.24	.09	.01	.96	.55	99.
75-b1	0.0-0.1	2.6	53.7	20.7	4.8	1.2	1.9	3.4	2.4	1.6	.70	.30	.09	.00	7.2	3.4	101.
75-b2	>0.1	2.7	58.5	17.1	3.6	2.7	3.2	6.3	3.8	1.9	.72	.32	.11	.02	.61	.3	99.
83-b1	0.0-0.2	2.5	51.0	15.9	7.7	2.2	6.2	5.4	2.9	2.3	1.8	.70	.15	.00	3.3	1.1	101.
83-b2	>0.2	2.7	53.2	16.5	4.0	4.0	6.6	7.9	3.5	2.0	1.5	.56	.12	.01	.62	.6	101.
79-b1	0.0-0.4	2.2	50.3	16.5	12.4	2.4	2.3	1.6	1.5	2.2	1.5	.24	.16	.02	6.1	2.0	99.
79-b2	0.4-0.9	2.3	52.5	14.8	10.6	3.5	4.1	2.3	2.0	2.3	1.6	.20	.18	.01	4.5	1.8	100.
79-b3	>0.9	2.7	55.8	18.6	4.8	2.7	3.3	6.4	3.1	1.6	.81	.25	.13	.02	2.1	.8	100.
84-a1	0.0-0.1	2.5	49.6	17.6	4.9	3.0	5.7	6.2	2.6	.98	.95	.25	.13	.00	5.1	1.6	99.
84-a2	>0.1	2.7	53.0	16.7	2.5	5.1	7.2	9.2	3.0	1.1	.86	.32	.13	.00	.73	.2	100.
89-a1	0.0-0.4	2.5	46.0	14.2	5.8	8.8	7.3	8.6	2.5	.59	2.3	.45	.23	.02	1.6	.3	99.
89-a2	>0.4	2.7	47.5	15.7	3.7	9.0	7.0	9.5	3.0	.44	2.0	.34	.17	.02	.42	.1	99.
85-a1	0.0-0.4	2.2	55.1	19.3	5.6	1.8	1.5	1.8	2.3	1.9	.84	.11	.12	.02	7.1	1.4	99.
85-a2	0.4-0.8	2.6	64.8	14.5	5.6	1.6	1.7	1.4	2.7	2.8	.89	.08	.10	.01	3.1	.7	100.
85-a3	>0.8	2.7	63.4	16.8	3.1	1.6	1.8	3.7	4.2	2.2	.59	.19	.08	.02	1.1	.45	99.
86-a1	0.0-0.6	2.4	36.7	23.6	7.1	2.4	3.9	1.9	.79	.69	.74	.21	.09	.01	14.0	8.4	101.
86-a2	0.6-0.9	2.5	41.0	17.8	4.4	5.4	9.1	4.0	.98	.49	.85	.25	.15	.01	9.2	6.4	100.
86-a3	>0.9	2.7	50.8	18.3	3.2	4.7	8.0	7.0	2.4	.49	.72	.13	.13	.01	3.5	1.4	101.

[1]See table 1 for description of samples.

[2]In mm, 0=rock surface.

[3]Estimated by comparison with Hendricks and Whittig's (1968) data for similar rock types, on the basis of ratios of Al_2O_3 and TiO_2 in the weathered rock to those in the fresh rock.

TABLE 10.—*Molecular percentages*
[Leaders (—), not analyzed]

Sample No	SiO_2	Al_2O_3	Fe_2O_3	FeO	MgO	CaO	Na_2O	K_2O	TiO_2	P_2O_5	MnO	CO_2	H_2O^+	Sum
109-a1	35.73	10.39	6.04	3.69	4.18	3.44	0.29	0.32	3.65	0.17	0.17	0.14	31.78	100.00
109-a2	34.92	6.49	7.25	—	7.25	7.09	.90	.47	2.71	.00	.14	.00	32.77	100.00
109-a3	37.93	6.53	6.26	—	7.30	8.23	1.65	.48	2.17	.00	.16	.00	29.30	100.00
109-a4	56.15	8.67	.75	8.56	6.54	9.07	2.83	1.00	1.74	.18	.18	.14	4.18	100.00
105-a1	55.33	10.20	2.72	2.59	4.15	5.97	2.20	.72	1.56	.13	.17	.14	14.11	100.00
105-a2	56.19	9.28	.79	7.91	6.58	9.13	2.85	.87	1.67	.18	.18	.14	4.21	100.00
104-a1	44.73	6.91	1.69	12.63	12.92	7.00	2.08	.46	2.63	.13	.17	.14	8.51	100.00
104-a2	46.00	7.33	1.26	13.40	13.57	8.87	2.43	.33	2.46	.18	.18	.14	3.84	100.00
104-a3	54.41	10.88	.88	2.05	12.02	11.41	3.40	.37	2.13	.15	.20	.16	1.95	100.00
102-a1	31.75	4.98	7.63	—	8.40	6.24	.82	.42	2.54	.00	.19	.00	37.04	100.00
102-a2	37.37	6.04	7.02	—	8.41	7.71	1.59	.44	2.26	.00	.19	.00	28.96	100.00
102-a3	48.54	8.33	5.32	—	6.29	9.21	2.98	.62	1.69	.00	.16	.00	16.85	100.00
98-a1	48.64	8.19	2.18	9.26	10.21	8.93	2.35	.47	2.64	.13	.18	.14	6.68	100.00
98-a2	51.82	9.93	1.60	8.78	10.28	10.47	2.98	.34	1.93	.13	.18	.14	1.42	100.00
118-a1	30.22	7.29	5.53	—	1.85	.24	.23	.36	1.53	.00	.06	.00	52.69	100.00
118-a2	31.38	3.41	8.17	—	2.93	.42	.38	.49	2.07	.00	.06	.00	50.69	100.00
118-a3	41.26	3.87	6.93	—	6.51	1.41	.81	.84	2.00	.00	.09	.00	36.29	100.00
118-a4	56.63	8.77	2.47	—	5.77	7.98	3.46	.76	.83	.00	.09	.00	13.25	100.00
95-a1	46.06	9.56	2.18	2.59	9.51	4.87	1.69	1.17	.81	.07	.19	.01	21.29	100.00
95-a2	52.25	6.75	1.60	5.29	16.06	6.68	1.92	1.01	.97	.05	.16	.01	7.26	100.00
95-a3	56.19	9.89	1.01	3.96	13.36	9.28	3.19	.79	.64	.11	.11	.03	1.44	100.00
119-a1	54.51	9.94	1.54	2.34	4.77	3.97	2.90	.89	.83	.17	.09	.03	18.00	100.00
119-a2	64.39	10.39	.93	3.24	6.25	7.27	4.27	1.23	.82	.16	.09	.03	.93	100.00
120-a1	56.46	10.21	1.87	1.39	3.19	2.61	2.27	.81	.89	.06	.07	.01	20.15	100.00
120-a2	59.19	8.39	1.94	2.76	6.00	3.87	2.60	1.97	1.02	.06	.10	.04	12.05	100.00
120-a3	62.87	10.30	.84	3.12	6.20	6.40	3.72	1.22	.78	.15	.09	03	4.27	100.00
121-a1	54.80	11.13	2.36	1.15	2.04	1.26	1.71	1.00	.89	.06	.06	.01	23.53	100.00
121-a2	66.04	7.89	1.68	3.56	6.04	2.12	2.72	1.32	1.18	.04	.10	.03	7.28	100.00
121-a3	64.67	8.67	1.18	4.10	6.53	2.80	3.03	1.20	1.03	.04	.11	.01	6.62	100.00
121-a4	65.27	11.14	.98	2.89	4.51	5.91	3.98	.97	.67	.11	.08	.01	3.46	100.00
75-b1	52.02	11.80	1.75	.97	2.74	3.53	2.25	.99	.51	.12	.07	.00	23.25	100.00
75-b2	64.00	11.00	1.48	2.47	5.21	7.38	4.02	1.32	.60	.15	.10	.03	2.22	100.00
83-b1	52.49	9.63	2.98	1.89	9.50	5.95	2.89	1.51	1.40	.30	.13	.00	11.32	100.00
83-b2	56.44	10.30	1.60	3.55	10.42	8.98	3.59	1.35	1.21	.25	.11	.01	2.19	100.00
79-b1	52.18	10.07	4.84	2.08	3.55	1.78	1.51	1.45	1.18	.11	.14	.03	21.09	100.00
79-b2	54.38	9.02	4.13	3.03	6.32	2.55	2.00	1.52	1.26	.09	.16	.01	15.54	100.00
79-b3	59.08	11.58	1.91	2.39	5.20	7.26	3.18	1.08	.65	.11	.12	.03	7.41	100.00
84-a1	49.35	10.30	1.83	2.49	8.44	6.61	2.50	.62	.72	.11	.11	.00	16.91	100.00
84-a2	55.48	10.28	.98	4.46	11.22	10.32	3.04	.73	.68	.14	.12	.00	2.55	100.00
89-a1	48.80	8.86	2.31	7.80	11.53	9.78	2.57	.40	1.85	.20	.21	.03	5.66	100.00
89-a2	51.26	9.97	1.50	8.12	11.25	10.98	3.13	.30	1.64	.16	.16	.03	1.51	100.00
85-a1	53.95	11.12	2.06	1.47	2.19	1.89	2.18	1.18	.62	.05	.10	.03	23.17	100.00
85-a2	67.26	8.85	2.19	1.39	2.63	1.56	2.71	1.85	.70	.04	.09	.01	10.73	100.00
85-a3	68.78	10.72	1.26	1.45	2.91	4.30	4.41	1.52	.48	.09	.07	.03	3.98	100.00
86-a1	32.85	12.43	2.39	1.80	5.20	1.82	.68	.39	.50	.08	.07	.01	41.78	100.00
86-a2	37.86	9.67	1.53	4.17	12.51	3.96	.88	.29	.59	.10	.12	.01	28.32	100.00
86-a3	50.23	10.64	1.19	3.88	11.78	7.42	2.30	.31	.54	.05	.11	.01	11.54	100.00

TABLE 11.—*Molecular ratios*
[Leaders (—), not analyzed]

Sample No.	Bases[1]	R_2O_3[2]	WPI[3]	PI[4]	Parker's Index[5]	SiO_2/R_2O_3	Bases/R_2O_2	Fe_2O_3/FeO
109-a1	8.24	21.92	-35.74	61.97	11.68	1.63	0.38	1.64
109-a2	15.71	16.46	-25.43	67.97	22.65	2.12	.95	—
109-a3	17.65	14.96	-16.51	71.71	26.48	2.53	1.18	—
109-a4	19.45	15.44	16.77	78.43	32.32	3.64	1.26	.09
105-a1	13.04	15.78	-1.27	77.81	22.32	3.51	.83	1.05
105-a2	19.44	15.71	16.67	78.15	31.99	3.58	1.24	.10
104-a1	22.46	17.54	16.46	71.83	32.12	2.55	1.28	.13
104-a2	25.21	17.75	24.02	72.15	36.04	2.59	1.42	.09
104-a3	27.20	14.91	26.16	78.49	40.85	3.65	1.82	.43
102-a1	15.87	15.14	-33.72	67.70	22.25	2.10	1.05	—
102-a2	18.15	15.33	-15.25	70.90	26.67	2.44	1.18	—
102-a3	19.11	15.34	2.71	75.99	31.15	3.17	1.25	—
98-a1	21.96	17.64	17.31	73.38	32.69	2.76	1.24	.24
98-a2	24.06	17.85	24.16	74.38	36.24	2.90	1.35	.18
118-a1	2.67	14.35	-105.86	67.80	4.48	2.11	.19	—
118-a2	4.23	13.65	-94.34	69.69	6.90	2.30	.31	—
118-a3	9.57	12.80	-42.00	76.32	14.91	3.22	.75	—
118-a4	17.97	12.06	5.45	82.44	30.74	4.70	1.49	—
95-a1	17.24	13.85	-5.25	76.89	27.03	3.33	1.25	.84
95-a2	25.66	11.97	20.48	81.36	36.89	4.36	2.14	.30
95-a3	26.62	13.52	26.13	80.61	40.37	4.16	1.97	.25
119-a1	12.53	13.49	-6.80	80.16	22.82	4.04	.93	.66
119-a2	19.03	13.75	18.62	82.40	34.47	4.68	1.38	.29
120-a1	8.88	13.66	-14.27	80.52	16.98	4.13	.65	1.35
120-a2	14.45	12.73	2.77	82.30	27.52	4.65	1.14	.70
120-a3	17.55	13.48	14.14	82.35	31.56	4.66	1.30	.27
121-a1	6.01	14.95	-23.12	78.56	12.95	3.66	.40	2.06
121-a2	12.20	12.54	5.42	84.05	22.80	5.27	.97	.47
121-a3	13.56	12.92	7.62	83.34	24.71	5.00	1.05	.29
121-a4	15.37	14.24	12.55	82.09	28.70	.58	1.08	.34
75-b1	9.51	14.54	-18.07	78.15	18.46	3.58	.65	1.80
75-b2	17.94	14.32	16.33	81.72	33.13	4.47	1.25	.60
83-b1	19.85	14.96	9.77	77.83	33.35	3.51	1.33	1.57
83-b2	24.35	14.87	23.16	79.15	40.08	3.80	1.64	.45
79-b1	8.29	17.12	-16.50	75.29	16.60	3.05	.48	2.32
79-b2	12.40	15.91	-3.80	77.36	22.47	3.42	.78	1.36
79-b3	16.72	15.34	10.21	79.39	29.54	3.85	1.09	.80
84-a1	8.18	14.10	1.55	77.78	28.46	3.50	1.29	.73
84-a2	25.31	14.18	23.97	79.64	38.82	3.91	1.79	.22
89-a1	24.27	16.93	20.68	74.25	35.71	2.88	1.43	.30
89-a2	25.67	17.16	25.67	74.92	38.35	2.99	1.50	.18
85-a1	7.44	14.54	-20.72	78.77	16.09	3.71	.51	1.40
85-a2	8.75	12.43	-2.24	84.40	20.30	5.41	.70	1.57
85-a3	13.14	13.19	9.63	83.90	28.05	5.21	1.00	.87
86-a1	8.10	16.22	-58.91	66.95	11.91	2.03	.50	1.33
86-a2	17.63	13.87	-15.40	73.18	23.21	2.73	1.27	.37
86-a3	21.80	14.32	11.89	77.82	31.48	3.51	1.52	.31

[1]Bases=$MgO+CaO+Na_2O+K_2O$.
[2]$R_2O_3=Al_2O_3+Fe_2O_3+TiO_2$.
[3]WPI=Weathering Potential Index=$100(\Sigma Bases\text{-}H_2O)/(\Sigma bases+\Sigma R_2O_3+SiO_2)$ (Reiche, 1950).
[4]PI=Product, Index=$100\ (SiO_2)/(SiO_2+\Sigma R_2O_3)$ (Reiche, 1950).
[5]Parker's (1970) Index=$100\ (Na_2O/0.35+MgO/0.9+CaO/0.7+K_2O/0.25)$.

TABLE 12.—*Standard-cell cations*

[Standard cell cations are the number of cations in a standard cell containing 160 oxygens, calculated by methods of Barth (1948). Leaders (—), not analyzed]

Sample No.	Si	Al	Fe^{3+}	Fe^{2+}	Mg	Ca	Na	K	Ti	P	Mn	C	H	Sum
109-a1	33.04	19.22	11.16	3.41	3.87	3.18	0.54	0.59	3.37	0.31	0.16	0.13	58.77	137.75
109-a2	33.84	12.57	14.06	—	7.03	6.87	1.74	.92	2.63	-	.14	.00	63.52	143.31
109-a3	36.63	12.61	12.09	—	7.05	7.94	3.18	.92	2.10	.00	.15	.00	56.58	139.26
109-a4	50.59	15.63	1.35	7.72	5.89	8.18	5.11	1.80	1.57	.32	.16	.13	7.54	105.97
105-a1	48.27	17.80	4.74	2.26	3.62	5.21	3.83	1.26	1.36	.23	.15	.12	24.62	113.48
105-a2	50.26	16.61	1.42	7.08	5.89	8.17	5.10	1.56	1.50	.32	.16	.13	7.53	105.72
104-a1	43.32	13.38	3.27	12.23	12.52	6.78	4.02	.88	2.55	.25	.17	.13	16.48	115.99
104-a2	44.20	14.10	2.42	12.87	13.04	8.52	4.68	.64	2.36	.34	.17	.14	7.38	110.88
104-a3	48.15	19.25	1.56	1.82	10.64	10.10	6.01	.66	1.88	.26	.18	.14	3.45	104.09
102-a1	31.85	9.99	15.30	—	8.43	6.26	1.64	.83	2.55	.00	.19	.00	74.31	151.35
102-a2	36.07	11.67	13.56	—	8.12	7.44	3.07	.85	2.19	.00	.18	.00	55.90	139.05
102-a3	43.75	15.01	9.59	—	5.67	8.30	5.38	1.11	1.52	.00	.15	.00	30.38	120.87
98-a1	45.06	15.18	4.04	8.58	9.46	8.27	4.35	.87	2.44	.25	.17	.13	12.38	111.18
98-a2	46.71	17.91	2.88	7.92	9.26	9.44	5.37	.61	1.74	.24	.16	.13	2.55	104.93
118-a1	30.72	14.83	11.25	—	1.88	.24	.47	.72	1.55	.00	.06	.00	107.12	168.85
118-a2	32.06	6.96	16.69	—	3.00	.43	.78	.99	2.12	.00	.06	.00	103.58	166.67
118-a3	40.04	7.52	13.45	—	6.32	1.37	1.57	1.63	1.94	.00	.09	.00	70.43	144.35
118-a4	50.36	15.59	4.38	—	5.13	7.10	6.16	1.35	.74	.00	.08	.00	23.56	114.45
95-a1	43.19	17.93	4.09	2.43	8.92	4.57	3.16	2.20	.76	.13	.18	.01	39.92	127.48
95-a2	49.14	12.70	3.01	4.98	15.10	6.28	3.60	1.90	.92	.09	.15	.01	13.65	111.52
95-a3	50.20	17.66	1.80	3.54	11.93	8.29	5.71	1.41	.57	.19	.10	.03	2.58	104.02
119-a1	48.72	17.77	2.76	2.09	4.26	3.54	5.19	1.59	.74	.31	.08	.02	32.18	119.27
119-a2	54.65	17.63	1.58	2.75	5.31	6.17	7.25	2.10	.69	.27	.08	.02	1.58	100.09
120-a1	49.70	17.98	3.29	1.22	2.81	2.30	3.99	1.42	.78	.11	.07	.01	35.48	119.15
120-a2	52.28	14.81	3.43	2.44	5.30	3.42	4.59	3.49	.90	.11	.08	.04	21.29	112.18
120-a3	53.92	17.66	1.45	2.68	5.32	5.49	6.38	2.10	.67	.26	.08	.02	7.32	103.34
121-a1	47.94	19.47	4.13	1.00	1.79	1.10	2.99	1.75	.78	.10	.05	.01	41.16	122.27
121-a2	56.65	13.54	2.88	3.06	5.18	1.82	4.66	2.27	1.01	.06	.08	.02	12.49	103.73
121-a3	55.76	14.94	2.03	3.54	5.63	2.41	5.23	2.07	.89	.08	.10	.01	11.41	104.09
121-a4	54.78	18.70	1.64	2.43	3.79	4.96	6.68	1.62	.56	.18	.07	.01	5.81	101.25
75-b1	46.21	20.96	3.11	.86	2.43	3.13	4.00	1.75	.46	.22	.07	.00	41.31	124.50
75-b2	53.84	18.52	2.49	2.08	4.38	6.21	6.77	2.23	.50	.25	.09	.03	3.74	101.12
83-b1	46.57	17.08	5.29	1.68	8.43	5.28	5.13	2.68	1.25	.54	.12	.00	20.09	114.13
83-b2	49.50	18.06	2.80	3.11	9.14	7.87	6.30	2.37	1.06	.44	.09	.01	3.85	104.60
79-b1	45.47	17.55	8.43	1.81	3.10	1.55	2.62	2.53	1.03	.18	.12	.02	36.76	121.18
79-b2	47.73	15.83	7.25	2.66	5.55	2.24	3.52	2.66	1.10	.15	.14	.01	27.27	116.12
79-b3	50.50	19.80	3.27	2.04	4.45	6.21	5.43	1.84	.56	.19	.10	.02	12.67	107.07
84-a1	45.18	18.86	3.36	2.28	7.73	6.05	4.58	1.14	.66	.19	.10	.00	30.97	121.11
84-a2	49.52	18.36	1.76	3.98	10.02	9.21	5.42	1.31	.61	.25	.10	.00	4.55	105.08
89-a1	44.92	16.31	4.26	7.18	10.61	9.00	4.73	.73	1.70	.37	19	.03	10.42	110.45
89-a2	46.47	18.07	2.72	7.36	10.20	9.96	5.68	.55	1.48	.28	.14	.03	2.74	105.68
85-a1	47.65	19.64	3.64	1.30	1.93	1.67	3.85	2.09	.55	.08	.09	.02	40.94	123.45
85-a2	56.58	14.90	3.68	1.17	2.21	1.31	4.56	3.11	.59	.06	.07	.01	18.05	106.30
85-a3	56.84	17.72	2.09	1.20	2.40	3.55	7.29	2.51	.40	.14	.06	.02	6.57	100.80
86-a1	32.19	24.35	4.68	1.76	5.09	1.79	1.34	.77	.49	.16	.07	.01	81.85	154.54
86-a2	37.57	19.19	3.03	4.13	12.41	3.93	1.74	.57	59	.19	.12	.01	56.20	139.68
86-a3	46.01	19.50	2.18	3.56	10.79	6.79	4.21	.57	.49	.10	.10	.01	21.13	115.45

TABLE 13.—*Weights per unit-volume*

[Calculations assume isovolumetric weathering; bulk density was estimated by comparison with Hendricks and Whittig's (1968) data for similar rock types, on the basis of ratios of Al_2O_3 and TiO_2 in the weathered rock to those in the fresh rock. Leaders (—), not analyzed]

Sample No.	Bulk density	SiO_2	Al_2O_3	Fe_2O_3	FeO	MgO	CaO	Na_2O	K_2O	TiO_2	P_2O_5	MnO	CO_2	H_2O^+	H_2O^-	Sum
109-a1	2.10	74.76	36.96	33.60	9.24	5.88	6.72	0.63	1.05	10.08	0.84	0.42	0.21	19.95	7.14	207.48
109-a2	2.40	91.20	28.80	50.40	—	12.72	17.28	2.42	1.94	9.36	.00	.43	.00	25.68	—	240.24
109-a3	2.60	106.60	31.20	46.80	—	13.78	21.58	4.78	2.11	8.06	.00	.52	.00	24.70	—	260.13
109-a4	2.80	150.36	39.48	5.32	27.44	11.76	22.68	7.84	4.20	6.16	1.12	.56	.28	3.36	.84	281.40
105-a1	2.70	144.72	45.36	18.90	8.10	7.29	14.58	5.94	2.97	5.40	.81	.54	.27	11.07	4.86	270.81
105-a2	2.80	149.52	42.00	5.60	25.20	11.76	22.68	7.84	3.64	5.88	1.12	.56	.28	3.36	1.40	280.84
104-a1	2.30	100.74	26.45	10.12	34.04	19.55	14.72	4.83	1.61	7.82	.69	.46	.23	5.75	.69	227.70
104-a2	2.60	114.14	30.94	8.32	39.78	22.62	20.54	6.24	1.30	8.06	1.04	.52	.26	2.86	.26	256.88
104-a3	2.80	130.20	44.24	5.60	5.88	19.32	25.48	8.40	1.40	6.72	.84	.56	.28	1.40	.56	250.88
102-a1	2.40	86.40	23.04	55.20	—	15.36	15.84	2.30	1.78	9.12	.00	.62	.00	30.24	—	239.90
102-a2	2.50	100.00	27.50	50.00	—	15.13	19.25	4.40	1.85	8.00	.00	.60	.00	23.25	—	249.98
102-a3	2.80	134.40	39.20	39.20	—	11.70	23.80	8.54	2.69	6.16	.00	.53	.00	14.00	—	280.22
98-a1	2.50	115.25	33.00	13.75	26.25	16.25	19.75	5.75	1.75	8.25	.75	.50	.25	4.75	.25	246.50
98-a2	2.80	136.64	44.52	11.20	27.72	18.20	25.76	8.12	1.40	6.72	.84	.56	.28	1.12	.28	283.36
118-a1	1.70	66.30	27.20	32.30	—	2.72	.49	.53	1.22	4.42	.00	.15	.00	34.68	—	170.02
118-a2	2.00	78.00	14.40	54.00	—	4.90	.98	.98	1.90	6.80	.00	.18	.00	37.80	—	199.94
118-a3	2.40	112.80	18.00	50.40	—	11.95	3.60	2.28	3.60	7.20	.00	.29	.00	29.76	—	239.88
118-a4	2.70	153.90	40.50	17.82	—	10.53	20.25	9.72	3.24	2.97	.00	.30	.00	10.80	—	270.03
95-a1	2.40	114.24	40.32	14.40	7.68	15.84	11.28	4.32	4.56	2.64	.41	.55	.02	15.84	5.76	237.86
95-a2	2.50	132.00	29.00	10.75	16.00	27.25	15.75	5.00	4.00	3.25	.28	.47	.03	5.50	2.75	252.02
95-a3	2.80	152.60	45.64	7.28	12.88	24.36	23.52	8.96	3.36	2.30	.70	.36	.06	1.18	.84	284.03
119-a1	2.50	136.25	42.25	10.25	7.00	8.00	9.25	7.50	3.50	2.75	1.03	.28	.05	13.50	7.50	249.10
119-a2	2.70	161.46	44.28	6.21	9.72	10.53	17.01	11.07	4.86	2.70	.95	.27	.05	.70	.54	270.35
120-a1	2.30	133.17	40.94	11.73	3.91	5.06	5.75	5.52	2.99	2.76	.35	.21	.02	14.26	5.75	232.42
120-a2	2.40	137.52	33.12	12.00	7.68	9.36	8.40	6.24	7.20	3.12	.34	.26	.07	8.40	2.88	236.59
120-a3	2.70	159.03	44.28	5.67	9.45	10.53	15.12	9.72	4.86	2.59	.92	.27	.05	3.24	1.21	266.95
121-a1	2.10	117.39	40.53	13.44	2.94	2.94	2.52	3.78	3.36	2.52	.29	.15	.02	15.12	5.67	210.67
121-a2	2.40	152.40	30.96	10.32	9.84	9.36	4.56	6.48	4.80	3.60	.19	.26	.05	5.04	1.92	239.78
121-a3	2.50	154.75	35.25	7.50	11.75	10.50	6.25	7.50	4.50	3.25	.25	.33	.03	4.75	2.75	249.35
121-a4	2.70	162.81	47.25	6.48	8.64	7.56	13.77	10.26	3.78	2.21	.65	.24	.03	2.59	1.48	267.76
75-b1	2.60	139.62	53.82	12.48	3.12	4.94	8.84	6.24	4.16	1.82	.78	.23	.00	18.72	8.84	263.61
75-b2	2.70	157.95	46.17	9.72	7.29	8.64	17.01	10.26	5.13	1.94	.86	.30	.05	1.65	.81	267.79
83-b1	2.50	127.50	39.75	19.25	5.50	15.50	13.50	7.25	5.75	4.50	1.75	.38	.00	8.25	2.75	251.63
83-b2	2.70	143.64	44.55	10.80	10.80	17.82	21.33	9.45	5.40	4.05	1.51	.32	.03	1.67	1.62	273.00
79-b1	2.20	110.66	36.30	27.28	5.28	5.06	3.52	3.30	4.84	3.30	.53	.35	.04	13.42	4.40	218.28
79-b2	2.30	120.75	34.04	24.38	8.05	9.43	5.29	4.60	5.29	3.68	.46	.41	.02	10.35	4.14	230.90
79-b3	2.70	150.66	50.22	12.96	7.29	8.91	17.28	8.37	4.32	2.19	.67	.35	.05	5.67	2.16	271.11
84-a1	2.50	124.00	44.00	12.25	7.50	14.25	15.50	6.50	2.45	2.38	.63	.33	.00	12.75	4.00	246.53
84-a2	2.70	143.10	45.09	6.75	13.77	19.44	24.84	8.10	2.97	2.32	.86	.35	.00	1.97	.54	270.11
89-a1	2.50	115.00	35.50	14.50	22.00	18.25	21.50	6.25	1.48	5.75	1.13	.58	.05	4.00	.75	246.73
89-a2	2.70	128.25	42.39	9.99	24.30	18.90	25.65	8.10	1.19	5.40	.92	.46	.05	1.13	.27	267.00
85-a1	2.20	121.22	42.46	12.32	3.96	3.30	3.96	5.06	4.18	1.85	.24	.26	.04	15.62	3.08	217.56
85-a2	2.60	168.48	37.70	14.56	4.16	4.42	3.64	7.02	7.28	2.31	.21	.26	.03	8.06	1.82	259.95
85-a3	2.70	171.18	45.36	8.37	4.32	4.86	9.99	11.34	5.94	1.59	.51	.22	.05	2.97	1.21	267.92
86-a1	2.40	88.08	56.64	17.04	5.76	9.36	4.56	1.90	1.66	1.78	.50	.22	.02	33.60	20.16	241.27
86-a2	2.50	102.50	44.50	11.00	13.50	22.75	10.00	2.45	1.22	2.13	.63	.38	.03	23.00	16.00	250.08
86-a3	2.70	137.16	49.41	8.64	12.69	21.60	18.90	6.48	1.32	1.94	.35	.35	.03	9.45	3.78	272.11

TABLE 14.—*Weights assuming TiO_2 constant*

[Data, in grams, represent the results of weathering 100 g of fresh rock. Leaders (—), not analyzed]

Sample No.	TiR[1]	SiO_2	Al_2O_3	Fe_2O_3	FeO	MgO	CaO	Na_2O	K_2O	TiO_2	P_2O_5	MnO	CO_2	H_2O^+	H_2O^-	Sum
109-a1	0.46	16.32	8.07	7.33	2.02	1.28	1.47	0.14	0.23	2.20	.18	0.09	0.05	4.35	1.56	45.28
109-a2	.56	21.44	6.77	11.85	—	2.99	4.06	.57	.46	2.20	.00	.10	.00	6.04	—	56.41
109-a3	.71	29.10	8.52	12.77	—	3.76	5.89	1.31	.57	2.20	.00	.14	.00	6.74	—	70.97
109-a4	1.00	53.70	14.10	1.90	9.80	4.20	8.10	2.80	1.50	2.20	.40	.20	.10	1.20	.30	100.50
105-a1	1.05	56.28	17.64	7.35	3.15	2.83	5.67	2.31	1.15	2.10	.32	.21	.10	4.31	1.89	105.31
105-a2	1.00	53.40	15.00	2.00	9.00	4.20	8.10	2.80	1.30	2.10	.40	.20	.10	1.20	.50	100.30
104-a1	.71	30.92	8.12	3.11	10.45	6.00	4.52	1.48	.49	2.40	.21	.14	.07	1.76	.21	70.24
104-a2	.77	33.99	9.21	2.48	11.85	6.74	6.12	1.86	.39	2.40	.31	.15	.08	.85	.08	76.49
104-a3	1.00	46.50	15.80	2.00	2.10	6.90	9.10	3.00	.50	2.40	.30	.20	.10	.50	.20	99.60
102-a1	.58	20.84	5.56	13.32	—	3.71	3.82	.56	.43	2.20	.00	.15	.00	7.29	—	57.89
102-a2	.69	27.50	7.56	13.75	—	4.16	5.29	1.21	.51	2.20	.00	.17	.00	6.39	—	68.75
102-a3	1.00	48.00	14.00	14.00	—	4.18	8.50	3.05	.96	2.20	.00	.19	.00	5.00	—	100.00
98-a1	.73	33.53	9.60	4.00	7.64	4.73	5.75	1.67	.51	2.40	.22	.15	.07	1.38	.07	71.71
98-a2	1.00	48.80	15.90	4.00	9.90	6.50	9.20	2.90	.50	2.40	.30	.20	.10	.40	.10	101.20
118-a1	.42	16.50	6.77	8.04	—	.68	.12	.13	.30	1.10	.00	.04	.00	8.63	—	42.31
118-a2	.32	12.62	2.33	8.74	—	.79	.16	.16	.31	1.10	.00	.03	.00	6.11	—	32.35
118-a3	.37	17.23	2.75	7.70	—	1.83	.55	.35	.55	1.10	.00	.04	.00	4.55	—	36.67
118-a4	1.00	57.00	15.00	6.60	—	3.90	7.50	3.60	1.20	1.10	.00	.11	.00	4.00	—	100.00
95-a1	.75	35.48	12.52	4.47	2.39	4.92	3.50	1.34	1.42	.82	.13	.17	.01	4.92	1.79	73.80
95-a2	.63	33.30	7.32	2.71	4.04	6.88	3.97	1.26	1.01	.82	.07	.12	.01	1.39	.69	63.71
95-a3	1.00	54.50	16.30	2.60	4.60	8.70	8.40	3.20	1.20	.82	.25	.13	.02	.42	.30	101.00
119-a1	.91	49.55	15.36	3.73	2.55	2.91	3.36	2.73	1.27	1.00	.37	.10	.02	4.91	2.73	90.91
119-a2	1.00	59.80	16.40	2.30	3.60	3.90	6.30	4.10	1.80	1.00	.35	.10	.02	.26	.20	100.00
120-a1	.80	46.32	14.24	4.08	1.36	1.76	2.00	1.92	1.04	.96	.12	.07	.01	4.96	2.00	80.80
120-a2	.74	42.31	10.19	3.69	2.36	2.88	2.58	1.92	2.22	.96	.10	.08	.02	2.58	.89	73.11
120-a3	1.00	58.90	16.40	2.10	3.50	3.90	5.60	3.60	1.80	.96	.34	.10	.02	1.20	.45	99.00
121-a1	.68	38.20	13.19	4.37	.96	.96	.82	1.23	1.09	.82	.10	.05	.01	4.92	1.84	68.33
121-a2	.55	34.71	7.05	2.35	2.24	2.13	1.04	1.48	1.09	.82	.04	.06	.01	1.15	.44	54.67
121-a3	.63	39.04	8.89	1.89	2.96	2.65	1.58	1.89	1.14	.82	.06	.08	.01	1.20	.69	63.08
121-a4	1.00	60.30	17.50	2.40	3.20	2.80	5.10	3.80	1.40	.82	.24	.09	.01	.96	.55	99.00
75-b1	1.03	55.23	21.29	4.94	1.23	1.95	3.50	2.47	1.65	.72	.31	.09	.00	7.41	3.50	103.89
75-b2	1.00	58.50	17.10	3.60	2.70	3.20	6.30	3.80	1.90	.72	.32	.11	.02	.61	.30	99.00
83-b1	.83	42.50	13.25	6.42	1.83	5.17	4.50	2.42	1.92	1.50	.58	.13	.00	2.75	.92	84.17
83-b2	1.00	53.20	16.50	4.00	4.00	6.60	7.90	3.50	2.00	1.50	.56	.12	.01	.62	.60	101.00
79-b1	.54	27.16	8.91	6.70	1.30	1.24	.86	.81	1.19	.81	.13	.09	.01	3.29	1.08	53.46
79-b2	.51	26.58	7.49	5.37	1.77	2.08	1.16	1.01	1.16	.81	.10	.09	.01	2.28	.91	50.63
79-b3	1.00	55.80	18.60	4.80	2.70	3.30	6.40	3.10	1.60	.81	.25	.13	.02	2.10	.80	100.00
84-a1	.91	44.90	15.93	4.44	2.72	5.16	5.61	2.35	.89	.86	.23	.12	.00	4.62	1.45	89.62
84-a2	1.00	53.00	16.70	2.50	5.10	7.20	9.20	3.00	1.10	.86	.32	.13	.00	.73	.20	100.00
89-a1	.87	40.00	12.35	5.04	7.65	6.35	7.48	2.17	.51	2.00	.39	.20	.02	1.39	.26	86.09
89-a2	1.00	47.50	15.70	3.70	9.00	7.00	9.50	3.00	.44	2.00	.34	.17	.02	.42	.10	99.00
85-a1	.70	38.70	13.56	3.93	1.26	1.05	1.26	1.62	1.33	.59	.08	.08	.01	4.99	.98	69.54
85-a2	.66	42.96	9.61	3.71	1.06	1.13	.93	1.79	1.86	.59	.05	.07	.01	2.06	.46	66.29
85-a3	1.00	63.40	16.80	3.10	1.60	1.80	3.70	4.20	2.20	.59	.19	.08	.02	1.10	.45	99.00
86-a1	.97	35.71	22.96	6.91	2.34	3.79	1.85	.77	.67	.72	.20	.09	.01	13.62	8.17	98.27
86-a2	.85	34.73	15.08	3.73	4.57	7.71	3.39	.83	.42	.72	.21	.13	.01	7.79	5.42	84.71
86-a3	1.00	50.80	18.30	3.20	4.70	8.00	7.00	2.40	.49	.72	.13	.13	.01	3.50	1.40	101.00

[1]Ti R=Ti Ratio=ratio of TiO_2 in the fresh rock to that in the weathered sample.

TABLE 15.—*Normalized molecular ratios*

[Molecular ratios are normalized to values in unaltered rock. Leaders (—), not analyzed]

Sample No.	Bases[1]	R_2O_3[2]	WPI[3]	PI[4]	Parker's Index[5]	SiO_2/R_2O_3	Bases/R_2O_3	Fe_2O_3/FeO
109-a1	0.42	1.42	-2.13	0.79	0.36	0.45	0.30	18.76
109-a2	.81	1.07	-1.52	.87	.70	.58	.76	—
109-a3	.91	.97	.98	.91	.82	.70	.94	—
109-a4	1.00	1.00	1.00	1.00	1.00	1.00	1.00	1.00
105-a1	.67	1.00	-.08	1.00	.70	.98	.67	10.50
105-a2	1.00	1.00	1.00	1.00	1.00	1.00	1.00	1.00
104-a1	.83	1.18	.63	.92	.79	.70	.70	.31
1 04-a2	.93	1.19	.92	.92	.88	.71	.78	.22
104-a3	1.00	1.00	1.00	1.00	1.00	1.00	1.00	1.00
102-a1	.83	.99	-12.43	.89	.71	.66	.84	—
102-a2	.95	1.00	-5.62	.93	.86	.77	.95	—
102-a3	1.00	1.00	1.00	1.00	1.00	1.00	1.00	—
98-a1	.91	.99	.72	.99	.90	.95	.92	1.30
98-a2	1.00	1.00	1.00	1.00	1.00	1.00	1.00	1.00
118-a1	.15	1.19	-19.41	.82	.15	.45	.13	—
118-a2	.24	1.13	-17.30	.85	.22	.49	.21	—
118-a3	.53	1.06	-7.70	93	.48	.69	.50	—
118-a4	1.00	1.00	1.00	1.00	1.00	1.00	1.00	—
95-a1	.65	1.02	.20	.95	.67	.80	.63	3.32
95-a2	.96	.89	.78	1.01	.91	1.05	1.09	1.19
95-a3	1.00	1.00	1.00	1.00	1.00	1.00	1.00	1.00
119-a1	.66	.98	.37	.97	.66	.86	.67	2.29
119-a2	1.00	1.00	1.00	1.00	1.00	1.00	1.00	1.00
120-a1	.51	1.01	-1.01	.98	.54	.89	.50	5.00
120-a2	.82	.94	.20	1.00	.87	1.00	.87	2.60
120-a3	1.00	1.00	1.00	1.00	1.00	1.00	1.00	1.00
121-a1	.39	1.05	-1.84	.96	.45	.80	.37	6.10
121-a2	.79	.88	.43	1.02	.79	1.15	.90	1.40
121-a3	.88	.91	.61	1.02	.86	1.09	.97	.85
121-a4	1.00	1.00	1.00	1.00	1.00	1.00	1.00	1.00
75-b1	.53	1.02	-1.11	.96	.56	.80	.52	3.00
75-b2	1.00	1.00	1.00	1.00	1.00	1.00	1.00	1.00
83.b1	.82	1.01	.42	.98	.83	.92	.81	3.50
83.b2	1.00	1.00	1.00	1.00	1.00	1.00	1.00	1.00
79-b1	.50	1.12	-1.62	.95	.56	.79	.44	2.91
79-b2	.74	1.04	-.37	.97	.76	.89	.71	1.70
79-b3	1.00	1.00	1.00	1.00	1.00	1.00	1.00	1.00
84-a1	.72	.99	.06	.98	.73	.89	.72	3.33
84-a2	1.00	1.00	1.00	1.00	1.00	1.00	1.00	1.00
89-a1	.95	.99	.81	.99	.93	.97	.96	1.60
89-a2	1.00	1.00	1.00	1.00	1.00	1.00	1.00	1.00
85-a1	.57	1.10	-2.15	.94	.57	.71	.51	1.61
85-a2	.67	.94	-.23	1.01	.72	1.04	.71	1.81
85-a3	1.00	1.00	1.00	1.00	1.00	1.00	1.00	1.00
86-a1	.37	1.13	-4.96	.86	.38	.58	.33	4.35
86-a2	.81	.97	-1.30	.94	.74	.78	.83	1.20
86-a3	1.00	1.00	1.00	1.00	1.00	1.00	1.00	1.00

[1]Bases=$MgO+CaO+Na_2O+K_2O$.

[2]$R_2O_3=Al_2O_3+Fe_2O_3+TiO_2$.

[3]WPI=Weathering Potential Index=$100(\Sigma Bases\text{-}H_2O)/(\Sigma bases+\Sigma R_2O_3+SiO_2)$ (Reiche, 1950).

[4]PI=Product Index=100 $(SiO_2)/(SiO_2+SR_2O_3)$ (Reiche, 1950).

[5]Parker's (1970) Index=100 $(Na_2O/0.35+MgO/0.9+CaO/0.7+K_2O/0.25)$.

TABLE 16.—*Normalized weights assuming TiO_2 constant*

[Weights assuming TiO_2 constant (table 14) are normalized to values in the fresh rocks. Leaders (—), not analyzed]

Sample No.	TiR[1]	SiO_2	Al_2O_3	Fe_2O_3	FeO	MgO	CaO	Na_2O	K_2O	TiO_2	P_2O_5	MnO	CO_2	H_2O^+	$H_2O_4^-$
109-a1	0.46	0.30	0.57	3.86	0.21	0.31	0.18	0.05	0.15	1.00	0.46	0.46	0.46	3.63	5.19
109-a2	.56	.40	.48	6.23	—	.71	.50	.20	.30	1.00	00	.51	.00	5.03	—
109-a3	.71	.54	.60	6.72	—	.90	.73	.47	.38	1.00	.00	.71	.00	5.62	—
109-a4	1.00	1.00	1.00	1.00	1.00	1.00	1.00	1.00	1.00	1.00	1.00	1.00	1.00	1.00	1.00
105-a1	1.05	1.05	1.18	3.67	.35	.67	.70	.82	.89	1.00	.79	1.05	1.05	3.59	3.78
105-a2	1.00	1.00	1.00	1.00	1.00	1.00	1.00	1.00	1.00	1.00	1.00	1.00	1.00	1.00	1.00
104-a1	.71	.66	.51	1.55	4.97	.87	.50	.49	.99	1.00	.71	.71	.71	3.53	1.06
104-a2	.77	.73	.58	1.24	.64	.98	.67	.62	.77	1.00	1.03	.77	.77	1.70	.39
104-a3	1.00	1.00	1.00	1.00	1.00	1.00	1.00	1.00	1.00	1.00	1.00	1.00	1.00	1.00	1.00
102-a1	.58	.43	.40	.95	—	.89	.45	.18	.45	1.00	.00	.79	.00	1.46	—
102-a2	.69	.57	.54	.98	—	1.00	.62	.40	.53	1.00	.00	.87	.00	1.28	—
102-a3	1.00	1.00	1.00	1.00	—	1.00	1.00	1.00	1.00	1.00	.00	1.00	.00	1.00	—
98-a1	.73	.69	.60	1.00	.77	.73	.62	.58	1.02	1.00	.73	.73	.73	3.45	.73
98-a2	1.00	1.00	1.00	1.00	1.00	1.00	1.00	1.00	1.00	1.00	1.00	1.00	1.00	1.00	1.00
118-a1	.42	.29	.45	1.22	—	.17	.02	.04	.25	1.00	.00	.35	.00	2.16	—
118-a2	.32	.22	.16	1.32	—	.20	.02	.04	.26	1.00	.00	.26	.00	1.53	—
118-a3	.37	.30	.18	1.17	—	.47	.07	.10	.46	1.00	.00	.40	.00	1.14	—
118-a4	1.00	1.00	1.00	1.00	—	1.00	1.00	1.00	1.00	1.00	.00	1.00	.00	1.00	—
95-a1	.75	.65	.77	1.72	.52	.57	.42	.42	1.18	1.00	.51	1.32	.37	11.71	5.96
95-a2	.63	.61	.45	1.04	.88	.79	.47	.39	.84	1.00	.28	.92	.32	3.30	2.31
95-a3	1.00	1.00	1.00	1.00	1.00	1.00	1.00	1.00	1.00	1.00	1.00	1.00	1.00	1.00	1.00
119-a1	.91	.83	.94	1.62	.71	.75	.53	.67	.71	1.00	1.06	1.00	.91	18.88	13.64
119-a2	1.00	1.00	1.00	1.00	1.00	1.00	1.00	1.00	1.00	1.00	1.00	1.00	1.00	1.00	1.00
120-a1	.80	.79	.87	1.94	.39	.45	.36	.53	.58	1.00	.35	.72	.40	4.13	4.44
120-a2	.74	.72	.62	1.76	.68	.74	.46	.53	1.23	1.00	.30	.81	1.11	2.15	1.97
120-a3	1.00	1.00	1.00	1.00	1.00	1.00	1.00	1.00	1.00	1.00	1.00	1.00	1.00	1.00	1.00
121-a1	.68	.63	.75	1.82	.30	.34	.16	.32	.78	1.00	.40	.53	.68	5.12	3.35
121-a2	.55	.58	.40	.98	.70	.76	.20	.39	.78	1.00	.18	.67	1.09	1.20	.80
121-a3	.63	.65	.51	.79	.93	.95	.31	.50	.81	1.00	.26	.91	.63	1.25	1.26
121-a4	1.00	1.00	1.00	1.00	1.00	1.00	1.00	1.00	1.00	1.00	1.00	1.00	1.00	1.00	1.00
75-b1	1.03	.94	1.25	1.37	.46	.61	.56	.65	.87	1.00	.96	.84	.00	12.14	11.66
75-b2	1.00	1.00	1.00	1.00	1.00	1.00	1.00	1.00	1.00	1.00	1.00	1.00	1.00	1.00	1.00
83-b1	.83	.80	.80	1.60	.46	.78	.57	.69	.96	1.00	1.04	1.04	.00	4.44	1.53
83-b2	1.00	1.00	1.00	1.00	1.00	1.00	1.00	1.00	1.00	1.00	1.00	1.00	1.00	1.00	1.00
79-b1	.54	.49	.48	1.39	.48	.38	.13	.26	.74	1.00	.52	.66	.54	1.57	1.35
79-b2	.51	.48	.40	1.12	.66	.63	.18	.33	.73	1.00	.41	.70	.25	1.08	1.14
79-b3	1.00	1.00	1.00	1.00	1.00	1.00	1.00	1.00	1.00	1.00	1.00	1.00	1.00	1.00	1.00
84-a1	.91	.85	.95	1.77	.53	.72	.61	.78	.81	1.00	.71	.91	.00	6.32	7.24
84-a2	1.00	1.00	1.00	1.00	1.00	1.00	1.00	1.00	1.00	1.00	1.00	1.00	.00	1.00	1.00
89-a1	.87	.84	.79	1.36	.85	.91	.79	.72	1.17	1.00	1.15	1.18	.87	3.31	2.61
89-a2	1.00	1.00	1.00	1.00	1.00	1.00	1.00	1.00	1.00	1.00	1.00	1.00	1.00	1.00	1.00
85-a1	.70	.61	.81	1.27	.79	.59	.34	.38	.61	1.00	.41	1.05	.70	4.53	2.19
85-a2	.66	.68	.57	1.20	.66	.63	.25	.43	.84	1.00	.28	.83	.33	1.87	1.03
85-a3	1.00	1.00	1.00	1.00	1.00	1.00	1.00	1.00	1.00	1.00	1.00	1.00	1.00	1.00	1.00
86-a1	.97	.70	1.25	2.16	.50	.47	.26	.32	1.37	1.00	1.57	.67	.97	3.89	5.84
86-a2	.85	68	.82	1.16	.97	.96	.48	.35	.85	1.00	1.63	.98	.85	2.23	3.87
86-a3	1.00	1.00	1.00	1.00	1.00	1.00	1.00	1.00	1.00	1.00	1.00	1.00	1.00	1.00	1.00

[1]TiR=Ti Ratio=ratio of TiO_2 in the fresh rock to that in the weathered sample.

☆U S GOVERNMENT PRINTING OFFICE: 1982—576-034/125